5-2015

Comparison of Analytical, Numerical and Semi-Analytical Methods for Modeling Matrix Diffusion Effects in Aquitards

Wenwen Wang
Clemson University, wenwenw@g.clemson.edu

COMPARISON OF ANALYTICAL, NUMERICAL AND SEMI-ANALYTICAL METHODS FOR MODELING MATRIX DIFFUSION EFFECTS IN AQUITARDS

A Thesis
Presented to
the Graduate School of
Clemson University

In Partial Fulfillment
of the Requirements for the Degree
Master of Science
Environmental Engineering and Science

---

by
Wenwen Wang
May 2015

Accepted by:
Dr. Ronald Falta, Committee Chair
Dr. Lawrence Murdoch
Dr. Timothy Devol

ABSTRACT

The invasion of dissolved chlorinated volatile organic compounds (CVOCs) into low permeability zones can cause contaminant persistence above maximum contaminant levels (MCLs) in adjacent aquifers due to the phenomenon of matrix diffusion. Numerical studies have been conducted to simulate matrix diffusion effects between aquifers and aquitards. However, existing numerical approaches for simulating matrix diffusion of CVOCs require fine discretization of the aquifer and aquitard into tens of layers of grid blocks, resulting in large computational effort. Considering the inefficiency of numerical approaches, a semi-analytical method was developed to only discretize the aquifer and mathematically approximate the diffusive response in the underlying aquitard.

The semi-analytical method was originally developed in petroleum reservoir engineering for approximating the conductive heat flux from a permeable reservoir into an underlying impermeable cap rock [Vinsome and Westerveld, 1980]. With some modification, a similar semi-analytical method can be applied directly to the problem of CVOC matrix diffusion. The objective of this study is to implement and test the new semi-analytical method for simulating matrix diffusion effects between an aquifer and an aquitard.

This study has three sub-objectives. First of all, grid refinement studies were performed by constructing two simple numerical models for simulating DNAPL pool dissolution in an aquifer with advection and vertical dispersion and matrix diffusion in an aquitard, respectively. The numerical simulations were validated with two simple

analytical solutions. The results showed that a grid spacing of $\Delta x = 1.0$ m and $\Delta z = 0.2$ m was fine enough to simulate both cases.

Second, a test was performed with the numerical method by comparing a two-layer numerical model with the more complex Dandy-Sale analytical solution (Sale et al., 2008) for 2-D transport in an aquifer with matrix diffusion in an underlying aquitard. In the numerical simulation, the two-layer model was constructed with fine grid spacing of $\Delta x = 1.0$ m and $\Delta z = 0.15$ m. The results showed that numerical solutions were in good quantitative agreement with analytical solutions in Dandy-Sale model.

Third, the new semi-analytical method was employed for the problem of CVOC matrix diffusion in the two-layer model and was tested against the more complex Dandy-Sale analytical solutions. The comparison of semi-analytical and analytical results indicated that the semi-analytical method is an accurate approximation of CVOC matrix diffusion effects between an aquifer and an aquitard.

DEDICATION

I would like to dedicate this to my parents and friends, for their understanding and love.

ACKNOWLEDGEMENTS

Firstly, I would like to express my sincere appreciation to my advisor. Dr. Ronald Falta, for his guidance, great patience and wisdom during my graduate study, and my committee members, Dr. Lawrence Murdoch and Dr. Timothy Devol, for their guidance and support throughout the course of this work.

I would especially like to acknowledge Dr. Falta for providing me the opportunity and financial support to work on such an interesting project. Finally, I would like to express gratitude to Mr. Zhou, for his understanding, continuous support from every aspect, and the encouragement during my time here.

The United States Department of Defense through the Environmental Security Technology Certification Program (ESTCP) provided funding for this work (project ER-201426). This support is also acknowledged gratefully.

TABLE OF CONTENTS

Table of Contents (Continued)

Page

LIST OF TABLES

LIST OF FIGURES

List of Figures (Continued)

Figure Page

List of Figures (Continued)

Figure Page

LIST OF ABBREVIATIONS

CVOCs	Chlorinated Volatile Organic Compounds
DNAPLs	Dense Non-aqueous Phase Liquids
LNAPLs	Light Non-aqueous Phase Liquids
NAPLs	Non-aqueous Phase Liquids
EPA	Environmental Protection Agency
MCL	Maximum Contaminant Level
PCE	Tetrachloroethene
TCE	Trichloroethylene
DOC	Dissolved Organic Carbon
EPA	Environmental Protection Agency
TMVOC	Multiphase Flow and Transport Code

LIST OF SYMBOLS IN EQUATIONS

D_w	Molecular diffusion coefficient of the chemical in water (m^2/s)
R	Retardation coefficient
τ	Tortuosity
C_0	TCE solubility in water (g/L)
D_T	Transverse hydrodynamic dispersion coefficient (m^2/s)
D_V	Transverse hydrodynamic dispersion coefficient (m^2/s)
D_L	Transverse hydrodynamic dispersion coefficient (m^2/s)
α_t	Transverse hydrodynamic dispersivity (m)
v	Pore water velocity (m/d)

CHAPTER 1

INTRODUCTION

Groundwater is one of the main sources for drinking water around the world, especially in rural areas. In the United States, groundwater supplies 42.1% of the population served by public water utilities and more than half of the population relies upon a groundwater source for their primary drinking water supply [Pierce and Perlman, 1993]. However, according to the data of the World Health Organization (WHO), the scarcity of water resources has created challenges for over 40% of the world population, i.e., more than 2 billion people have no access to enough water or clean water.

The quality of groundwater resources globally has been under serious threat due to their exposure to a broad spectrum of contaminants [Taste 1992; Schipper et al., 2010]. Non-aqueous phase liquids (NAPLs) persisting in the subsurface are the most toxic and prevalent contaminants found in the groundwater [Schwille, 1988]. Over the last 25 years, many contaminated sites in North America, particularly those of industrial origin, have exhibited non-aqueous phase liquids (NAPLs) residing in porous media below the water table [Freeze, 2000]. These contaminated liquids often originate from leaking underground storage tanks, ruptured pipelines, surface spills, hazardous wastes landfills, and disposal sites [Doherty, 2000; Pankow and Cherry, 1996].

NAPLs are organic liquids immiscible with water. Based on the density relative to water, NAPLs can be further subcategorized into light non-aqueous phase liquids (LNAPLs) or dense non-aqueous phase liquids (DNAPLs). When a NAPL spill infiltrates a subsurface, a portion of it may be trapped and immobilized within the unsaturated

porous formation by capillary force and the remaining fluid will continue to move downward through the unsaturated zone under the influence of gravity. Upon reaching the water table, LNAPLs will tend to spread laterally and float above the water table in the form of entrapped ganglia (blobs) and pools whereas DNAPLs with density heavier than water, will continue to migrate vertically through the saturated zone until they encounter an impermeable layer, where a flat source zone or pool starts to form [Seagren et al., 1999； Albert et al., 1994; Schwille, 1988].

As groundwater flows through trapped ganglia and DNAPL pools, the soluble chemicals in DNAPLs, such as tetrachloroethylene (PCE) and trichloroethylene (TCE), will undergo interphase mass transfer from the non-aqueous phase to the aqueous phase, slowly creating large dissolved contaminant plumes in groundwater. These plumes are subject to advection, dispersion, matrix diffusion, sorption and a variety of potential degradation processes. Although the solubility of DNAPL compounds is generally low, it is frequently several orders of magnitude higher than the maximum contaminant level (MCLs) for drinking water standards [Pankow et al., 1996]. Therefore, a small amount of DNAPL may contaminate a large volume of groundwater.

Over the past two decades, the growing concern of DNAPL-contaminated sites has led to extensive research in the removal or destruction of contaminant source. However, clean-up goals have hardly been met if the subsurface formation contains low permeability units (e.g. clays or rock matrix) [Johnson and Pankow, 1992; Ball et al., 1997; Liu and Ball, 2002; Chapman and Parker, 2005; Lipson et al., 2005; Parker et al., 2008; Seyedabbasi et al., 2012; Chapman and Parker, 2012]. Historically, the existence of

low permeability units in the subsurface was thought to be an effective barrier to further vertical migration of DNAPLs. However, once these low permeability zones are contaminated, they can also act as long-term reservoirs for contaminants due to the phenomenon of matrix diffusion [Mckay et al., 1993; Parker et al., 1994; Ball et al., 1997; Liu and Ball, 2002; Chapman and Parker, 2005; Seyedabbasi et al., 2012].

Matrix diffusion characterizes transport process whereby dissolved chemicals diffuse between high permeability zones (e.g. sandy layers or fractures) and low permeability zones. When dissolved chemicals are initially introduced into high permeability zones, they will diffuse rapidly into adjacent low permeability zones due to a sharp concentration contrast and a significant amount of contaminants will be stored in the low permeability zone. Once the source is removed from the high permeability zone through natural or manmade process, the dissolved chemicals in low permeability zones can slowly diffuse back into high permeability zones due to the reversal of the concentration gradient [Parker et al., 1994; Slough et al., 1999; Reynold and Kueper, 2001; Chapman and Parker, 2005; Falta et al., 2005; Lipson et al., 2005; Parker et al., 2008; Sale et al., 2008].

Matrix diffusion has the potential to increase the remediation timeframe (i.e. the time required to reach regulatory concentration goals) at chlorinated solvent sites because diffusion-controlled release of contaminants back into transmissive zones occurs at relatively slow rates [Parker et al., 2008; West and Kueper, 2010]. Previously, the importance of contaminant back diffusion from clayey aquitards on aquifer restoration has been widely investigated by numerical techniques [Liu and Ball, 2002; Chapman and

Parker, 2005; Parker et al., 2008; Chapman and Parker, 2012]. However, existing numerical models can only simulate the process of matrix diffusion under ideal circumstances, using computationally intensive fine grids.

A much more efficient alternative is application of a semi-analytical method, which requires no explicit discretization of the low permeability zones. This semi-analytical method was originally developed in petroleum reservoir engineering for calculating the conductive heat flux from permeable reservoir and underlying impermeable cap rock during thermally enhanced oil recovery [Vinsome and Westerveld, 1980]. This method was shown to give excellent accuracy for heat exchange between reservoir fluids and confining beds in petroleum and geothermal injection and production operations [Pruess and Wu, 1993; Pope et al., 1999; Varavei and Sepehrnoori, 2009]. With some modification, a similar semi-analytical method can be applied to the problem of CVOC matrix diffusion. Instead of discretizing the aquitard, the semi-analytical method only discretizes the aquifer and mathematically approximates the diffusive response in the underlying aquitard.

The main motivation of this study is to employ the new semi-analytical method for the problem of CVOC matrix diffusion and verify its accuracy with existing analytical solutions.

CHAPTER 2

LITERATURE REVIEW

This chapter summarizes the scientific literature relevant to the physical processes of NAPL dissolution, matrix diffusion and transport mechanisms of dissolved NAPLs in the groundwater.

2.1 NAPL Dissolution

The dissolution of NAPL organic contaminants in the subsurface has been the subject of intensive investigation and increasing concern over the past two decades. Many common NAPLs have very low aqueous solubilities, thus they may serve as long-term sources of groundwater contamination. Based on the results of several experimental studies [e.g., Schwille, 1988; Pearce et al., 1994; Voudrias and Yeh, 1994], DNAPL pools in the saturated zone can be expected to persist for years to decades in the case of small pools (i.e., <1–2 liters of NAPL) and on the order of decades to centuries in the case of larger pools (i.e., hundreds of liters of NAPL). This persistence is mainly caused by slow dissolution kinetics of the contaminants from the DNAPL pool, which is affected by many factors, including the DNAPL source, porous media properties, boundary conditions, and the DNAPL- aqueous mass transfer relation.

2.1.1 NAPL Pool Dissolution

The study of NAPL pool dissolution has received much attention. A majority of the studies available in the literature focused on theoretical investigations. Hunt et al. [1988] used a two-dimensional steady-state equation, accounting for transverse dispersion into a semi-infinite porous medium to describe the process of NAPL

dissolution. The authors suggested that because of mass transfer limitations in liquid phase dissolution, ground water extraction at contaminated sites is ineffective for removing the DNAPL within a reasonable amount of time. The authors also suggest that steam displacement as an enhancement for remediation could rapidly vaporize and mobilize trapped volatile NAPLs. Anderson et al. [1992] presented a three-dimensional analytical solution describing characteristics of downgradient contaminant plume resulting from the dissolution of a NAPL pool. They concluded that the observed concentrations in the field are generally above 1mg/L and the main reason is that NAPLs below water table tend to accumulate as stagnant pools, which have a slow dissolution rate controlled by vertical dispersion. Johnson and Pankow [1992] presented quantitative estimates of pool source strengths in the saturated zone. The authors were able to estimate the time required for complete pool dissolution and also suggested that the removal times can be reduced by increasing the groundwater velocities. However, they also provided a strong possibility that DNAPL components will remain within an aquitard or a low-permeability layer on which the pool originally formed after the pool has been totally dissolved away. Chrysikopoulos et al. [1994] presented a mathematical model describing the transport of a decaying contaminant resulting from the dissolution of a single component NAPL pool. The study showed a good agreement between the simulated concentration profiles and the experimental data. Seagren et al. [1994] presented a two-dimensional analytical solution to develop quantitative tools and criteria for assessing the effectiveness of NAPL pool remediation techniques such as flushing and biodegradation. Chrysikopoulos [1995] presented three-dimensional analytical solutions for

contaminant transport resulting from the dissolution of a well-defined elliptic or rectangular stagnant NAPL pool. This study demonstrated through synthetic examples that the more elongated the pool along the direction of the flow, the higher the dissolved peak concentration. Chrysikopoulos [2003] developed analytical relationships for the average mass transfer coefficient and the concentration boundary layer thickness applicable to dissolving NAPL pools in saturated, homogeneous and isotropic porous formations.

Several experimental studies on NAPL dissolution have been conducted. Schwille [1998] conducted several visual NAPL displacement experiments and concluded that a pool of NAPL will form if the spill is sufficiently large. Furthermore, this study also concluded that NAPL removal rate increases with higher flow rates. Voudrias and Yeh [1994] performed a dissolution experiment with a toluene pool floating at the water table under constant and variable hydraulic gradients. They concluded that pulsed pumping is more efficient than continuous pumping for remediation of contaminated aquifers. Whelan et al. [1994] designed and constructed a two-dimensional experimental aquifer to observe the dissolution behavior of DNAPL pools. They also performed a two component pool dissolution experiment, and found that the dissolved concentrations measured were much lower than the respective DNAPL solubility. Pearce et al. [1994] investigated factors affecting the dissolution kinetics of single-component DNAPL pools covering the bottom of a two-dimensional experimental aquifer and also concluded that measured concentrations were a small fraction of the respective DNAPL solubility. Chrysikopoulos [2000] designed a unique three-dimensional bench-scale model aquifer to

carry out DNAPL pool dissolution experiments, allowing for a constant, well-defined pool-water interface. The authors suggested that the model is useful for the validation of numerical and analytical DNAPL pool dissolution models and the estimates of pool size, location, and projected longevity under homogeneous conditions. Lee [2002] developed an experimental mass transfer correlation for circular TCE pools dissolving in three-dimensional, water-saturated porous media and showed a relatively good agreement between the newly developed correlation and experimental data.

2.1.2 Multicomponent NAPL Dissolution

As a majority of groundwater contaminations sites involve multicomponent NAPLs, the study on multicomponent NAPL systems has also recently received attention. Leinonen and Mackay [1973] concluded that in a multicomponent mixture, complex and substantial changes in the effective solubility of each component may occur. Banerjee [1984] conducted numerous experiments to determine the solubility of multicomponent mixture by using both structurally similar and different chemical mixtures. The authors concluded that mixtures of structurally related hydrophobic liquids were near ideal in the organic phase and in the aqueous phase the activity coefficient of a component was unaffected by the presence of cosolutes. They also concluded that for mixtures of structurally unrelated liquids, the solubility calculations can be estimated using the unique function-group activity coefficients (UNIFAC) method. Lee and Chrysikopoulos [1995] developed a three-dimensional, finite-difference numerical model to simulate contaminant transport resulting from the dissolution of multicomponent NAPL pools in homogeneous saturated porous media.

2.1.3 Numerical Modeling Methods

Many efforts have been devoted to numerically modeling the impacts of source zone architecture on NAPL dissolution. Powers et al. [1998] used MODFLOW [Zheng and Wang, 1999] to simulate NAPL dissolution in two-dimensional (2D) flow through systems containing a sand lens contaminated with NAPL and surrounded by a clean sand matrix. Saba and Illangasekare [2000] used a modified version of the transport code MT3D [Zheng and Wang, 1999] to evaluate the effects of flow dimensionality on NAPL dissolution. Instead of assuming local equilibrium, a mass transfer rate correlation was determined from experiments and incorporated into the model. Mayer and Miller [1996] developed a 2D multiphase flow and species transport model to simulate NAPL emplacement and dissolution in both homogeneous and heterogeneous porous media using either the local equilibrium assumption (LEA) or empirical mass transfer correlations. In a more recent work, Christ et al. [2006] developed an upscaled mass transfer model by incorporating source zone parameters, i.e., the initial concentration and source zone ganglia-to-pool (GTP) mass ratio. This model was demonstrated to use as a screening tool to relate DNAPL mass removal and flux-weighted concentrations when mass removal is less than 80% and the model was shown to be applicable to a range of source zones with GTP greater than 0.4.

Several numerical codes for three-phase flow in porous media have been developed [e.g., White and Lenhard, 1995; Falta et al., 1995; Pruess and Battistelli, 2002]. White and Lenhard [1995] presented a three-dimensional, three-phase compositional model that incorporated fluid entrapment and hysteresis in constitutive

functions. This model is for has been used successfully to simulate DNAPL infiltration and entrapment in a heterogeneous porous matrix [Oostrom et al., 1999]. The multiphase compositional model (CompFlow) can be applied to simulate in detail the nonaqueous and aqueous phase plume migration patterns arising from a synthetic dense nonaqueous phase liquid (DNAPL) release in the aquifer [Unger, 1995; Unger et al., 1996]. T2VOC [Falta et al., 1995] and TMVOC [Pruess and Battistelli, 2002] are part of the TOUGH2 family of codes. T2VOC can be used to model three-phases, three-component, non-isothermal flow of water, air, and a volatile organic compound (VOC) in multi-dimensional heterogeneous porous media. TMVOC is capable of simulating multiphase flow, heat transfer and transport of multiple volatile organic compounds in three-dimensional heterogeneous porous media or fractured rock.

A number of simplified modeling approaches have also been developed for multi-dimensional systems based on analytical or semi-analytical solutions. Nambi and Powers [2003] both developed mass transfer correlations using a 1D transport model to simulate NAPL pool dissolution in heterogeneous systems. In comparison with other published dissolution correlations, the slower mass transfer rate was characterized with a significantly higher exponent on the NAPL saturation term. Parker and Park [2004] investigated field-scale DNAPL dissolution kinetics using high-resolution numerical simulations of DNAPL releases and dissolved phase transport. Sale and McWhorter [2001] simulated NAPL dissolution from discrete source zones located within a 2D homogeneous porous medium using a multiple analytical source superposition technique (MASST). NAPL was distributed in discrete rectangular zones, and these zones were

arranged in different configurations. Falta [2003] formulated a sub-grid pool dissolution model that simulates dissolution of multiple heterogeneously distributed NAPL pools in a 2D dual permeability flow field. The calculation of the advective and dispersive mass flux of chemical leaving each NAPL zone was done using an integral finite difference method, and the calculated interphase mass transfer rate was shown to match experimental data and an analytical solution for DNAPL pool dissolution. Fure et al. [2006] showed that the stream tube model was adequate in capturing NAPL dissolution profiles from experiments performed in 2D heterogeneous systems.

2.2 Solute Transport Mechanisms

There are three important types of processes in solute transport: advection, dispersion and diffusion. In general, transport by advection and dispersion dominates in zones of high permeability of a porous medium, such as aquifer and fractures, while diffusion dominates in zones of low permeability, such as clay layers.

In high permeability zones, the transient solute transport in a 3-D system with uniform flow in the x-direction groundwater flow system can be described via the advection-dispersion equation [Fetter, 2001].

$$R\,\frac{\partial C(x,t)}{\partial t} = -v_x\frac{\partial C(x,t)}{\partial x} + D_L\frac{\partial^2 C(x,t)}{\partial x^2} + D_T\frac{\partial^2 C(x,t)}{\partial y^2} + D_V\frac{\partial^2 C(x,t)}{\partial z^2} \qquad (1)$$

Where R is the retardation factor, D_L is the longitudinal hydrodynamic dispersion coefficient, D_T is the transverse hydrodynamic dispersion coefficient, D_V is the vertical hydrodynamic dispersion coefficient, C is the solute concentration, v_x is ground water

pore velocity in the x-direction, t is the time after release of solute, and x is the distance from the source.

The longitudinal hydrodynamic dispersion coefficient, D_L , accounts for mechanical mixing via the mechanical dispersion coefficient, D_m, and diffusion via the effective diffusion coefficient, D* [Shackelford, 1991; Fetter, 2001].

$$D_L = \alpha_L v + D^*$$

$$D_T = \alpha_T v + D^*$$

$$D_V = \alpha_V v + D^*$$

where α_L is longitudinal hydrodynamic dispersivity, α_T is transverse hydrodynamic dispersivity, α_V is vertical hydrodynamic dispersivity, v is pore water velocity, D^* is the product of the tortuosity, τ, and the aqueous molecular diffusion coefficient, D_w.

For 1-D diffusion in a low permeability zones, equation (1) reduces to the following equation which is for Fick's second law for diffusion of non-reactive solutes in porous media:

$$R\,\frac{\partial C(x,t)}{\partial t} = D^*\,\frac{\partial^2 C(x,t)}{\partial x^2} \qquad (2)$$

2.3 Matrix diffusion

Matrix diffusion refers to the transport process whereby solutes dissolved in groundwater diffuse either from higher permeability zones (e.g. sandy layer or fractures) into the lower permeability zones (e.g. clayey layer or porous rock matrix), or from the lower permeability zones into higher permeability zones [Pankow and Cherry 1996]. Recognition of matrix diffusion as an important process in aquifers with silty or clayey

strata was provided conceptually by Mackay and Cherry [1989]. They discussed the problem of dissolved contaminants invading low permeability strata via diffusion, and subsequent slow rate of release of the contaminants by reverse diffusion during pump-and-treat/aquifer flushing causing long-term tailing. Parker et al. [1994] proposed the concept of NAPL disappearance based on mass transfer rates and times-to-disappearance calculated using one-dimensional analytical model for several common chlorinated solvents. The authors suggested that the model was valid for matrix blocks of a sufficiently large size, so that diffusion from each fracture was not influenced by diffusion from other fractures. Parker et al. [1997] extended the analysis by Parker et al. [1994] to include DNAPL mass flux and disappearance from fractures into matrix blocks of finite size where diffusion effects from fractures bordering the same matrix block were included. Ball et al. [1997] applied a newly developed analytical solution of the two-layer diffusion problem toward the interpretation of measured concentration profiles in a groundwater aquitard at Dover Air Force Base. In this study, independent estimates of sorption and diffusion properties in the aquitard layers were used and a mathematical model based on diffusion in laminate slabs was applied to make inferences regarding the historical concentration in the overlying aquifer.

Much recent work has focused on numerical modeling for matrix diffusion effects from low permeability zones to adjacent high permeability zones. Liu and Ball [2002] used computer modeling to investigate the previous bimodal history of groundwater contamination at the sites and make predictions of contamination flux under hypothesized remediation conditions. The authors also suggested that the field results provided direct

evidence of a case where the underlying confining layer was contaminated from an overlying groundwater plume and subsequently released its contaminant back to the aquifer. Parker et al. [2004] presented a field study of aquitard integrity in a small area (<0.1ha) at a large industrial site in Connecticut, where a persistent zone of TCE DNAPL occuured on top of a clayey silt aquitard. The study provided evidence that some aquitards were capable of preventing deep DNAPL migration and even DNAPL entry, providing long-term protection of underlying aquifer. Lipson et al. [2005] evaluated the influence of bedrock physical and chemical properties on the matrix diffusion process, with particular emphasis on plume attenuation at a former industrial site. The study demonstrated that back diffusion from rock matrix to the open fractures can occur for a very long periods of time following the removal of DNAPL sources in fractured bedrock. Chapman and Parker [2005] provided a case study involving full-scale source-zone isolation at an industrial site. Using detailed aquifer and aquitard sampling along a transect downgradient of the isolated source, along with numerical modeling of site conditions, they showed that back diffusion from the clayey aquitard strongly impacts the overlying aquifer groundwater quality, causing a persistent plume predicted to last many decades or longer before declining to inconsequential levels. Sale et al. [2008] explored the effects of reduced contaminant loading on downgradient water quality using an idealized two-layer scenario by conducting a laboratory sand tank experiment and also developed exact analytical solution for the two-layer scenario, which was consistent with the laboratory data. Parker and Chapman [2008] presented a field study of a TCE DNAPL site where the DNAPL source zone was hydraulically isolated and the rate of

groundwater quality improvement in the downgradient area was monitored for 5 years. The study used a model with very fine discretization and time-step constraints to accurately capture the diffusion process. Wilking et al. [2012] conducted an experimental study of effects of DNAPL distribution on mass rebound and showed the persistence of the plume as a result of mass rebound from low permeability zones after DNAPL source has depleted. This led to in important practical conclusion that complete removal of a DNAPL mass from a source area did not suggest that the site was fully remediated and the plume can persist for significantly long periods as controlled by DNAPL morphology and site-specific geologic conditions. Chapman and Parker [2012] explored the validity of using numerical models in high resolution mode to simulate scenarios involving diffusion into and out of low permeability zones. This study showed that two finite element models, HydroGeoSphere [Therrien and Sudicky, 1996] and FEFLOW [Trefry and Muffels, 2007]. It also presented finite difference model (MODFLOW/MT3DMS) [Zheng and Wang, 1999] with adequate spatial and temporal discretization. The results provided a close match to experimental data from a laboratory sand tank experiment.

CHAPTER 3

RESEARCH OBJECTIVES

The main motivation of this study is to develop and test the accuracy of a new semi-analytical method for simulating matrix diffusion effects of dissolved chemicals between aquifers and aquitards. This research focused on three main objectives:

The first objective was to investigate the effect of grid resolution on the accuracy of numerical methods by comparing numerical solutions with two simple analytical solutions. Two simple numerical models were constructed to simulate the DNAPL pool dissolution in an aquifer and matrix diffusion effects in an aquitard, respectively. The comparison of numerical simulations and analytical solutions were performed with different levels of grid refinement.

The second objective was to perform additional tests with a two-layer numerical model by comparing it with a more complex analytical solution known as the Dandy-Sale model [Sale et al., 2008]. The numerical model was constructed with fine grid discretization for simulating 2-D contaminant transport in an aquifer with matrix diffusion in an underlying aquitard**.**

The third objective was to employ a new semi-analytical method into the problem of matrix diffusion and verify its accuracy by comparing it with the existing analytical solutions. The semi-analytical simulation was conducted by performing numerical simulation for only the aquifer and mathematically approximating matrix diffusion effects in the aquitard by using an analytical trial function that was updated at each time-step.

CHAPTER 4

NUMERICAL SIMULATION OF MATRIX DIFFUSION AND DNAPL DISSOLUTION USING TWO SIMPLE MODELS

The objective of this chapter is to simulate matrix diffusion effects in an aquitard and DNAPL pool dissolution in an aquifer through two simple numerical models. The numerical models were constructed using TMVOC multiphase flow and transport code [Pruess and Battistelli, 2002] with PetraSim interface [Thunderhead Engineering, 2011]. The TMVOC multiphase flow and transport code is a numerical simulator developed at the Lawrence Berkeley National Laboratory to simulate multiphase flow with volatile organic chemicals in multidimensional heterogeneous porous media. The TMVOC code has been widely used and validated with experimental results for a variety of isothermal and non-isothermal problem [Pruess and Battistelli, 2003; Tse et al., 2006].

4.1 Matrix Diffusion Model

4.1.1 Numerical Model Setup

We consider a one-dimensional, homogeneous and isotropic model consisting of a single aquifer grid block and a large thickness aquitard (Figure 4.1). The top aquifer layer is a uniform transmissive porous media (e.g., sand), and the other layers are uniform porous media with low permeability (e.g., clay), where groundwater flow is considered negligible and the transport of dissolved TCE is assumed to be only driven by molecular diffusion without advection. The model is initialized as a fully water-saturated media without an unsaturated zone.

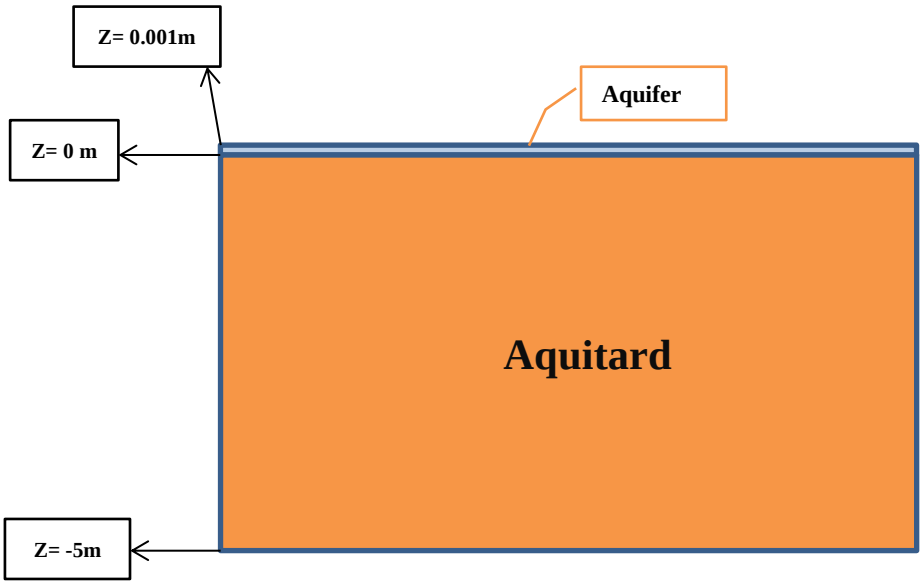

Figure 4.1 Geometry of matrix diffusion model

The mesh size of the numerical model is 10.0 m × 1.0 m × 5.001 m (L x W x H = x, y, z) with resolution of 1 cell in x-, 1 cell in y-, and up to 51 cells in z-direction, creating a 1-D model domain of up to 51 cells (Figure 4.2). The thickness of the single aquifer layer is 0.001m and the thickness of other layers in the aquitard is 0.1m.

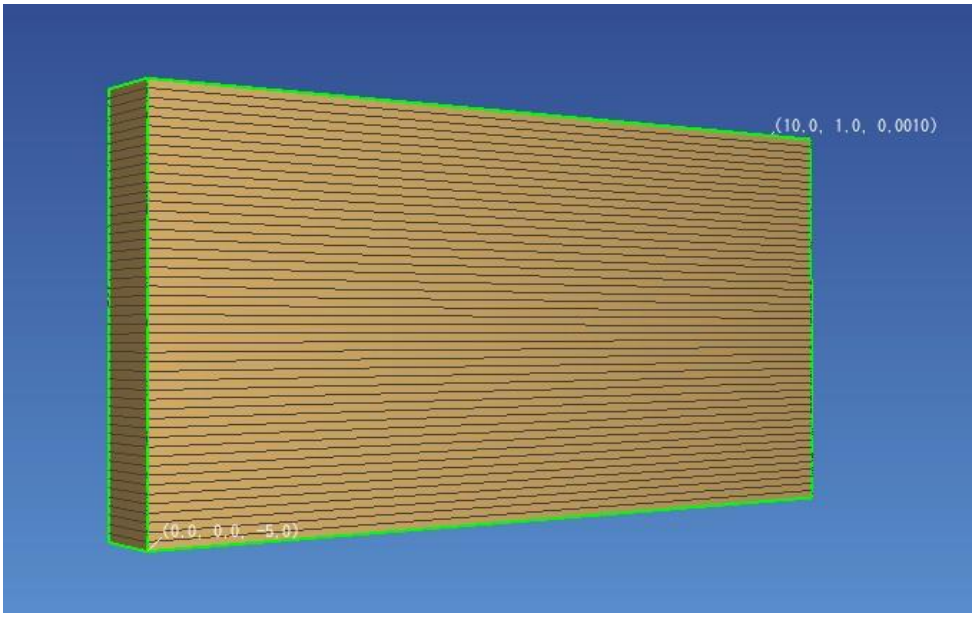

Figure 4.2 Model domain and discretization in PetraSim

The input values used in the model were presented in Table 4.1.

Table 4.1 Input parameters used in matrix diffusion model

Parameter	Aquifer	Aquitard
Bulk density,ρ_b (kg/m^3)	1690	1430
Permeability, k (m^2)	1E-13	1E-18
Porosity, ϕ	0.35	0.45
Tortuosity, τ	0.737	0.737
Retardation factor, R	1.73	1.48
Diffusion coefficient of TCE, D_w (m^2/s)	1.0E-9	1.0E-9
Aqueous solubility of TCE, C_0 (mg/L)	1000	
Saturation of DNAPL source, S_n	0.1	
Time-step, Δt (s)	2.4E6	

Two stages were used for development of TCE concentration profiles in the aquitard. In the first stage, a constant TCE source (S_n=0.1) was maintained for 50 years in the top aquifer grid block (Figure 4.3a). As chemicals dissolved in the aquifer, the dissolved TCE concentration at the interface was much higher than that in the aquitard, causing mass transfer into the underlying aquitard by molecular diffusion. In the second stage, the result of the first stage was loaded as the initial condition. After the TCE source was removed, clean water was flushed into the aquifer for additional 50 years. In the absence of a TCE source, flushing the permeable aquifer caused a rapid decline in the TCE concentration at the interface and an expanding zone of reverse diffusion formed in the uppermost part of the aquitard (Figure 4.3b).

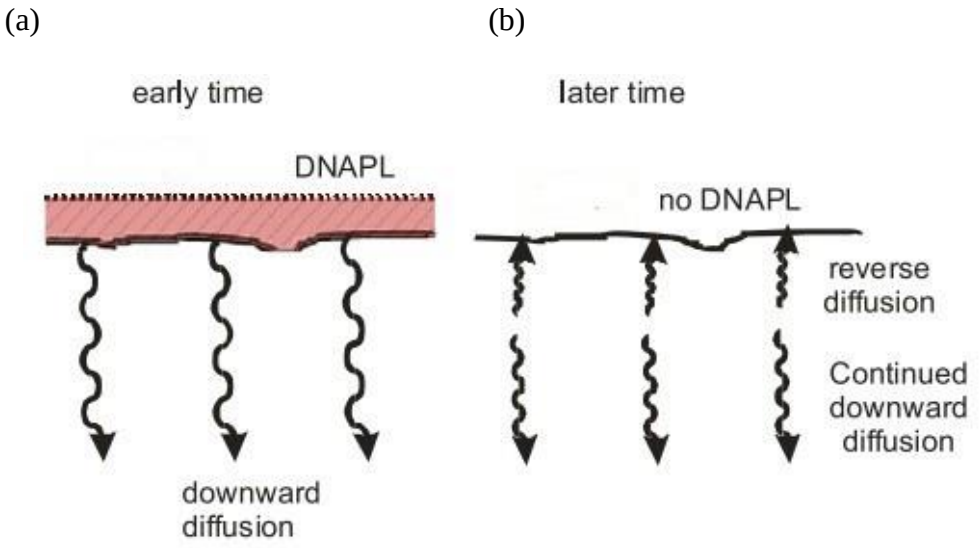

Figure 4.3 Schematic illustration of the aquitard diffusion problem: (a) Temporary TCE source for the first 50 years (b) A removal of the TCE source for another 50 years.

Figure 4.4 shows the TCE concentration profile as a function of depth at different times for each scenario. In the first scenario, the TCE source persisted through the loading period, creating a constant and maximum aqueous concentration (TCE solubility=1000 mg/L) at the interface. The TCE concentration profile shows that the aqueous concentration decreased with depth into the aquitard (Figure 4.4a). In the second scenario, after the TCE source was removed and clean water flushed in the aquifer, the TCE concentration at the interface was instantaneously dropped back to zero and therefore caused contaminant in the aquitard to diffuse back into the aquifer due to the reversal of the concentration gradient at the interface. As a consequence, the TCE concentration increased first until reaching its maximum value at some depth below the interface, and then the concentration began to decrease with depth (Figure 4.4b).

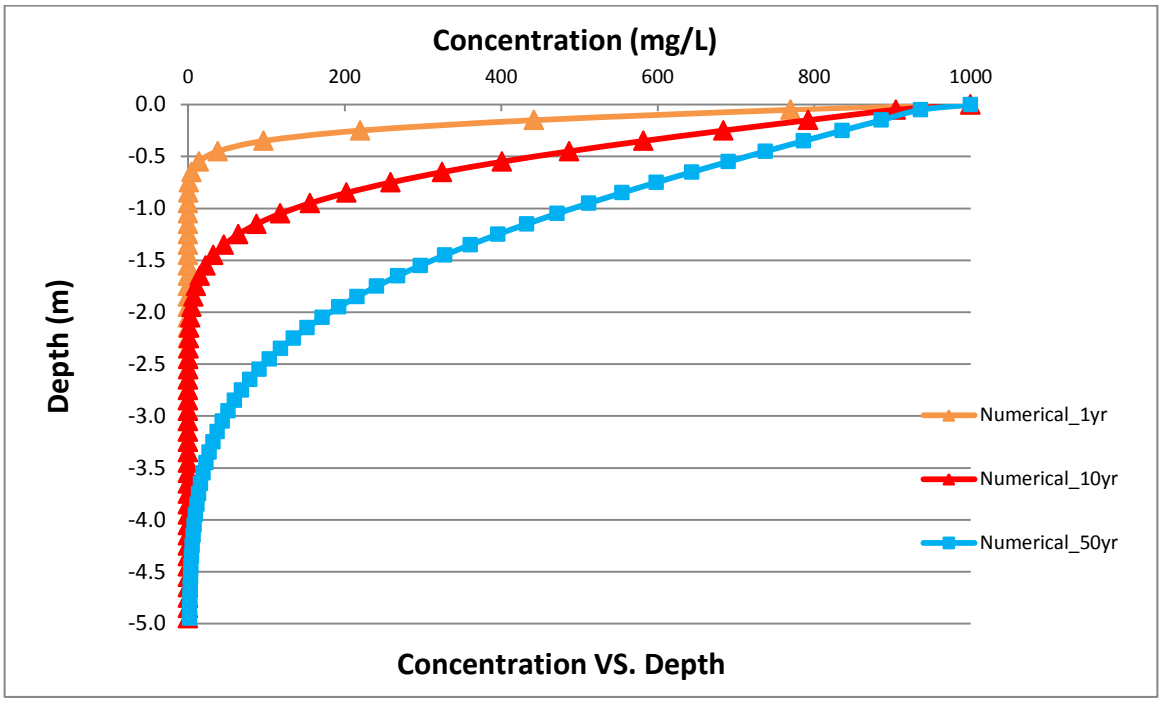

Figure 4.4a TCE concentration profiles for temporary TCE source at times of 1, 10 and 50 years.

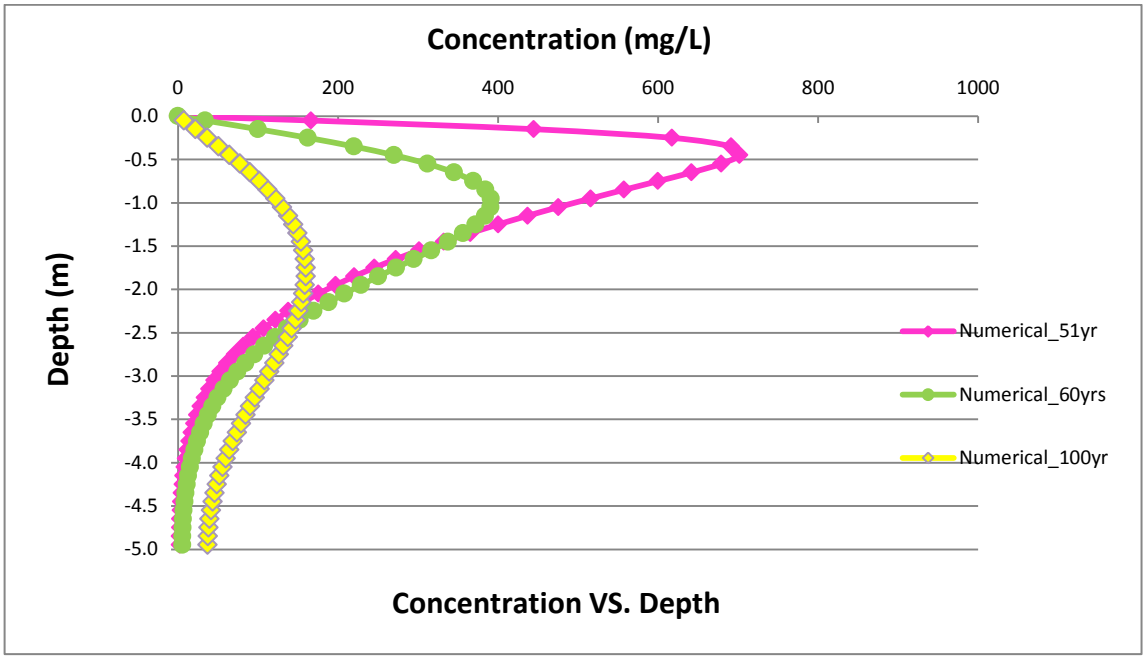

Figure 4.4b TCE concentration profiles after a removal of TCE source at times of 51, 60 and 100 years.

4.1.2 Analytical Solution

The analytical solutions for estimating matrix diffusion effects in aquitards were originally presented by Parker et al. [1984] and modified in Matrix Diffusion Toolkit [Sale et al., 2008]. The key assumption employed in the solution was to assume that the contaminant concentration at the interface between high and low permeability zones was uniformly and instantaneously decreased to zero when DNAPL source was completely depleted. Estimates of concentration profile at a given time within the low permeability zone are:

$$C_{(z,\ t)} = C_0 erfc\left\{\frac{z}{2\sqrt{\alpha t}}\right\}\ ; \qquad t < t_1 \qquad (4\text{-}1)$$

and

$$C_{(z,\ t)} = C_0\left[erfc\left\{\frac{z}{2\sqrt{\alpha t}}\right\} - erfc\left\{\frac{z}{2\sqrt{\alpha(t-t_1)}}\right\}\right]\ ; \qquad t > t_1 \qquad (4\text{-}2)$$

Where C_0 the TCE solubility in water, z is the vertical distance into the aquitard from the interface and t_1 is the time when contaminant source is removed from the high-permeability zone. The parameter α is the effective molecular diffusivity divided by the retardation factor:

$$\alpha = \tau\ D_w/R$$

The diffusive flux for the exact analytical solution was calculated using the "square root" method, which is a part of the current Matrix Diffusion Toolkit [Farhat et al., 2012]. By combining Fick's law,

$$F = -\phi\tau D_w \left.\frac{\partial C}{\partial z}\right|_{z=0}$$

and equations (4-1) and (4-2), the diffusive mass flux across the interface, *F*, can be quantified as:

$$F = \phi\tau D_w C_0 \frac{1}{\sqrt{\pi\alpha t}} \; ; \qquad t < t_1 \qquad (4\text{-}3)$$

$$F = \phi\tau D_w C_0 \left(\frac{1}{\sqrt{\pi\alpha t}} - \frac{1}{\sqrt{\pi\alpha (t-t_1)}}\right) \; ; \qquad t > t_1 \qquad (4\text{-}4)$$

By integrating the mass flux across the aquifer/aquitard interface with respect to time, the total mass in the aquitard as a function of time can be calculated analytically [Seyedabbasi et al., 2012]. The accumulated mass per unit area in the aquitard after a certain time is:

$$M = 2\phi\tau D_w C_0 \sqrt{\frac{t}{\alpha\pi}} \; ; \qquad t < t_1 \qquad (4\text{-}5)$$

$$M = 2\phi\tau D_w C_0 \left(\sqrt{\frac{t}{\alpha\pi}} - \sqrt{\frac{t-t_1}{\alpha\pi}}\right) ; \qquad t > t_1 \qquad (4\text{-}6)$$

4.1.3 Testing

4.1.3.1 TCE Concentration

The accuracy of the numerical model for modeling matrix diffusion effects in aquitard can be verified with exact analytical solutions, equations (4-1) and (4-2). A comparison of numerical and analytical solutions for TCE concentration distribution in aquitard is presented in Figure 4.5. The result shows that the numerical solutions at different times are extremely consistent with the analytical solutions.

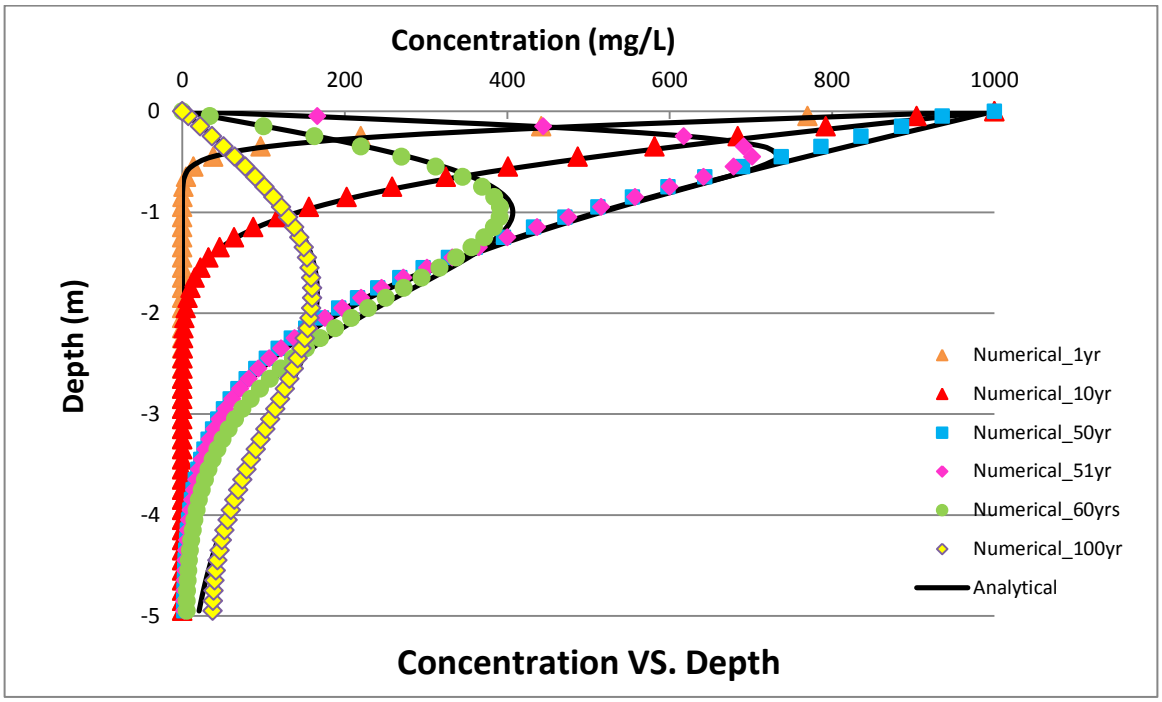

Figure 4.5 Comparison of numerical and analytical solution for TCE concentration profile in an aquitard at times of 1, 10, 50, 51, 60 and 100 years.

4.1.3.2 Diffusive Flux

To further investigate the accuracy of the numerical model, the time-series of diffusive mass flux into and out of the aquitard is generated (Figure 4.6). The numerical and analytical solutions compare well except at very early time, and immediately after the source removal. During the first 50 years, the TCE mass slowly diffused from the aquifer to the underlying aquitard by forward diffusion. As the TCE mass stored in the aquitard increased, the concentration gradient at the interface decreased with time, slowing the process of forward diffusion into the aquitard. Therefore, the magnitude of mass flux into the aquitard decreased with time. After removing the source at t = 50 years, the dissolved TCE concentration in the aquifer decreased sharply and then the concentration gradients

at the interface was reversed, driving the TCE mass stored in the aquitard to diffuse back into the aquifer. Therefore, the magnitude of diffusive flux out of the aquitard rose to its maximum value suddenly at t= 50 years and then reduced continuously with time.

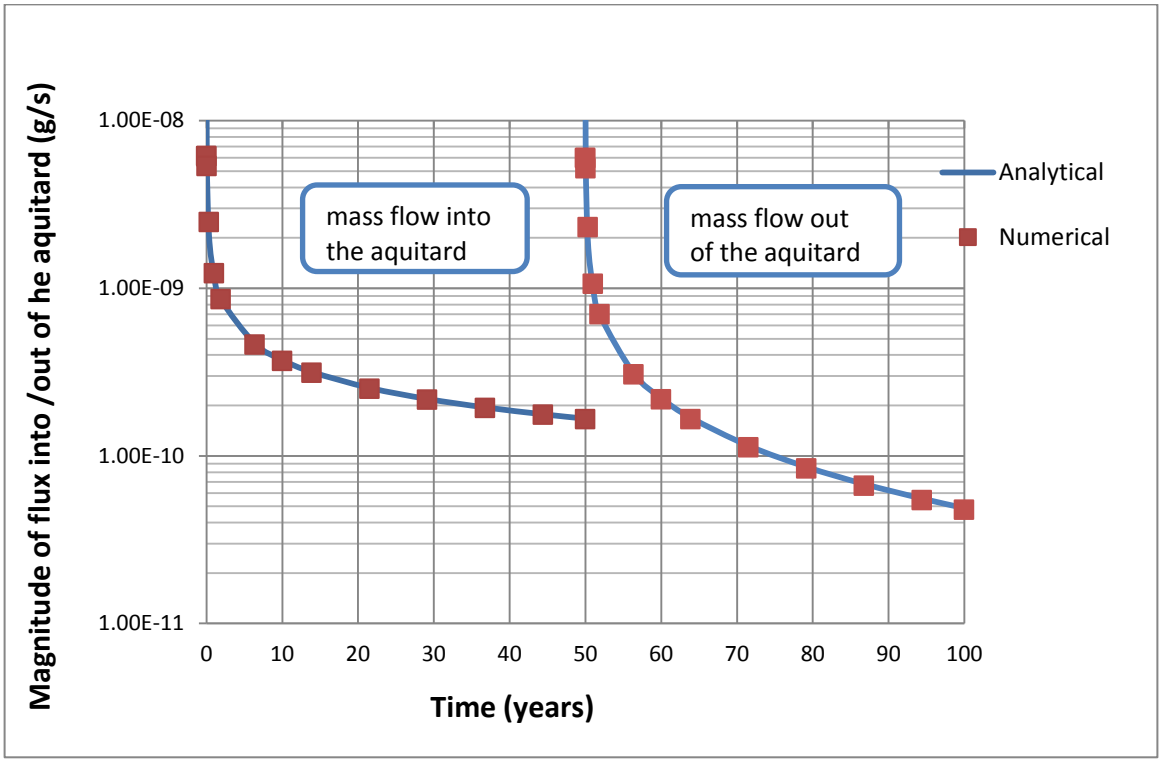

Figure 4.6 Magnitude of diffusive mass flux across the aquifer/aquitard interface.

4.1.3.3 TCE Mass

Finally, an additional comparison of numerical and analytical results was to investigate the total mass of TCE in the aquitard. During the loading period, the mass stored in the aquitard accumulated gradually by forward diffusion until reaching a maximum value at t=50 years. When the source was removed, the TCE mass in the aquitard diffused back into the aquifer, resulting in a sudden drop of the total mass in aquitard (Figure 4.7).

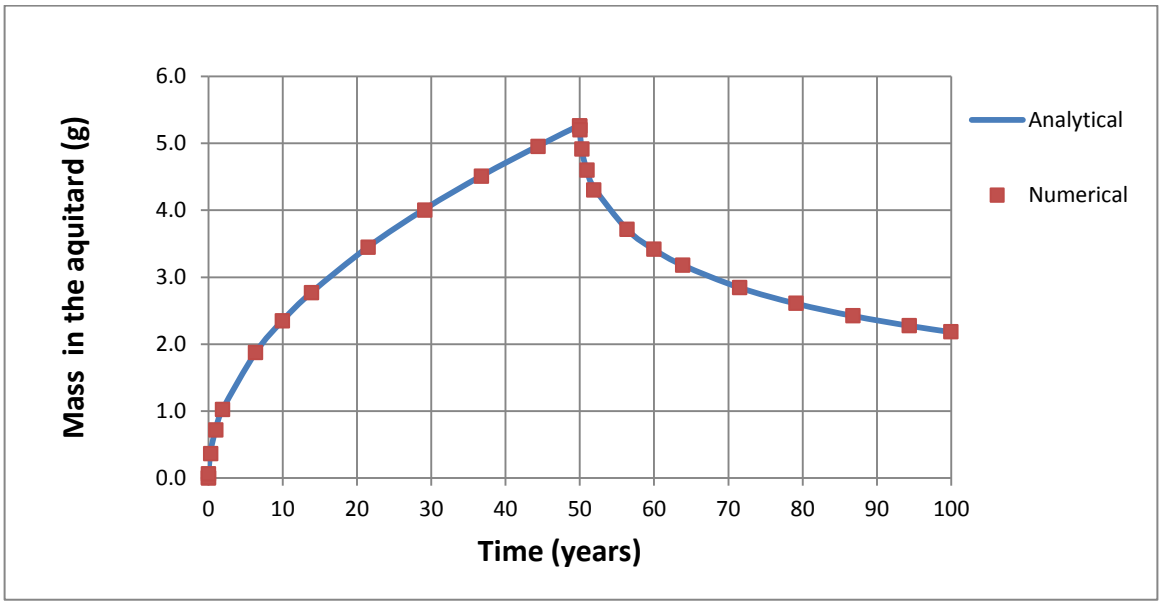

Figure 4.7 Total mass of TCE in the aquitard during the simulation.

4.1.4 Grid Refinement Study

It is widely recognized that a key requirement for numerical simulation is use of adequate spatial discretization to capture the system geometry. However, fine grid discretization requires higher computational requirements and increases the processing time. The base numerical model required about 40 seconds to complete the 100 year simulation. To investigate model sensitivity with respect to grid resolution, we perform several additional cases with coarser grid spacing of 0.2 m, 0.4 m, 0.6 m, 0.8 m and 1.2 m to examine how the discretization of elements need to be optimized to accurately simulate matrix diffusion effects in the aquitard.

4.1.4.1 TCE Concentration

The comparison of numerical and analytical solution with different levels of grid refinement for TCE concentration profiles is presented in Figure 4.8.

(a)

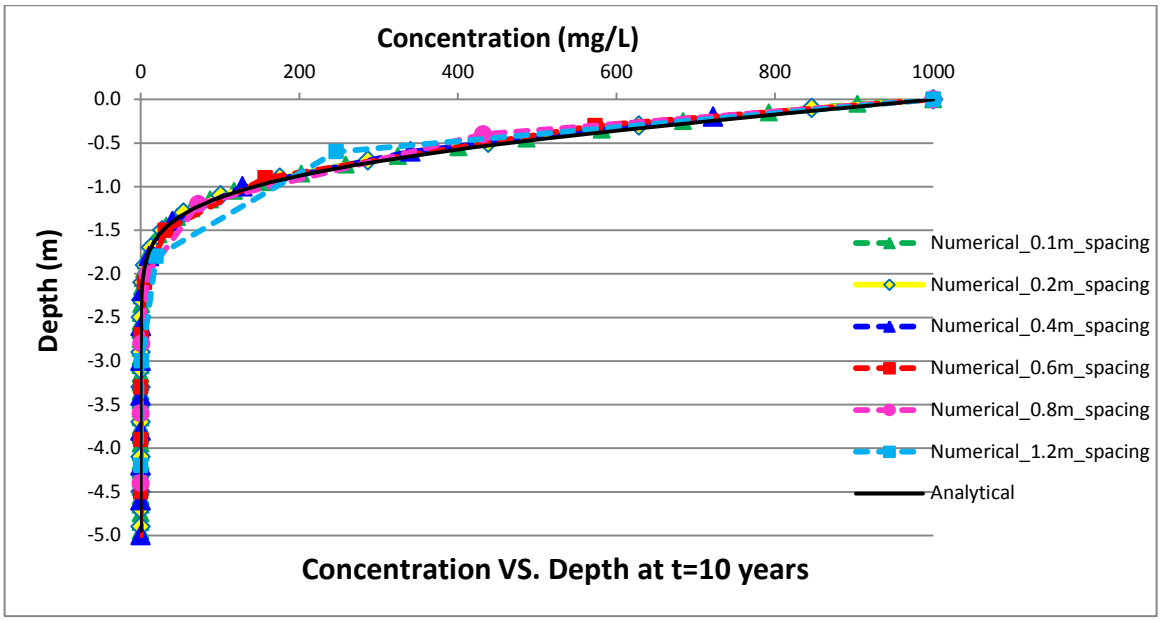
Concentration (mg/L)
0
200
400
600
800
1000
0.0
-0.5
-1.0
-1.5
-2.0
-2.5
-3.0
-3.5
-4.0
-4.5
-5.0
Depth (m)
Numerical_0.1m_spacing
Numerical_0.2m_spacing
Numerical_0.4m_spacing
Numerical_0.6m_spacing
Numerical_0.8m_spacing
Numerical_1.2m_spacing
Analytical
Concentration VS. Depth at t=10 years

(b)

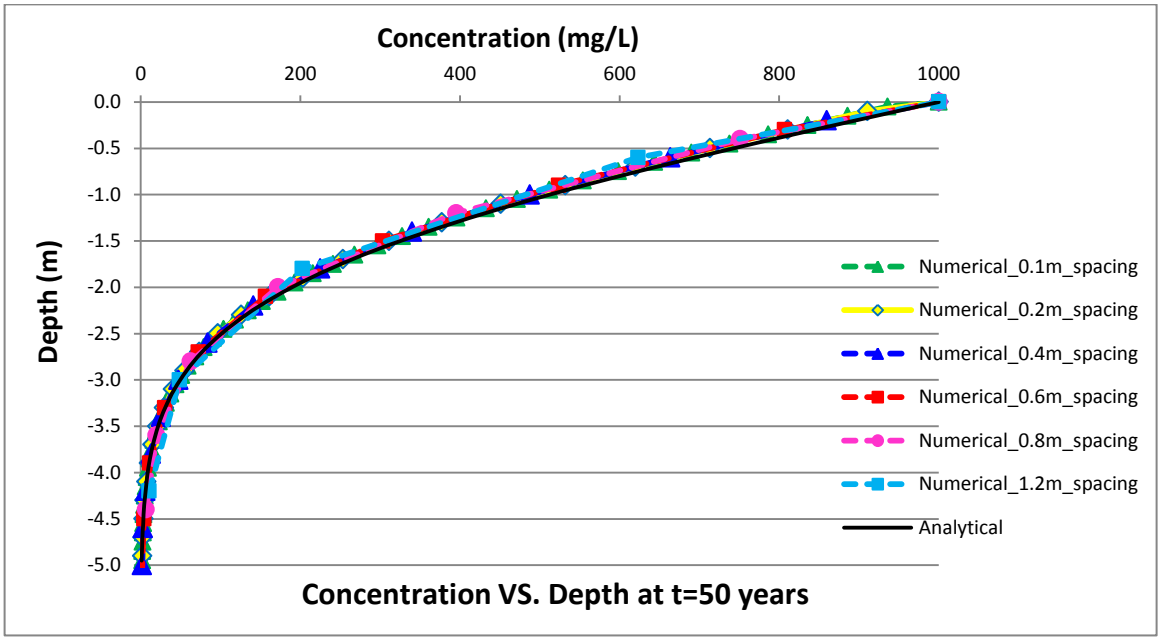
Concentration (mg/L)
0
200
400
600
800
1000
0.0
-0.5
-1.0
-1.5
-2.0
-2.5
-3.0
-3.5
-4.0
-4.5
-5.0
Depth (m)
Numerical_0.1m_spacing
Numerical_0.2m_spacing
Numerical_0.4m_spacing
Numerical_0.6m_spacing
Numerical_0.8m_spacing
Numerical_1.2m_spacing
Analytical
Concentration VS. Depth at t=50 years

(c)

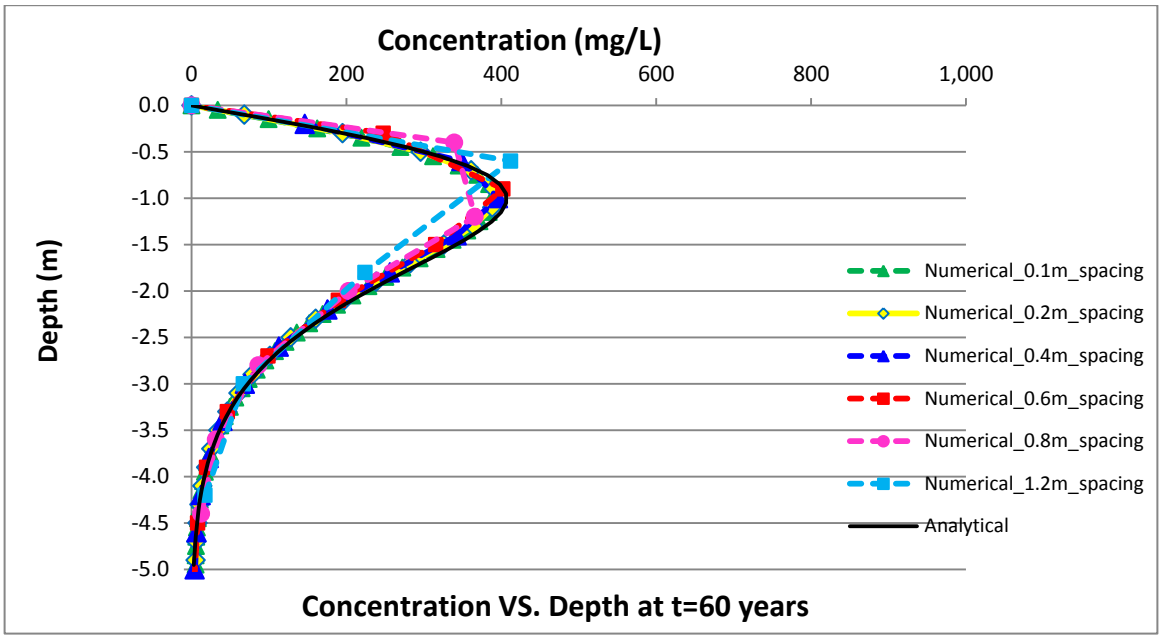

(d)

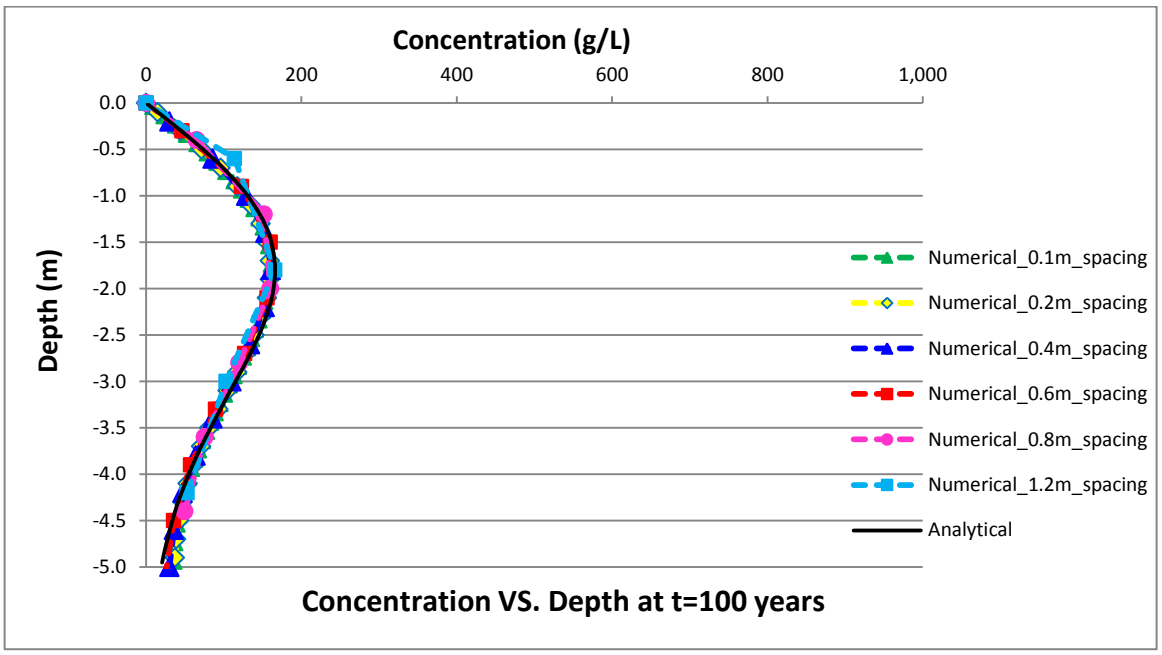

Figure 4.8 Grid discretization used for numerical simulations at times of (a) 10 years, (b) 50 years, (c) 60 years and (d) 100 years.

To illustrate the deviation more quantitatively, we use statistics method to quantify the deviation between numerical solutions and analytical solutions. In statistics, the coefficient of determination, R^2, is a number that indicates how well the data fit a statistic model. The value of R^2 ranges from 0 to 1. In this problem, R^2 is used to quantify the deviation between numerical solutions and analytical solutions, which is computed as follows:

$$R^2 = 1 - \frac{SS_{res}}{SS_{tot}}$$

where SS_{res} and SS_{tot} is defined as:

$$SS_{res} = \sum_i (y_i - f_i)^2$$

$$SS_{tot} = \sum_i (y_i - \overline{y_i})^2$$

Where $\{y_1, y_2 \dots y_n\}$ are the values of numerical solutions, $\{f_1, f_2 \dots f_n\}$ are the values of analytical solutions, n stands for the size of the comparison and $\overline{y_i}$ is the mean of the numerical data.

Table 4.2 Coefficient of determination between numerical and analytical solutions for concentration.

Time / Grid spacing	10 years	50 years	60 years	100 years
0.1 m	0.996	0.998	0.992	0.993
0.2 m	0.993	0.996	0.991	0.992
0.4 m	0.988	0.991	0.977	0.982
0.6 m	0.981	0.983	0.975	0.976
0.8 m	0.974	0.985	0.947	0.963
1.2 m	0.948	0.954	0.932	0.941

The values of R^2 at various grid spacing and times are arranged in Table 4.2. In this study, we assume that the R^2 with values higher than 0.99 indicates a good comparison between numerical and analytical results. It is observed that the value of R^2 increases with the increasing grid spacing at each year. As the values of R^2 with grid spacing of 0.1 m and 0.2 m are more than 0.99 for all the time, we conclude that the grid spacing of 0.2 m is fine enough to reproduce the main parts of the concentration profile in the aquitard for this matrix diffusion model.

4.1.4.2 Diffusive Flux

Figure 4.9 presents the numerical results for estimating the diffusive flux across the interface with different levels of grid discretization. The result shows that the numerical solutions with grid spacing of 0.1m and 0.2 m are in good qualitative agreement with the analytical solution. Moreover, it is observed that the numerical solution with coarser spatial discretization could greatly underestimate the mass flow into and out of the aquitard at very early times and immediately after the source removal,

which may be due to the fact that the numerical solution with coarse spatial discretization cannot accurately resolve the concentration gradients adjacent to the interface.

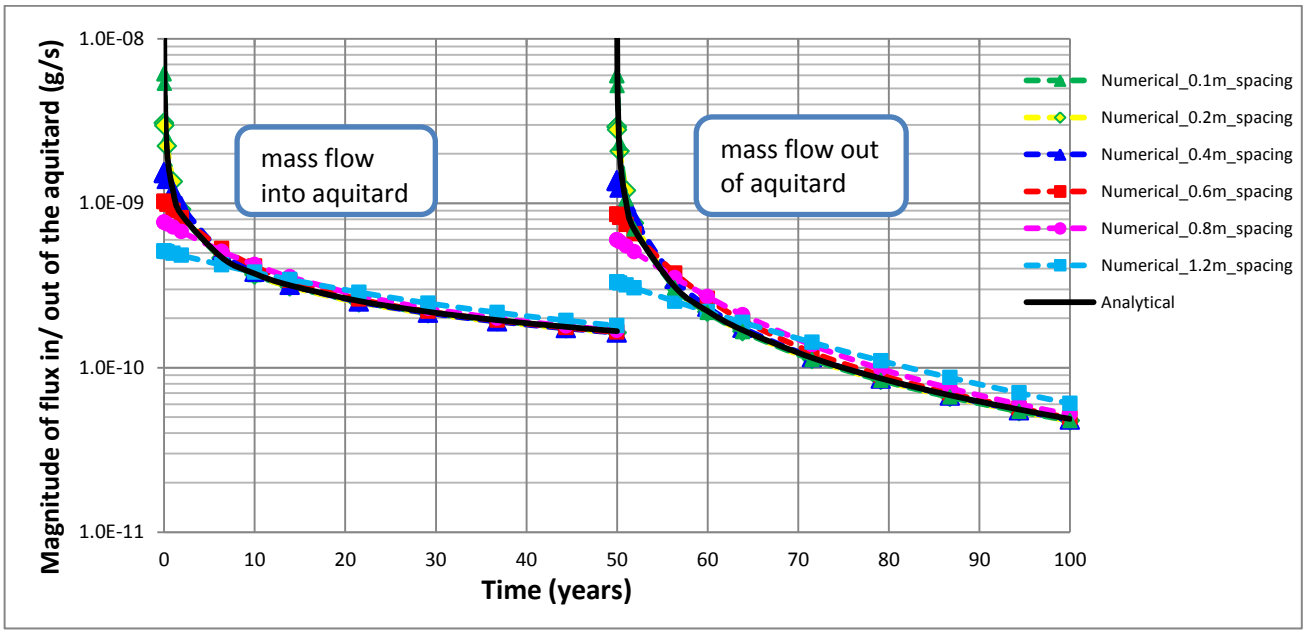

Figure 4.9 Magnitude of diffusive mass flux across the aquifer/aquitard interface with different spatial discretization.

Table 4.3 Coefficient of determination between numerical and analytical solutions for flux.

Grid spacing	R^2
0.1 m	0.995
0.2 m	0.993
0.4 m	0.984
0.6 m	0.978
0.8 m	0.967
1.2 m	0.942

To quantify the deviation between numerical solutions and analytical solutions for flux, we use same statistics method as introduced before. The values of R^2 for flux at

various grid spacing are listed in Table 4.3. It is shown that the coefficient of determination between the numerical and analytical solutions also increases with the increasing grid spacing.

4.1.4.3 TCE Mass

The numerical solution for total mass in the aqutard with different spatial discretization is compared to the exact analytical solution (Figure 4.10). The comparisons illustrate that an insufficient discretization of the elements can underestimate the total mass in the aquitard during the loading time and overestimate the total mass after removing the source. The results of coefficient of determination also show that coarser discretization can cause larger deviation between two solutions (Table 4.4). In Figure 4.10, it can be observed that the numerical solution with grid spacing of 0.1 m and 0.2 m compares extremely well with the analytical solution.

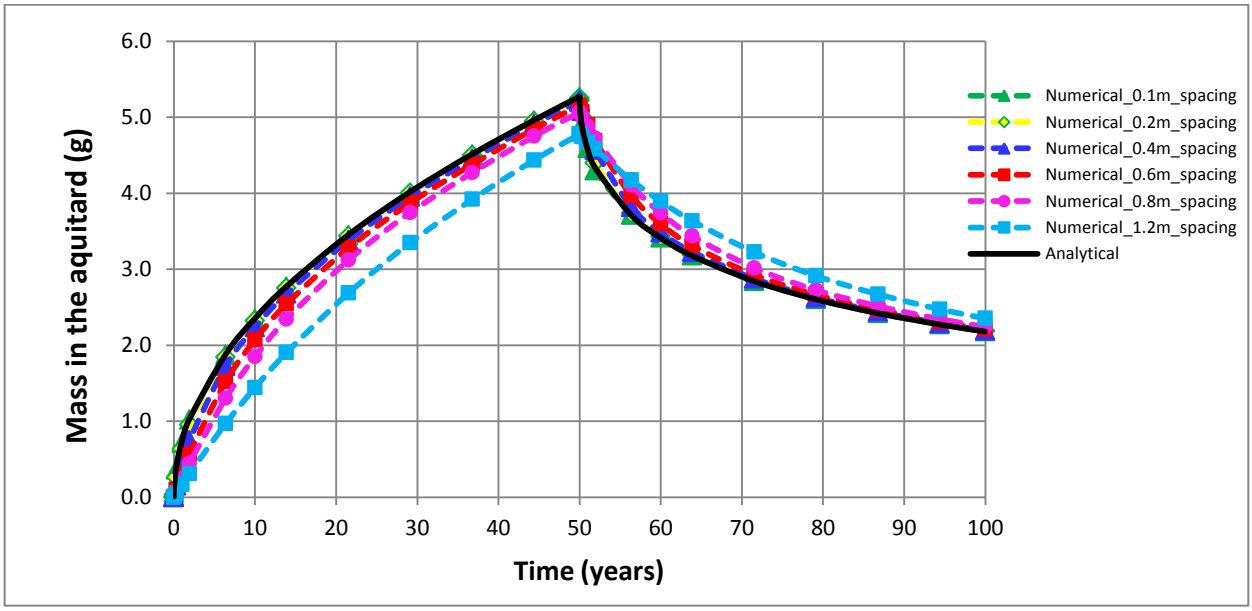

Figure 4.10 Total mass of TCE in the aquitard during numerical simulation with different spatial discretization.

Table 4.4 Coefficient of determination between numerical and analytical solutions for total mass.

Grid spacing	σ
0.1 m	0.995
0.2 m	0.992
0.4 m	0.985
0.6 m	0.978
0.8 m	0.966
1.2 m	0.942

In summary, numerical simulations with very coarse spatial discretization can cause the results to be less accurate. In this numerical model, based on grid refinement studies above, the grid spacing of 0.2 m was fine enough to accurately evaluate the dissolved concentration, diffusive flux and total mass in the aquitard.

4.2 DNAPL Pool Dissolution Model

4.2.1 Numerical Model Setup

We consider a two-dimensional, homogenous and isotropic porous medium (Figure 4.11). A very thin DNAPL pool that is denser than water forms at the top of a low permeability layer (e.g., clay) and groundwater flow is ignored in the DNAPL pool layer. The other layers above are uniform transmissive granular porous media (e.g., sand). Hydraulically, the sandy layers have active groundwater flow parallel to the layers, providing a constant groundwater velocity of 0.5 m/d. Groundwater in the low permeability layer was considered negligible. According to dispersion theory [Fried et al., 1975], the dissolution behavior of DNAPL pool was controlled by diffusion and vertical

dispersion of dissolved solvents up and away from the pool. The model was initialized as a fully water-saturated media without an unsaturated zone.

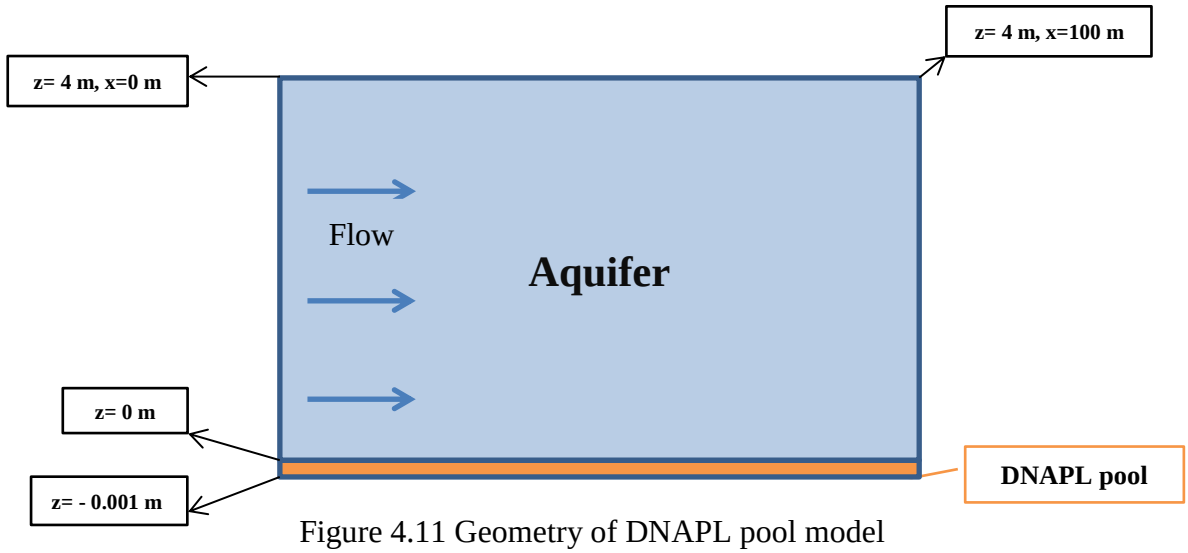

Figure 4.11 Geometry of DNAPL pool model

The domain of the numerical model was 100.0 m × 1.0 m × 4.001 m (L x W x H = x, y, z) with resolution of 10 cell in x-, 1 cell in y-, and 21 cells in z-direction, creating a 2-D model domain of 201 cells (Figure 4.12). The thickness of the DNAPL pool layer was 0.001 m and the aquifer above was discretized with grid spacing of $\Delta z = 0.2$ m and $\Delta x = 10$ m. The initial pressure was assumed to be hydrostatic pressure and clean water was flushed into the left hand side of the aquifer. A constant TCE source (S_n=0.1) was applied at the bottom DNAPL pool layer for 50 years and the right side of the model was defined as constant hydrostatic pressure boundary with zero concentration.

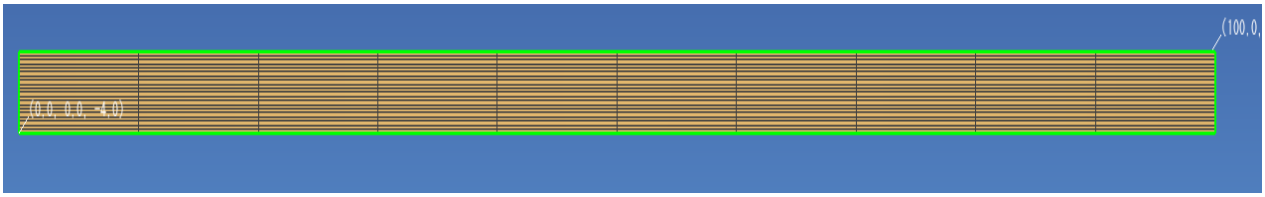

Figure 4.12 Model domain and discretization in PetraSim

In numerical model, the TMVOC code does not include the process of dispersion, therefore a new effective diffusion coefficient is applied to mimic the transverse dispersion coefficient. For constant velocity, the transverse dispersion coefficient was substituted by the product of an apparent tortuosity (τ*) and molecular diffusion coefficient.

$$D_T = \tau^* D_W \tag{4-7}$$

where the transverse dispersion coefficient is a function of the effective molecular diffusivity (τD_W) combined with a term representing mechanical dispersion ($\alpha_t v$):

$$D_T = \alpha_t v + \tau D_W \tag{4-8}$$

where α_t is transverse hydrodynamic dispersivity, v is pore water velocity.

By substituting the equation (4-8), the apparent tortuosity in aquifer can be determined as :

$$\tau^* = \tau + \frac{\alpha_t v}{D_W} \tag{4-9}$$

The input values used in the model were presented in Table 4.5.

Table 4.5 Input parameters used in DNAPL pool dissolution model.

Parameter	Aquifer	DNAPL pool
Bulk density, ρ_b (kg/m^3)	1690	1430
Permeability, k (m^2)	1E-13	1E-18
Porosity, ϕ	0.35	0.45
Tortuosity, τ	0.737	0.737
Retardation factor, R	1.73	1.48
Diffusion coefficient of TCE, D_w (m^2/s)	1.0E-9	1.0E-9
Transverse hydrodynamic dispersivity, α_t (m)	0.001	
Apparent tortuosity, τ^*	6.254	
Aqueous solubility of TCE, C_0 (mg/L)	1000	
Time-step, Δt (s)	2.4E6	

The dissolved TCE plume developed in the groundwater perpendicular to the flow direction above the pool until it reached a steady state. Figure 4.13 presents a steady-state TCE mass fraction distribution for the x, z cross-section. The vertical spreading of the dissolved TCE plume increases with the direction of groundwater flow. A corresponding vertical concentration profile at different downstream locations (x = 5 and 15 m) is shown in Figure 4.14 and both of the curves indicated that the TCE concentration decreased almost one order of magnitude with the short distance of 0.5 m above the pool. Observation of these curves reveals that dissolved concentrations at a given vertical height increased with distance from the up-gradient end of the pool.

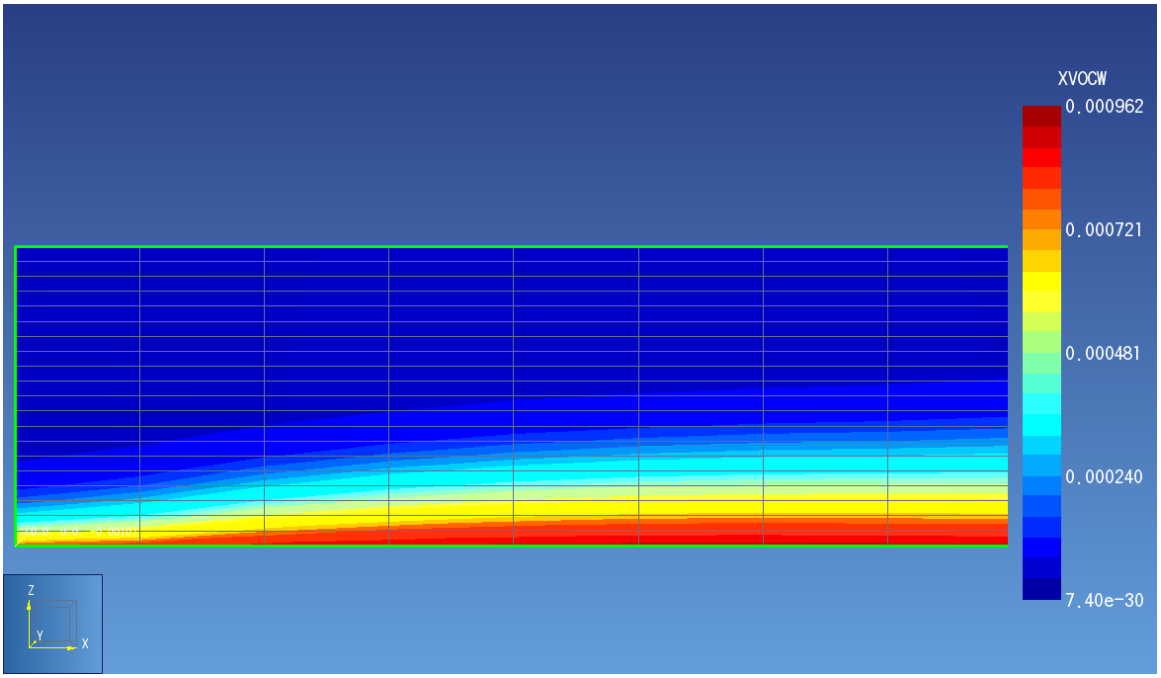

Figure 4.13 TCE mass fraction distributions in x, z plane at steady state.

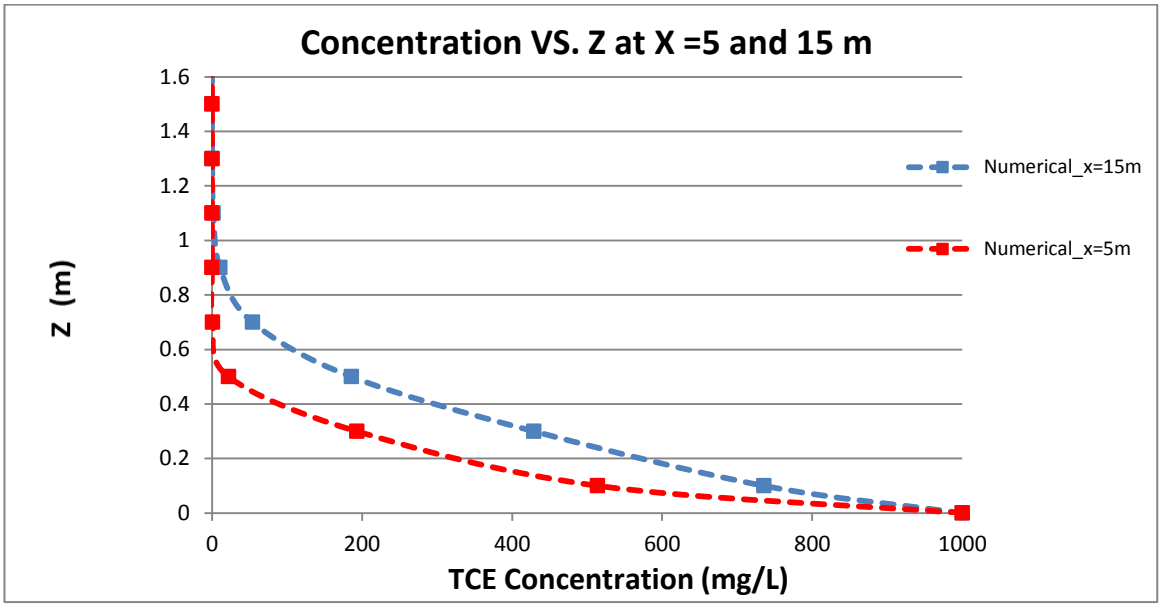

Figure 4.14 TCE concentration profiles for x = 5 and 15 m at steady state.

4.2.2 Analytical Solution

The DNAPL pool dissolution model was first proposed by Hunt et al. [1988]. The transport of dissolved DNAPL components in the saturated, isotropic porous medium can be described using the following steady-state form of the two-dimensional advection-dispersion equation.

$$v\frac{\partial C}{\partial x} = D_T\frac{\partial^2 C}{\partial z^2} \tag{4-10}$$

Equation (4-7) assumes that advective transport in the direction of groundwater flow (x) is much greater than the dispersive transport in the direction of flow; thus, longitudinal dispersion can be neglected. The boundary conditions are given below:

$C(x, z = 0) = C_0$

$C(x = 0, z) = 0$

$C(x, z = \infty) = 0$

Where C_0 is DNAPL solubility in water, z is the vertical distance from DNAPL pool, and x is the distance in direction of flow.

The transverse dispersion coefficient is a function of the effective molecular diffusivity combined with a term representing mechanical dispersion:

$$D_T = D_e + \alpha_t v$$

Where D_e is the product of the tortuosity and the aqueous molecular diffusion coefficient.

The vertical concentration profile at the downgradient edge of the pool ($x = L_p$) is then given by [Hunt et al., 1988]:

$$C_{(L_p,\ z)} = C_0 erfc\left\{\frac{z}{2\sqrt{D_t L_p / v}}\right\} \quad (4\text{-}8)$$

4.2.3 Testing

The numerical data from the pool dissolution model were tested with the steady-state mathematical solution. The comparison between the numerical simulations and analytical solutions is illustrated in Figure 4.15, showing a reasonable agreement between the two solutions.

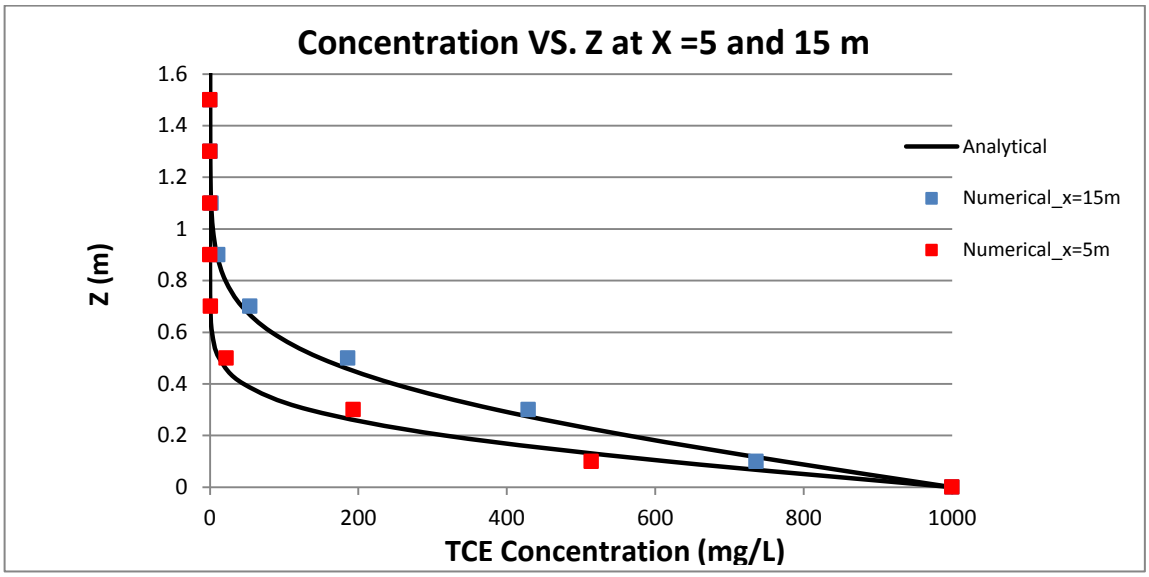

Figure 4.15 TCE concentration profiles at each location of x = 5 m and 15 m with the grid spacing of $\Delta z = 0.2$m, $\Delta x = 10$ m.

4.2.4 Grid Refinement Study

A uniform grid spacing of 0.2 m in z-direction and 10 m in x-direction was used in this model. To understand model sensitivity with respect to grid resolution, we perform additional numerical simulations with two different levels of horizontal and vertical grid discretization of $\Delta z = 0.1$ m, $\Delta x = 10$ m (Figure 4.16-a) and $\Delta z = 0.2$ m, $\Delta x = 5$ m (Figure 4.16-b).

(a)

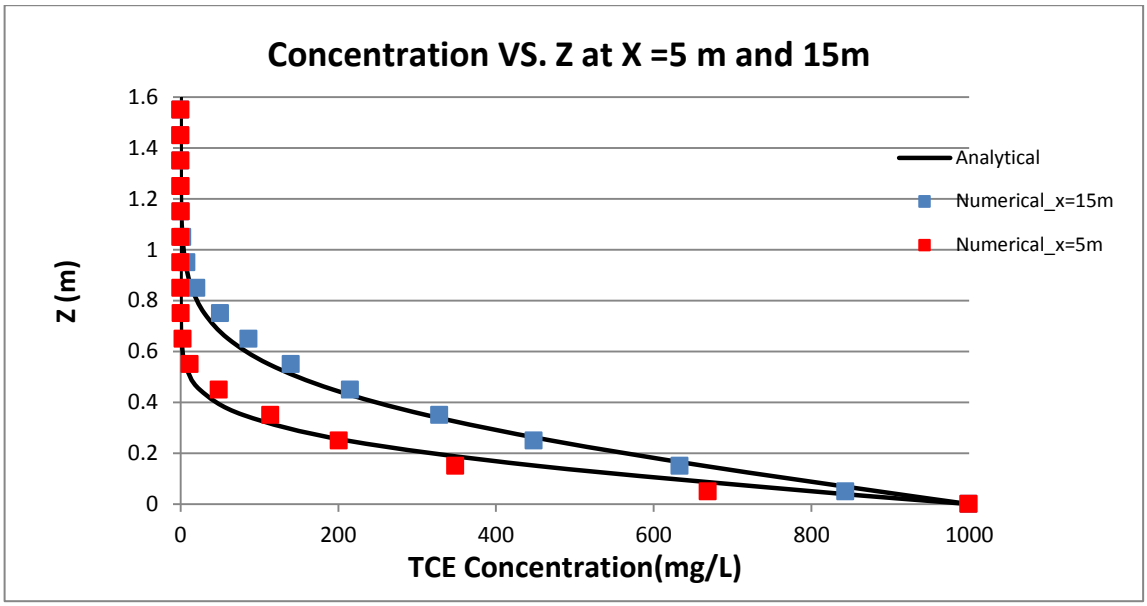

Figure 4.16a TCE concentration profiles at each location of x = 5 m and 15 m with the grid spacing of $\Delta z = 0.1$m, $\Delta x = 10$ m.

(b)

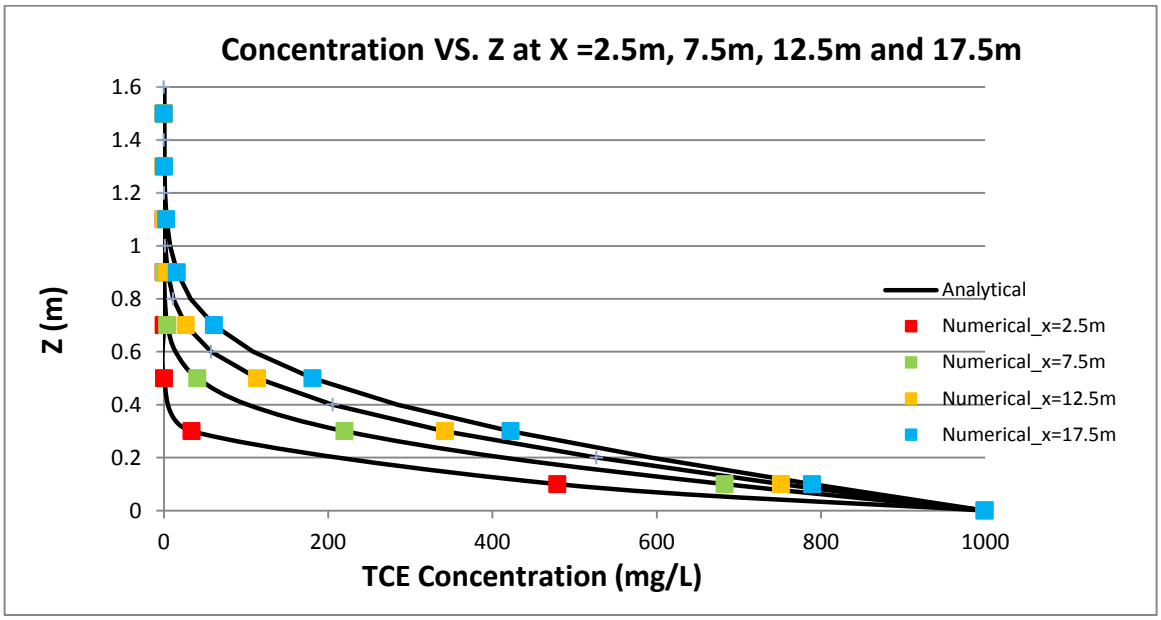

Figure 4.16b TCE concentration profiles at each location of x = 2.5 m, 7.5 m, 12.5 m and 17.5 m with the grid spacing of $\Delta z = 0.2$m, $\Delta x = 5$ m.

Table 4.6 Coefficient of determination between numerical and analytical solutions for concentration.

Grid spacing	R^2
Δz=0.2m, Δx= 10 m	0.974
Δz=0.1m, Δx= 10 m	0.978
Δz=0.2m, Δx= 5 m	0.991

The numerical solutions with finer grid spacing (0.1m) in vertical direction still shows some difference with the analytical solution (Figure 4.16-a). In Table 4.6, it is shown that the values of R^2 with grid spacing of $\Delta z = 0.1\text{m}, \Delta x = 10\text{m}$ are still less than 0.99. If only refining the grid spacing to 5m in x-direction, the numerical results shows to be much closer with analytical solution (Figure 4.16-b) and its coefficient of determination is more than 0.99, which indicates a good comparison between numerical and analytical solutions. In this grid refinement study, we can see that the grid refinement in horizontal direction plays an important role in this model, because there exists a grid dependent numerical error in the x-direction. In summary, based on the results above, the grid spacing of 0.2m in z-direction and 5m in x-direction is fine enough to accurately characterize the concentration profile in DNAPL dissolution model.

CHAPTER 5

NUMERICAL SIMULATION OF A TWO-LAYER MODEL

5.1 Introduction

A number of researchers have recognized that contaminants stored in low permeability zones can sustain plumes with adverse contaminant concentrations for a long time after the original DNAPL source is depleted [Liu and Ball, 2002; Lipson et al., 2005; Chapman and Parker, 2005; Wilking et al., 2012]. Liu and Ball [2002] observed a slow release of chlorinated solvents from an aquitard after a source removal from an overlying sand unit. Lipson et al. [2005] evaluated the influence of bedrock physical and chemical properties on the matrix diffusion process, with particular emphasis on plume attenuation at an industrial site. The author demonstrated that back diffusion from rock matrix to the open fractures could occur for a very long periods of time following the removal of DNAPL sources in fractured bedrock. Chapman and Parker [2005] employed high resolution numerical modeling methods to demonstrate that releases from low permeability zones can sustain adverse concentration in a transmissive zone for 100 years after source isolation. Wilking et al. [2012] conducted an experimental study of effects of DNAPL distribution on mass rebound and showed the persistence of the plume as a result of mass rebound from low permeability zones after DNAPL source was depleted.

The objective of this chapter is to develop an idealized two-layer numerical model to simulate matrix diffusion of dissolved TCE between an aquifer and an aquitard. The accuracy of numerical model for the two-layer scenario can be validated with the Dandy-Sale Model [Sale et al., 2008].

5.2 Dandy-Sale Model

Sale et al. [2008] developed an exact 2-D analytical solution to estimate the distribution of aqueous and sorbed phase in transmissive and low permeability zones as a function of time. The conceptual frame work of the two-layer scenario is shown in Figure 5.1. The transmissive layer is situated above the low permeability layer. The DNAPL source existed upgradient at the contact of the two layers, which was active first and then removed after a certain time. Primary assumptions were made as follows: (1) the transmissive and low permeability layers were uniform, homogeneous, isotropic and infinite in $z \rightarrow \infty$ (transimissive layer) and $z \rightarrow -\infty$ (low permeability layer); (2) the lateral transport in the transimissive layer was dominated by advection such that longitudinal dispersion can be neglected; (3) the hydraulic conductivity in the low permeability layer was sufficiently low that the solute transport within that layer would occur only by molecular diffusion; (4) no degradation was considered in either layer.

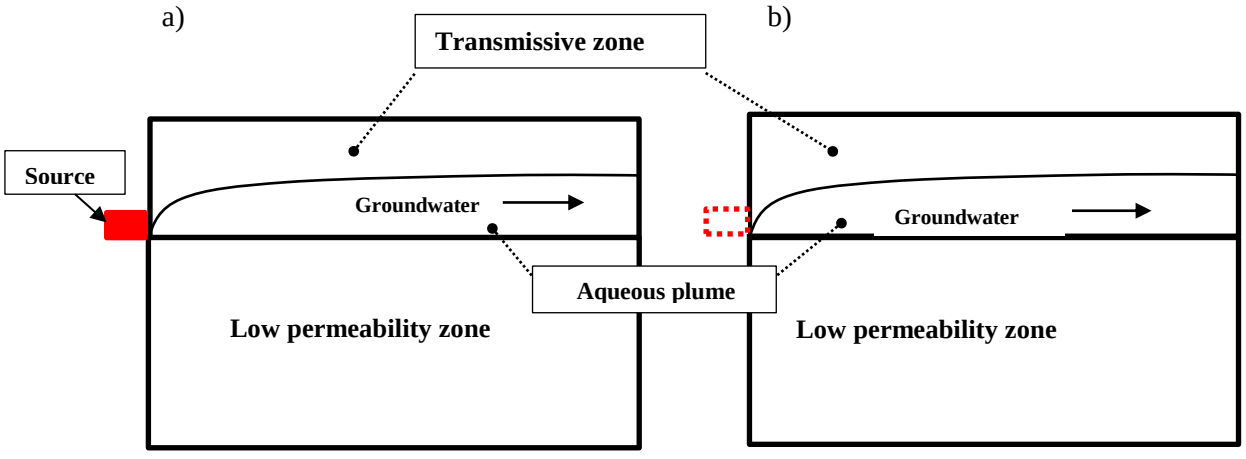

Figure 5.1 The two-layer scenario conceptual model: (a) Active source (b) Depleted source

These simplifications reduced the two-layer system to a two-dimensional domain with a single velocity component. Equations governing solute transport were described for each layer due to their differences in hydraulic conductivity and porosity.

In the transmissive layer, the transient solute transport is described by the advection-dispersion equation:

$$R\,\frac{\partial C}{\partial t} = -v_x \frac{\partial C}{\partial x} + D_T \frac{\partial^2 C}{\partial z^2} \tag{5-1}$$

In the low permeability zone, the solute transport was described by an equation similar to equation (5-1), but without advection.

$$R\frac{\partial C(x,t)}{\partial t} = \mathrm{D}^* \frac{\partial^2 C(x,t)}{\partial z^2} \tag{5-4}$$

The initial and boundary conditions are given below:

$$C(x,z,0) = 0 \qquad (\mathrm{z} \geq 0)$$

$$C'(x,z,0) = 0 \qquad (-\infty \leq z < 0)$$

$$C(x, z \to \infty, t) = 0$$

$$C'(x, z \to -\infty, t) = 0$$

$$C(x,0,t) = C'(x,0,t)$$

$$\phi D_T \frac{\partial C}{\partial z}(x,0,t) = \phi D^* \frac{\partial C'}{\partial z}(x,0,t)$$

where $C(x,z,t)$, ϕ and D_T are the solute concentration, porosity and transverse dispersion coefficient in the transmissive layer and $C'(x,z,t)$, ϕ' and D^* are the solute concentration, porosity and effective molecular diffusion coefficient in low permeability layer, respectively.

The source occurs in the transmissive layer at the upstream model boundary. It drops exponentially with increasing vertical distance from the interface into the transmissive layer (Figure 5.2). This source configuration is intended to create a source that is similar to a thin pool of DNAPL, which is used as a boundary condition in the Dandy-Sale model. The aqueous concentration associated with the source is mathematically modeled as:

$$\mathrm{C}(0,\mathrm{z},\mathrm{t}) = C_0 e^{-\frac{z}{2}\sqrt{\frac{v\pi}{LD_T}}}[1 - H(t - t_1)] \qquad (z \geq 0) \qquad (5\text{-}5)$$

Where C_0 is the aqueous concentration at x=0, z=0, v the water is pore velocity in the longitudinal direction, D_T is the transverse dispersion coefficient in the vertical direction, L is the length of DNAPL source zone located upstream of the model, t_1 is the persistence time of the source and H is the Heaviside step function, such that:

$$\mathrm{H}(\mathrm{t} - t_1) = \begin{cases} 0, & if\ t \leq t_1 \\ 1, & if\ t > t_1 \end{cases}$$

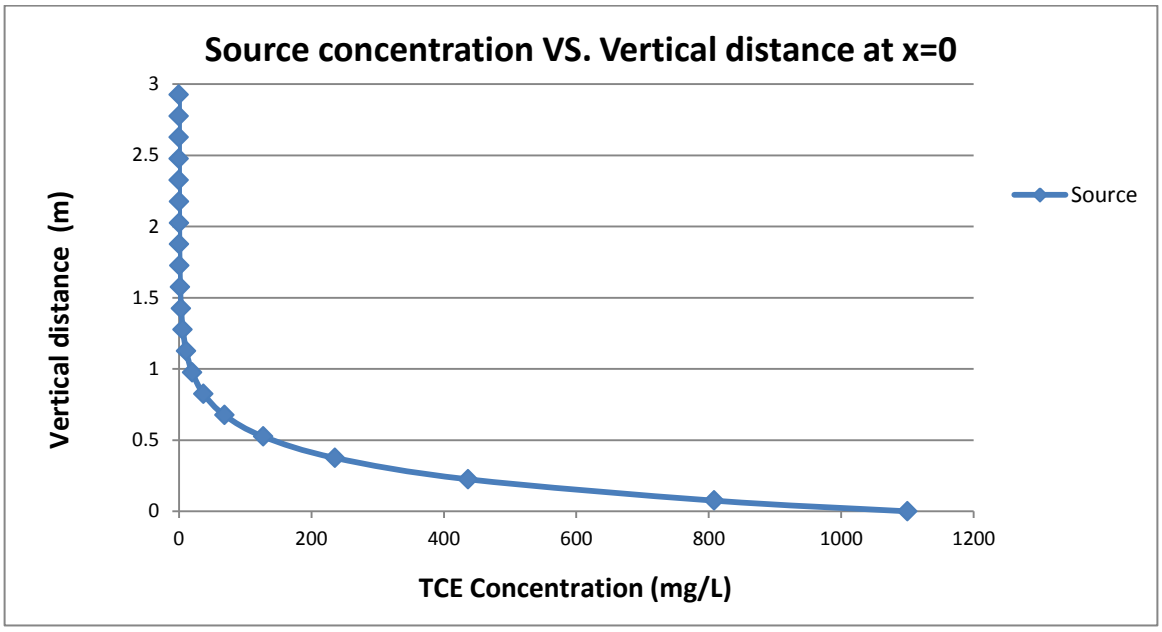

Figure 5.2 Source concentrations as a function of vertical distance from the interface into the transmissive layer, used as the upstream boundary condition in the Dandy-Sale model.

The analytical solution of contaminant concentrations in the transmissive and low permeability layer at a desired location and time are given as [Sale et al., 2008]:

$$C_{trans.}(x,z,t) = C_0\left[\frac{1}{2}e^{\frac{b^2x}{\emptyset}}\left[e^{bz}erfc\left(\frac{b}{\emptyset}\sqrt{x}+\frac{\emptyset z}{2\sqrt{x}}\right)+e^{-bz}+e^{-bz}erfc\left(\frac{-b}{\emptyset}\sqrt{x}+\frac{\emptyset z}{2\sqrt{x}}\right)\right]+\right.$$

$$\left.\frac{-\emptyset\gamma}{\pi}e^{bz}\sqrt{t-\frac{x}{v_c}}\int_0^x\frac{e^{\frac{b^2\xi}{\emptyset}}}{\sqrt{x-\xi}}\left(\frac{erfc\left(\frac{b}{\emptyset}\sqrt{\xi}+\frac{\emptyset z}{2\sqrt{\xi}}\right)}{\gamma^2(x-\xi)+\emptyset^2(t-\frac{x}{v_c})}\right)d\xi\right] \quad (5\text{-}6)$$

Where $\emptyset$, γ, v_c and b are defined as:

$$\emptyset = \sqrt{\frac{v}{D_T}} \quad (5\text{-}7)$$

$$\gamma = \frac{n'\sqrt{R'D^*}}{nD_T} \quad (5\text{-}8)$$

$$\mathrm{b} = \frac{1}{2}\sqrt{\frac{v\pi}{LD_T}} \tag{5-9}$$

and R and R' are retardation factors of the transmissive and low permeability layer, respectively.

$$C_{low\ k.}(x,z,t) = C_0\left[\frac{1}{\sqrt{\pi}}\int_0^x \frac{I_1(x,z,t,\xi)}{\sqrt{x-\xi}}\left[\frac{1}{\sqrt{\pi\xi}} - \frac{b}{\emptyset}e^{\frac{b^2\xi}{\emptyset}}erfc\left(\frac{b}{\emptyset}\sqrt{\xi}\right)\right]d\xi\right] \tag{5-10}$$

where,

$$I_1(x,z,t,\xi) = \mathrm{erfc}\left(\frac{\frac{z}{\sqrt{\frac{D^*}{R'}}}}{2\sqrt{t-\frac{x}{v_c}}}\right) - \gamma\frac{\mathrm{erfc}\left(\frac{\frac{\gamma z}{\sqrt{\frac{D^*}{R'}}}}{2(t-\frac{x}{v_c})\sqrt{\frac{\gamma^2}{t-\frac{x}{v_c}}+\frac{\emptyset^2}{x-\xi}}}\right)}{\sqrt{t-\frac{x}{v_c}}\sqrt{\frac{\gamma^2}{t-\frac{x}{v_c}}+\frac{\emptyset^2}{x-\xi}}exp\left[\frac{\frac{\emptyset^2 z^2}{\frac{D^*}{R'}}}{4[\gamma^2(x-\xi)+\emptyset^2\left(t-\frac{x}{v_c}\right)]}\right]} \tag{5-11}$$

The Dandy-Sale model has been programmed in the Matrix Diffusion Toolkit [2012], which can solve the Dandy-Sale analytical solutions in less than 5 minutes. Based on the Microsoft Excel platform, the Matrix Diffusion Toolkit is an easy-to-use software tool for estimating concentration both in the tramsmissive zone and low permeability zone. Furthermore, this software can provide planning-level estimates of mass discharge in the tramsmissive zone.

5.3 Numerical Model Setup

To compare with the Dandy-Sale model, we consider a two-dimensional, vertically oriented, two-layer system (Figure 5.3). Hydraulically, the transmissive layer had active groundwater flow parallel to the layers while groundwater in the low

permeability layer was considered negligible. The model was initialized as a fully water-saturated media without an unsaturated zone.

The mesh size of the numerical model was 250.0 m × 40.0 m × 9.0 m (L x W x H = x, y, z) with resolution of 250 cell in x-, 1 cell in y-, and 60 cells in z-direction, creating a 2-D model domain of 15000 cells. The domain was discretized with grid spacing of $\Delta x = 1\text{m}$ and $\Delta z = 0.15\text{m}$. The thickness of the transmissive and low permeability zones were 3m and 6 m respectively. It was assumed that the solute plume did not contact the vertical boundaries of the domain, which were defined as no-flow boundaries. The initial pressure was assumed to be hydrostatic pressure. The DNAPL source at the upstream boundary was intended to create a boundary layer coming to the transmissive zone. The right side column of the transmissive zone was defined as constant hydrostatic pressure boundary and was fixed at zero concentration.

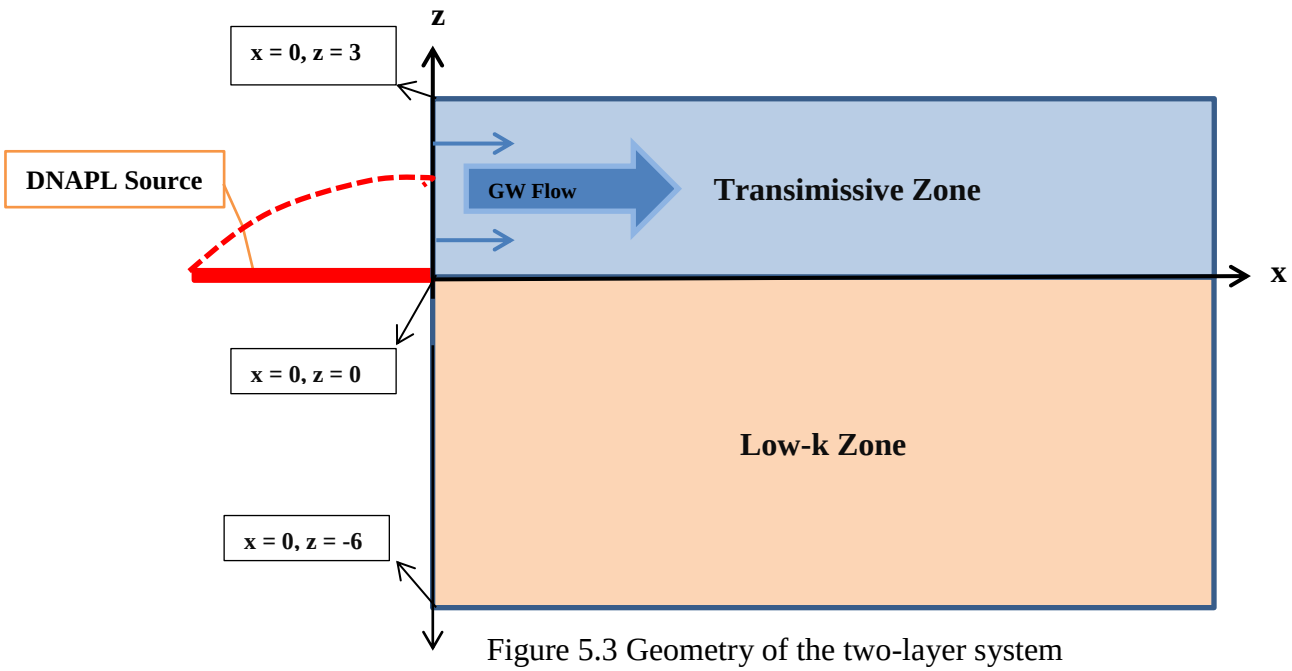

Figure 5.3 Geometry of the two-layer system

In this study, the source (equation 5-5) occurred in the upstream of the model domain, which was active for 50 years (t_1) then shut completely off allowing clean water to flush through the transimissive layer for additional 50 years. The conceptual numerical model for the two-layer scenario was consistent with the Dandy-Sale Model (Figure 5.1).

The solute transport of dissolved contaminant in the two-layer system was assumed to undergo three important types of mechanisms, including advection, dispersion and molecular diffusion. No degradation was considered in either layer. Advection and dispersion dominated groundwater flow and contaminant transport in transmissive layer while molecular diffusion was the only transport mechanism considered in low permeability layer due to its low hydraulic conductivity.

In numerical simulation, as discussed before (Chapter 4), as TMVOC does not account for dispersion, the transverse dispersion coefficient was substituted by the product of tortuosity and molecular diffusion coefficient. The apparent tortuosity of the aquifer can be determined as:

$$\tau^* = \tau + \frac{\alpha_t v}{D_W}$$

This results in a constant and isotropic dispersion coefficient. It is slightly different than the Dandy-Sale model which assumes zero longitudinal dispersion. The input values used in this numerical model are consistent with values used for the Dandy-Sale model in Matrix Diffusion Toolkit [2012].

Table 5.1 Input parameters used in the two-layer model.

Parameter	Transmissive zone	Low permeability zone
Bulk density,ρ_b (kg/m^3)	1700	1500
Permeability, k (m^2)	1E-13	1E-18
Porosity, ϕ	0.35	0.45
Tortuosity, τ	0.707	0.715
Retardation factor, R	1.17	1.17
Pore velocity, v (m/d)	0.37	0
Diffusion coefficient of TCE, D_w (m^2/s)	9.1E-10	9.1E-10
Transverse hydrodynamic dispersivity, α_t (m)	0.001	
Apparent tortuosity, τ^*	5.41	
Aqueous solubility of TCE, C_0 (mg/L)	1100	
Time-step, Δt (s)	1.0E8	

5.4 Results

The contaminant plume developed with the groundwater flow through the domain. Figure 5.4 presents TCE mass fraction distribution for the x, z cross-section with the active source at different times and the dashed line indicates the interface between the two layers. It was clearly observed that the dissolved TCE plume evolved in the down-gradient direction until it reached the boundary. Due to the mechanisms of molecular diffusion and vertical dispersion, the plume continued to expand in the vertical direction until the source was removed.

(a)

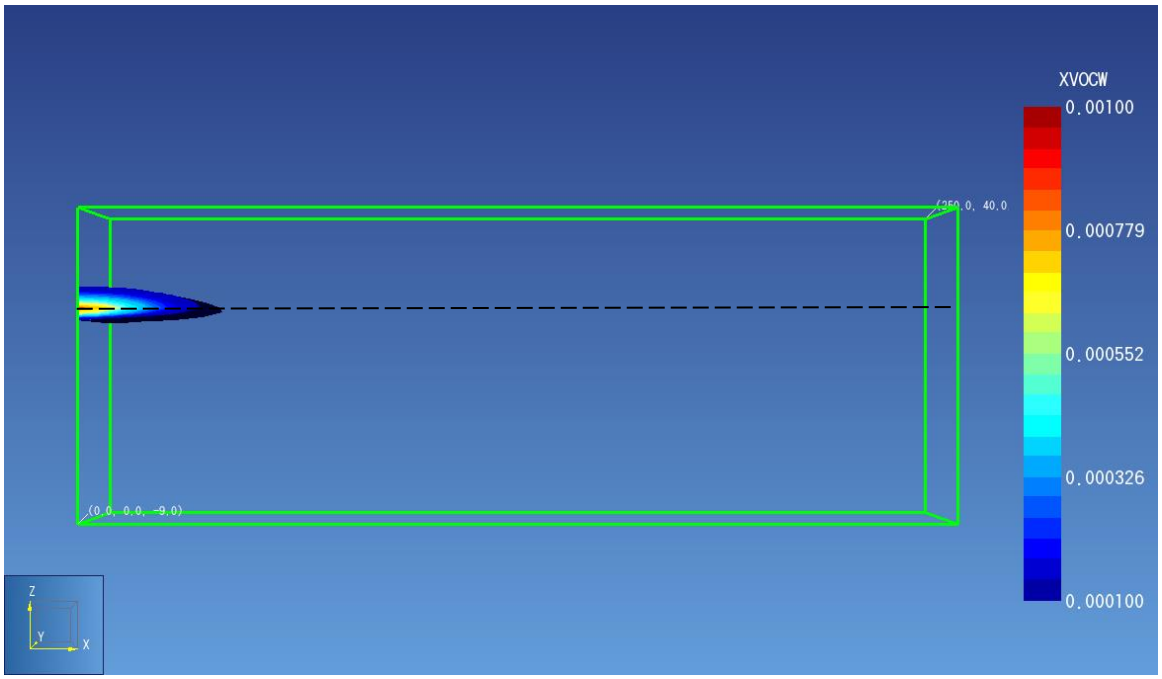
XVOCW
0.00100
0.000779
0.000552
0.000326
0.000100
(0.0, 0.0, -9.0)
Z
Y
X

(b)

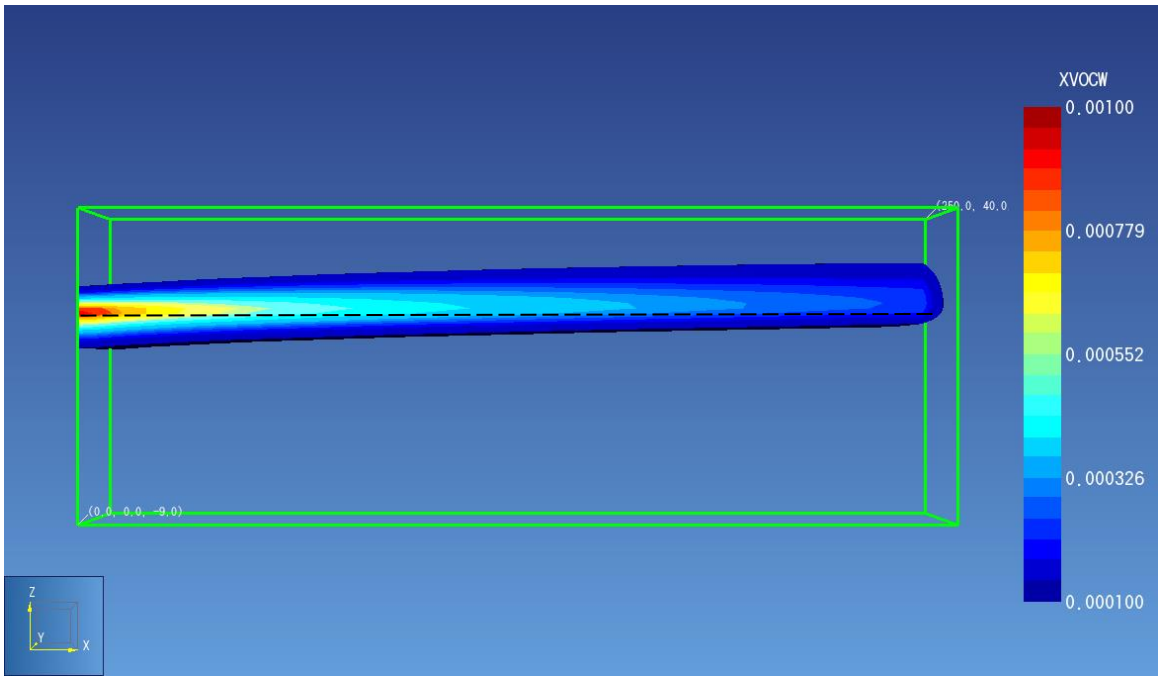
XVOCW
0.00100
0.000779
0.000552
0.000326
0.000100
(0.0, 0.0, -9.0)
Z
Y
X

(c)

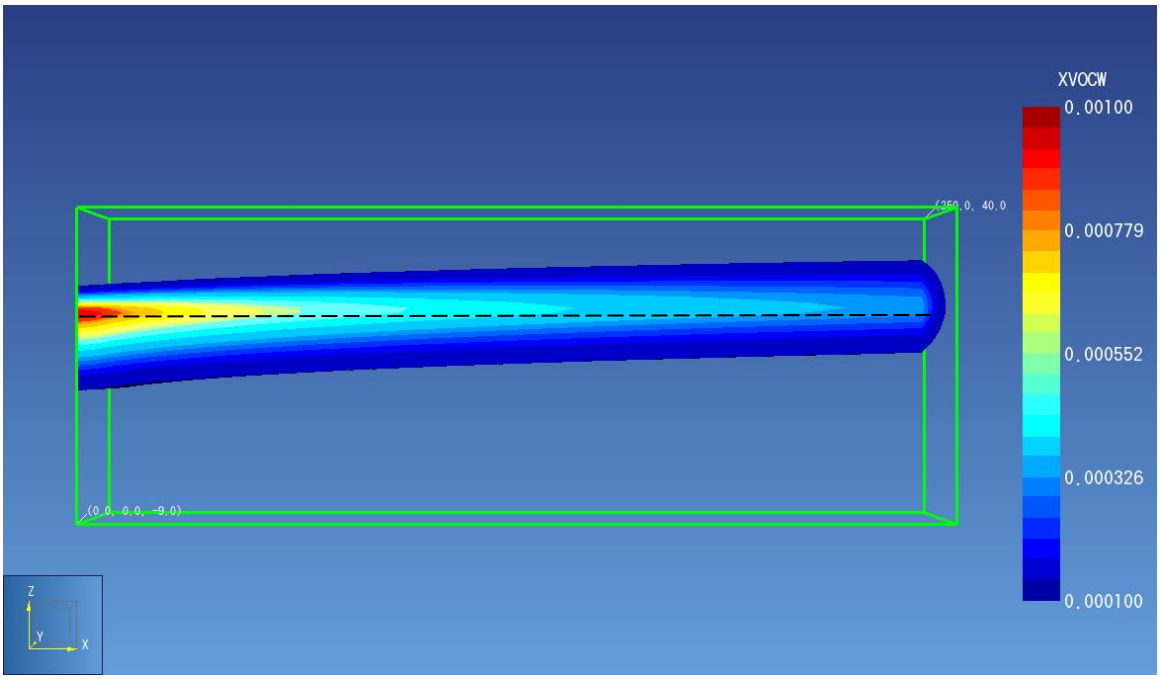

Figure 5.4 Distribution of TCE mass fractions in x, z plane for active source scenario at times of (a) 100 days, (b) 3 years and (c) 50 years.

During the unloading period, the entire source at $x < 0$ was removed allowing clean water to flush through the transmissive layer for another 50 years. Figure 5.5 shows the TCE mass fraction distribution without source at times of 51 years, 60 years and 100 years. Flushing in the transmissive layer caused the contaminant plume to shrink from the up-gradient edge of plume and it was also observed that the TCE mass fraction decreased by orders of magnitude with plume recession. However, the low permeability zones still remained contaminated after 100 years (Figure 5.5-d).

(a)

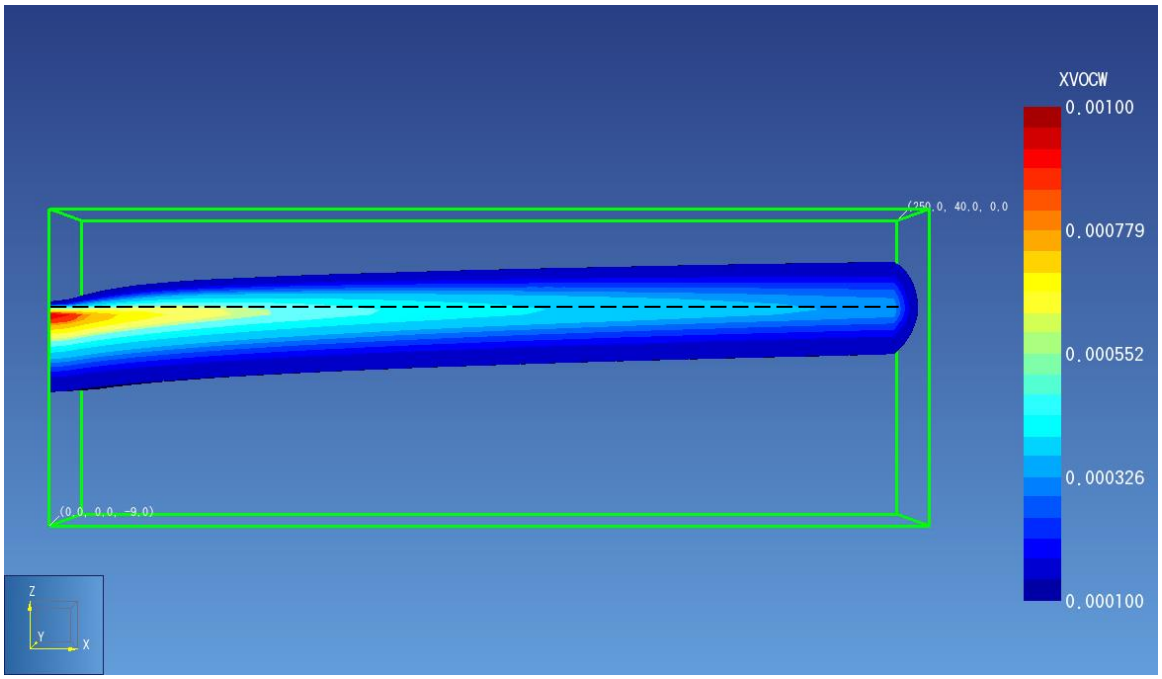
XVOCW
0.00100
0.000779
0.000552
0.000326
0.000100
(250.0, 40.0, 0.0
(0.0, 0.0, -9.0)
Z
Y
X

(b)

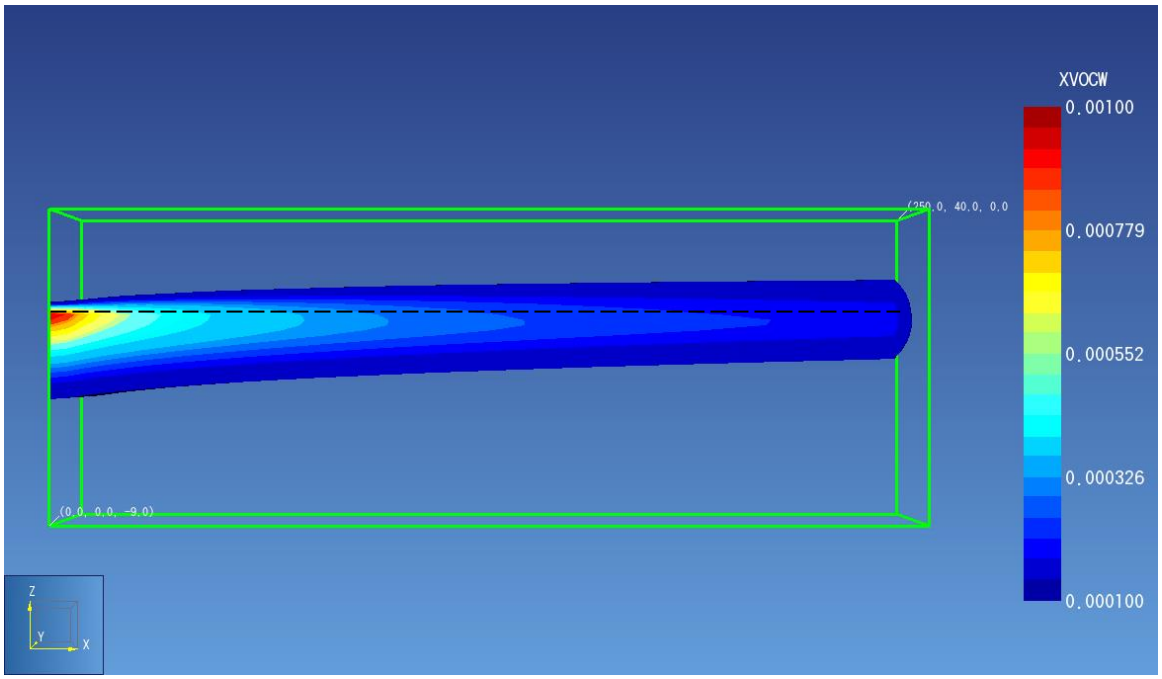
XVOCW
0.00100
0.000779
0.000552
0.000326
0.000100
(250.0, 40.0, 0.0
(0.0, 0.0, -9.0)
Z
Y
X

(c)

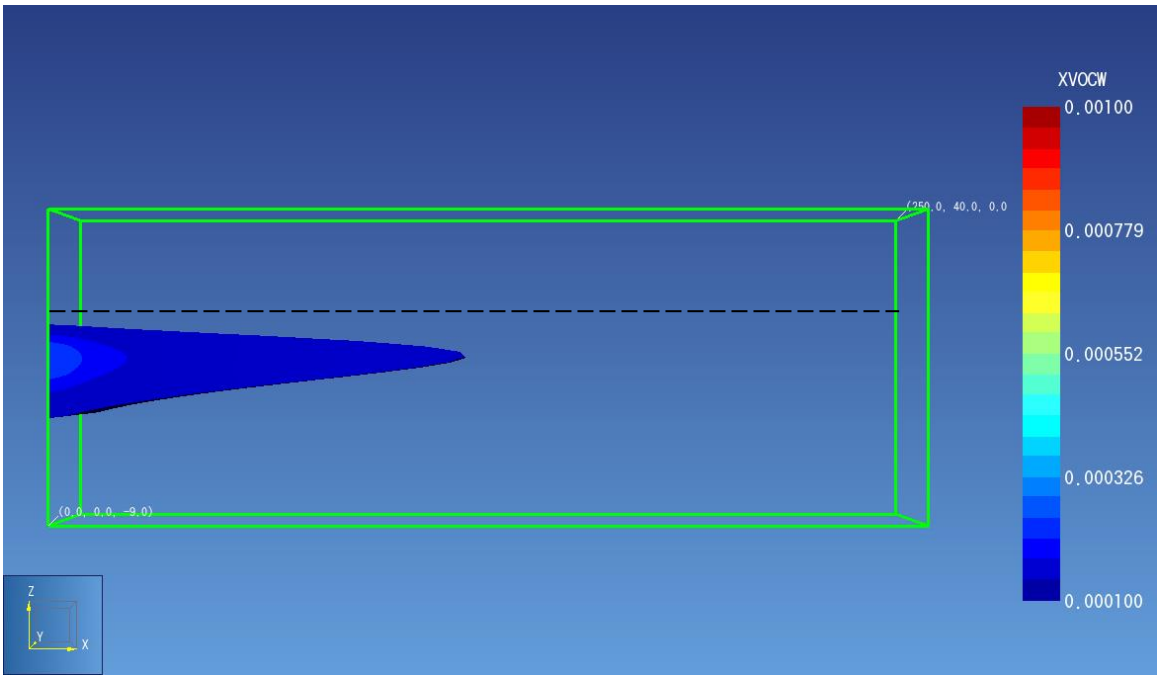

Figure 5.5 Distribution of TCE mass fractions in x, z plane for depleted source scenario at times of (a) 51 years, (b) 60 years and (c) 100 years.

To illustrate the process of back diffusion, several line plots for the TCE concentration at x = 2.5 m for different times were created (Figure 5.6). In the scenario of an active source, the maximum concentration of contaminant was observed at the interface between the two layers (Figure 5.6-b). After the source was depleted, the concentration gradient at the interface was reversed as the clean water flushed through the transmissive layer. Therefore, the contaminant mass stored in low permeability layer began to diffuse slowly back into the transmissive layer. In Figures 5.6-c, d, it was observed that the maximum TCE concentration decreased sharply after removing the source and the position where maximum TCE concentration occurred moved downward from the interface to a depth of 1.5 m below the interface.

(a) 10 years

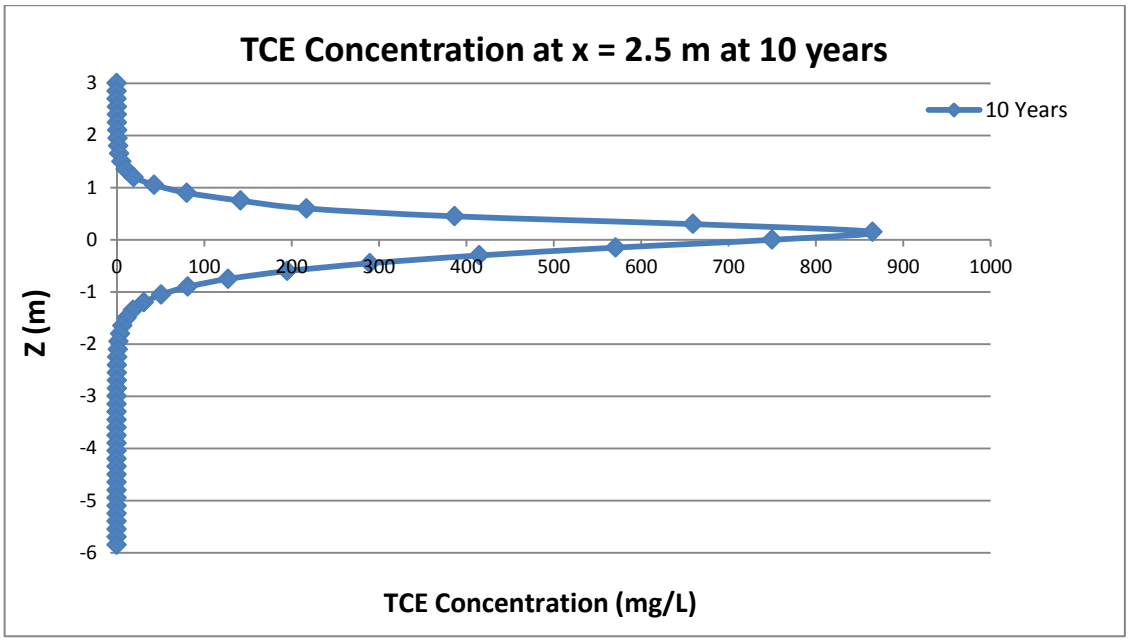

(b) 50 years

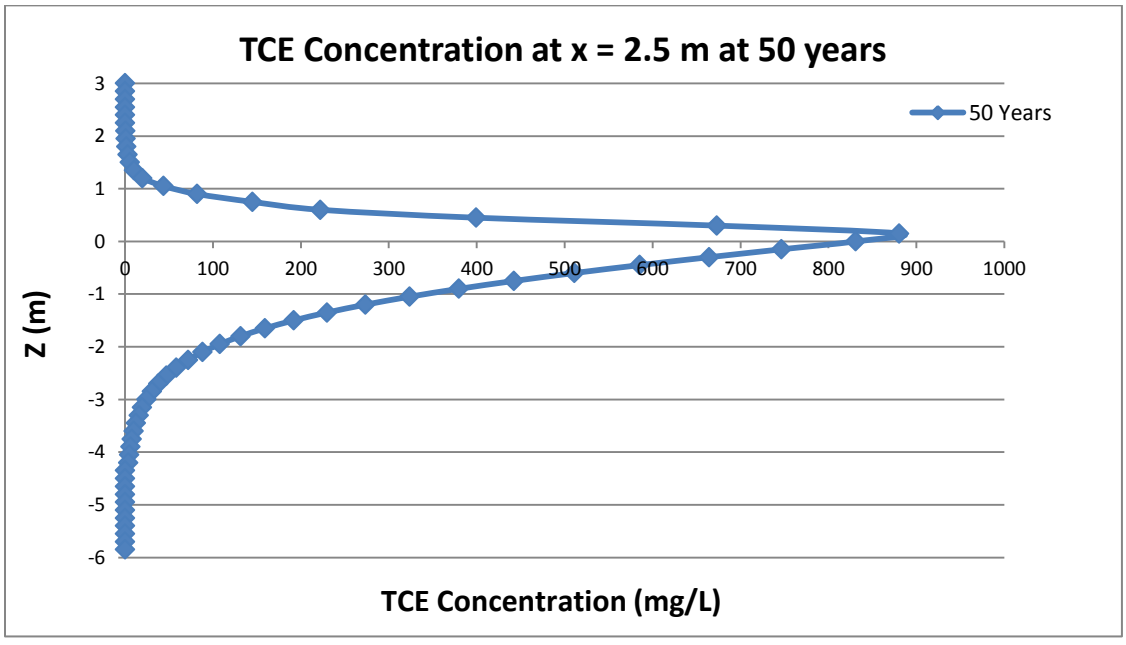

(c) 60 years

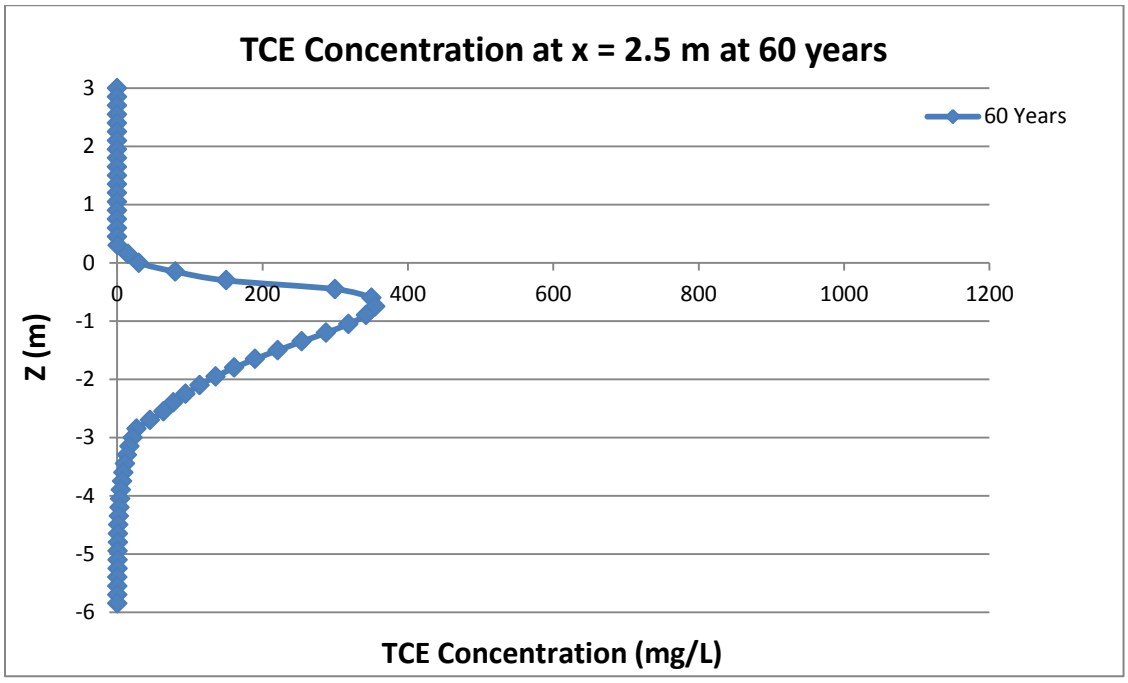

(d) 100 years

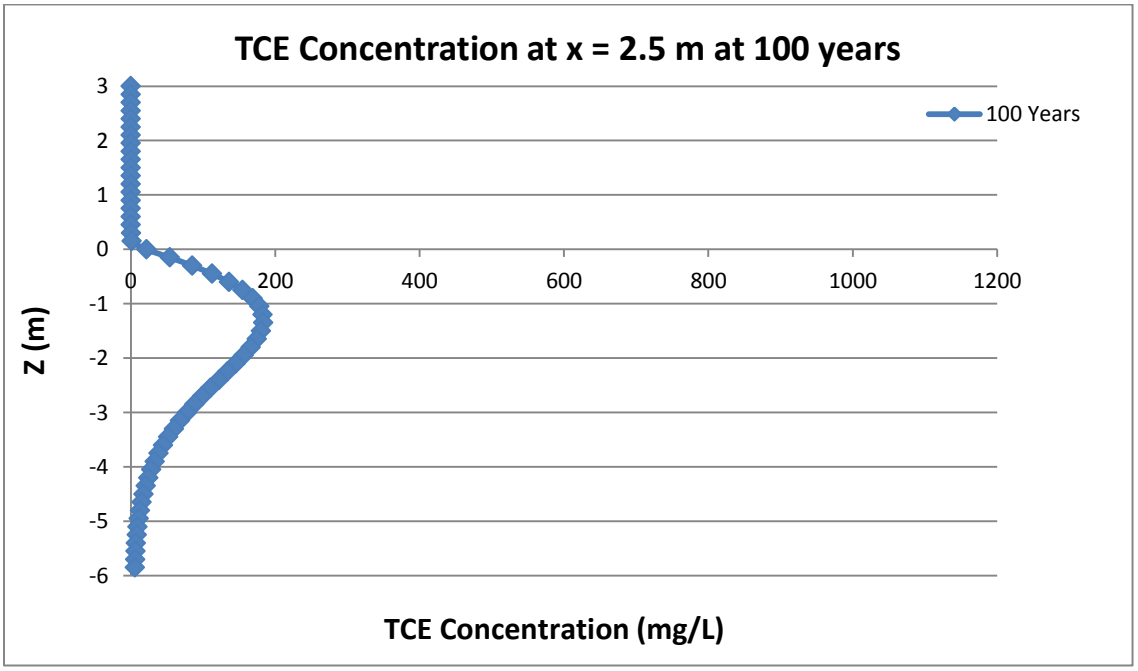

Figure 5.6 Line plots for the TCE concentration at x = 2.5 m at times of: (a) 10 years, (b) 50 years, (c) 60 years and (d) 100 years.

A corresponding TCE concentration profile in the low permeability layer at x = 2.5 m is shown in Figure 5.7. In the first 50 years, the TCE concentration decreased with depth into the low permeability layer. After removing the source, the TCE concentration at the interface was almost instantaneously reduced to zero, and therefore caused matrix diffusion back from the low permeability layer to the transmissive layer. The curves for t = 100 years revealed that the dissolved TCE concentration increased with depth into the low permeability layer until reaching its maximum value at z = -1.5 m, and then started to decrease with depth.

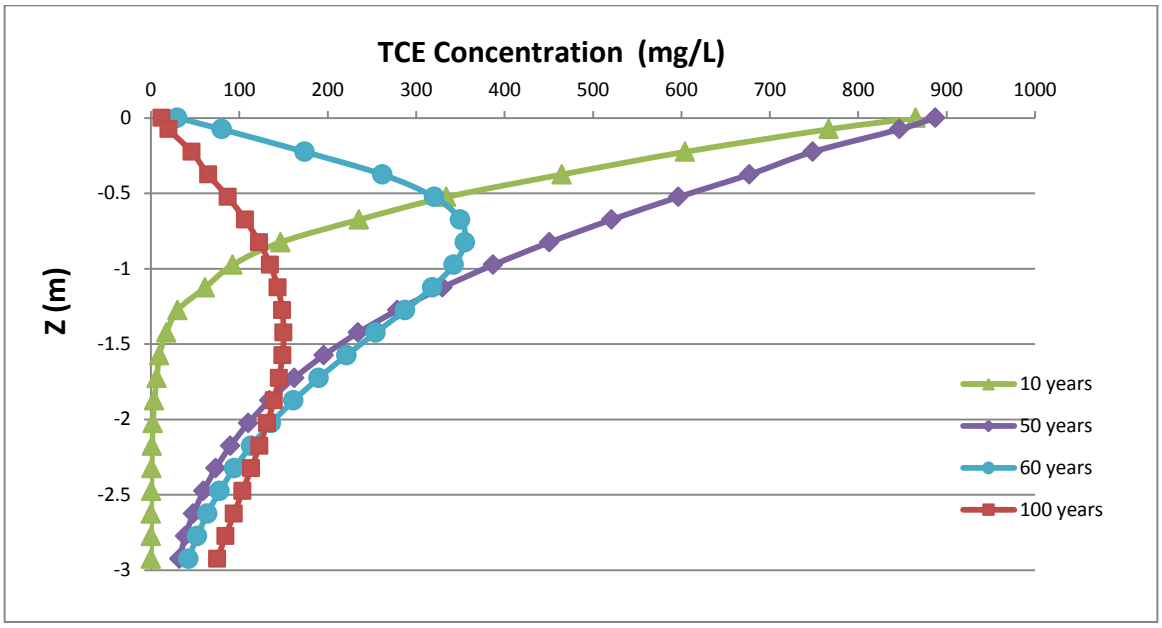

Figure 5.7 TCE concentration profiles in the low-k layer at x = 2.5 m for t = 10, 50, 60 and 100 years

5.5 Testing

The numerical solution was verified against the analytical solutions (equations 5-10 and 5-11) in Dandy-Sale Model [Sale et al., 2008]. In both models, the DNAPL source

was active on for 50 years and off for another 50 years and all the input parameters were set to be the same.

5.5.1 TCE Concentration in the Transmissive Layer

The concentration profiles in the transmissive layer as a function of lateral distance from the source at the times of 10, 50, 60 and 100 years are presented in Figure 5.8. The concentration is calculated by assuming a 10-foot (3 m) screened interval as is done in the Matrix Diffusion Toolkit [2012]. The 10-foot screened interval was selected because contamination diffusing from a low permeability zone might not spread vertically above 10 feet at actual field site [Matrix Diffusion Toolkit, 2012]. In the models, the concentrations over the bottom 10feet of the aquifer are averaged to get the well concentration.

(a)

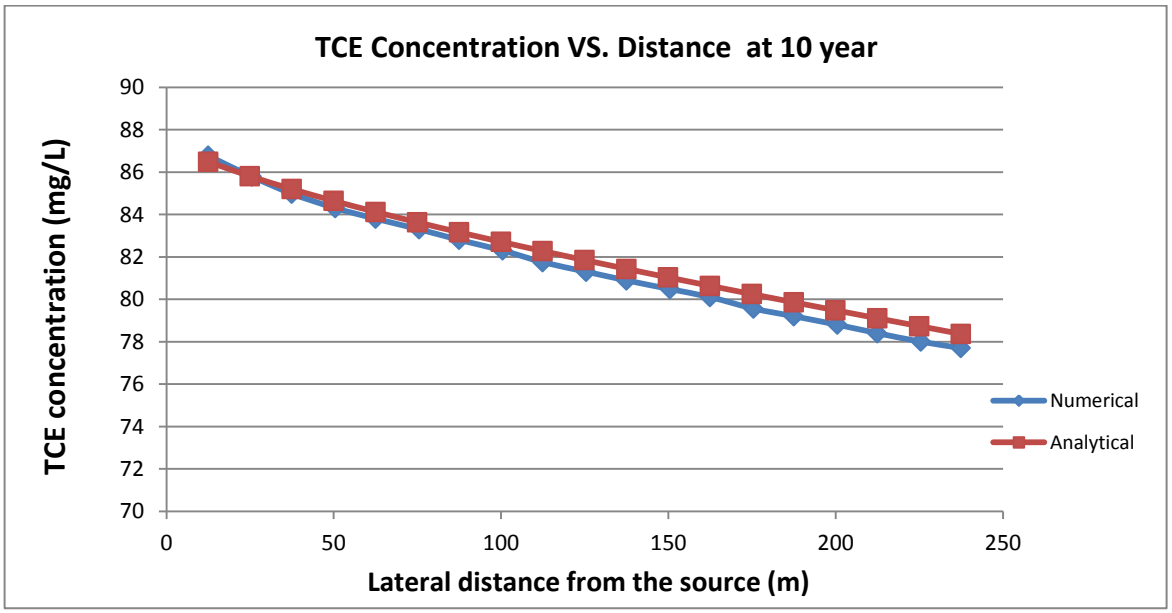

(b)

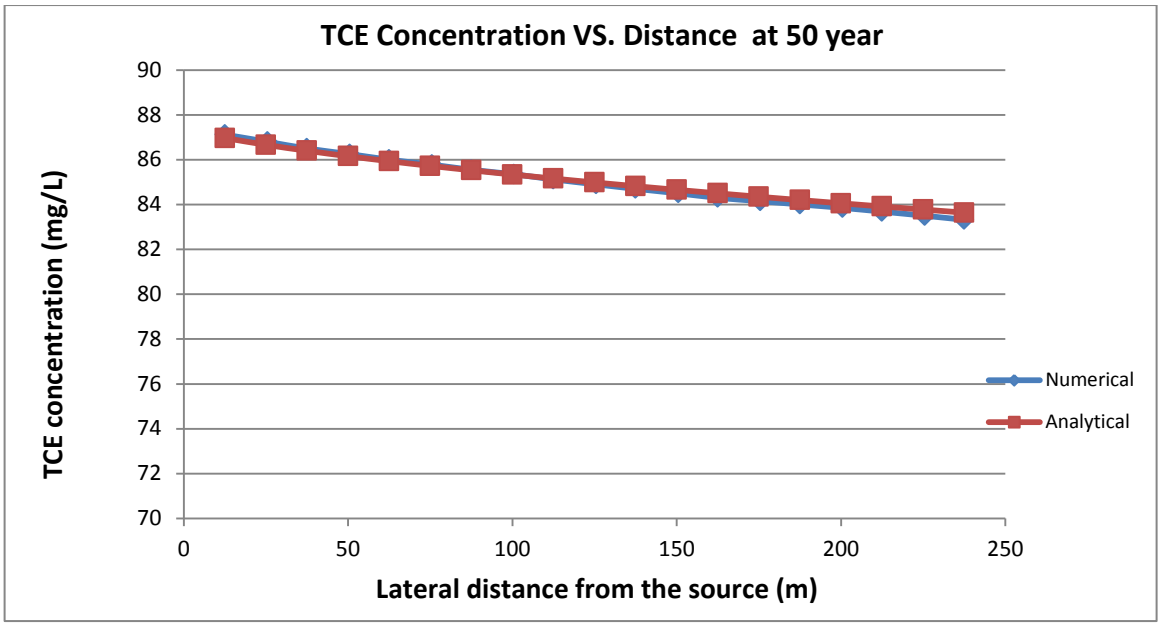
TCE Concentration VS. Distance at 50 year
TCE concentration (mg/L)
90
88
86
84
82
80
78
76
74
72
70
0
50
100
150
200
250
Lateral distance from the source (m)
Numerical
Analytical

(c)

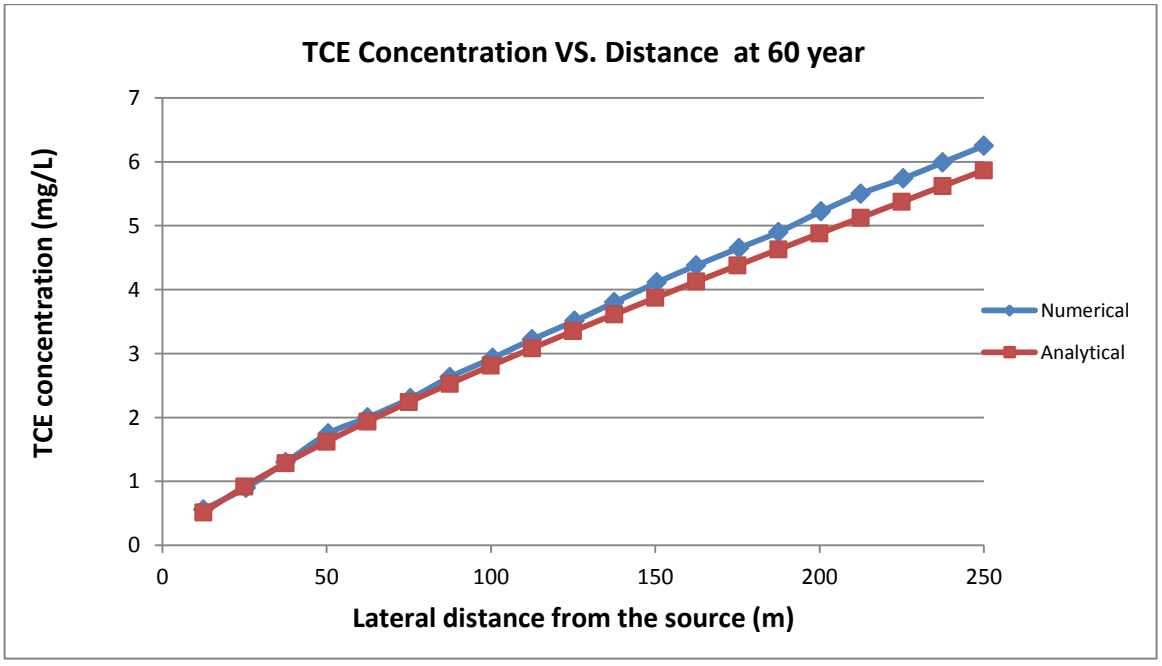
TCE Concentration VS. Distance at 60 year
TCE concentration (mg/L)
7
6
5
4
3
2
1
0
0
50
100
150
200
250
Lateral distance from the source (m)
Numerical
Analytical

(d)

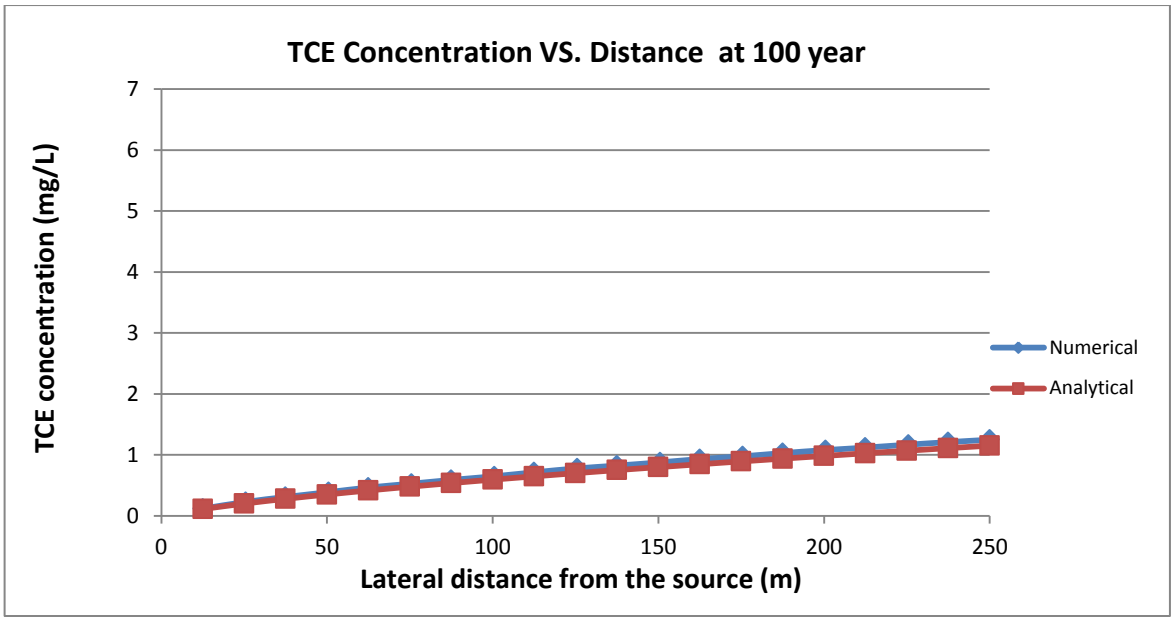

Figure 5.8 TCE concentration profiles in the transmissive layer at the times of: (a) 10 years, (b) 50 years, (c) 60 years and (d) 100 years.

Table 5.2 Coefficient of determination between numerical and analytical solutions for concentration in the aquifer at different times.

Time	R^2
10 years	0.993
50 years	0.995
60 years	0.972
100 years	0.952

The coefficient of determination between two solutions at different years is presented in Table 5.2. All the numerical results showed a good agreement with Dandy-Sale solutions especially for the active source scenario. In Figure 5.8-c, d, it is shown that there existed a slight deviation between two solutions after removing the source, which

can be attributed to two possible reasons: (1) the numerical model considered both longitudinal and vertical dispersion while Dandy-Sale model only had vertical dispersion in the transmissive layer; (2) there was grid dependent numerical dispersion when applying an "on-off" source in the numerical model which would not be present in the analytical model.

To test the effect of grid dependent numerical dispersion, the numerical model was rebuilt by using a coarser grid spacing of $\Delta x = 5$ m. Figure 5.9 illustrates that the numerical results with finer discretization schemes shows a closer comparison with the analytical solution.

(a)

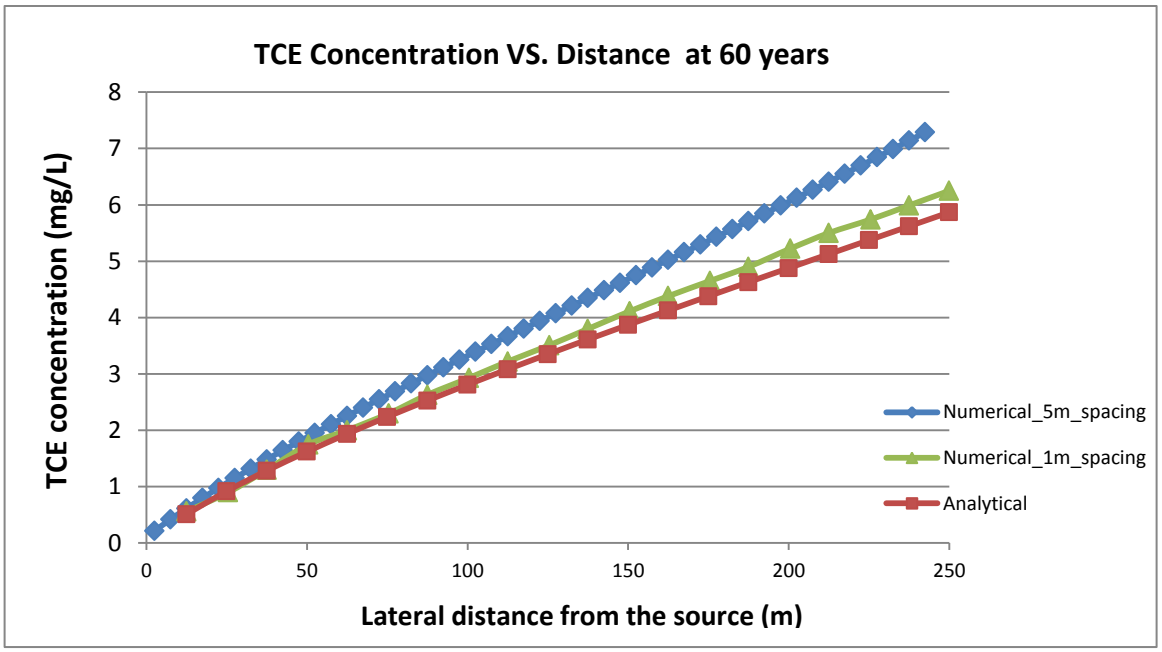

(b)

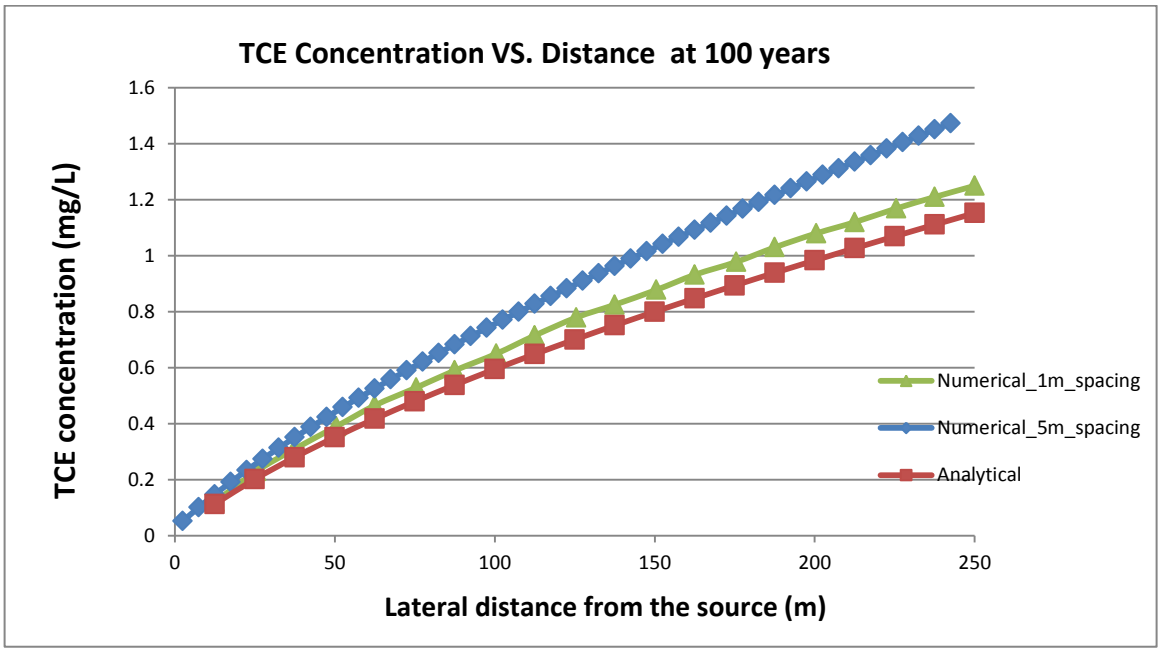

Figure 5.9 Comparison of numerical results with a grid spacing of 1 m and 5 m and analytical solution for the transmissive layer at the times of: (a) 60 years and (b) 100 years.

5.5.2 TCE Concentration in the Low Permeability Layer

Figure 5.10 presents the comparison of the numerical results with the Dandy-Sale solution for the low permeability layer. The coefficient of determination between two solutions at different locations at various times is listed in Table 5.3. Based on the results, the comparisons of these two solutions at locations of x= 2.5 m and 12.5 m were excellent. However, when comparing the TCE concentration at more than 50 m down-gradient the plume, there was a slight deviation between the numerical and Dandy-Sale

solutions, which may be due to the inaccuracy of concentration in the transmissive layer that can affect the boundary condition at the interface.

(a)

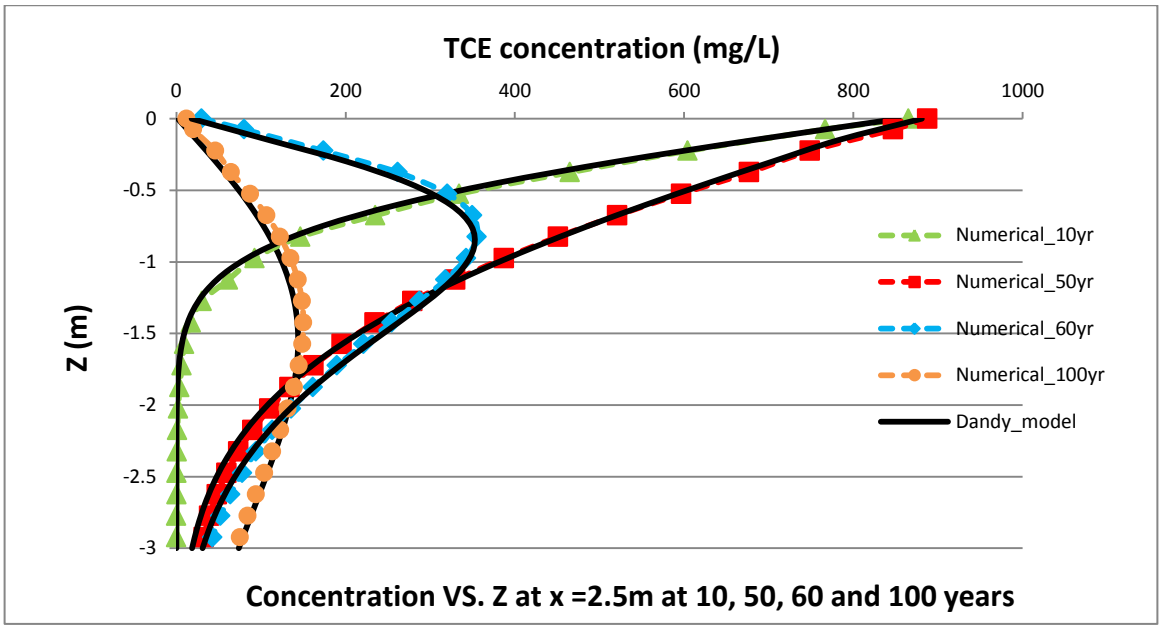

(b)

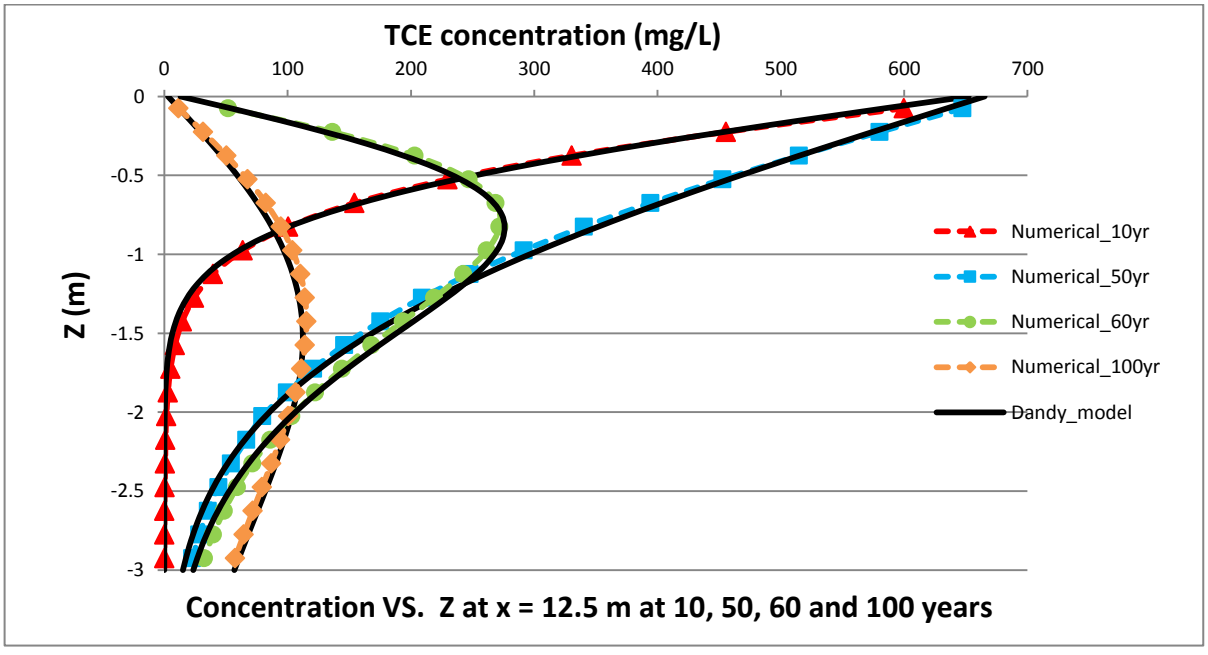

(c)

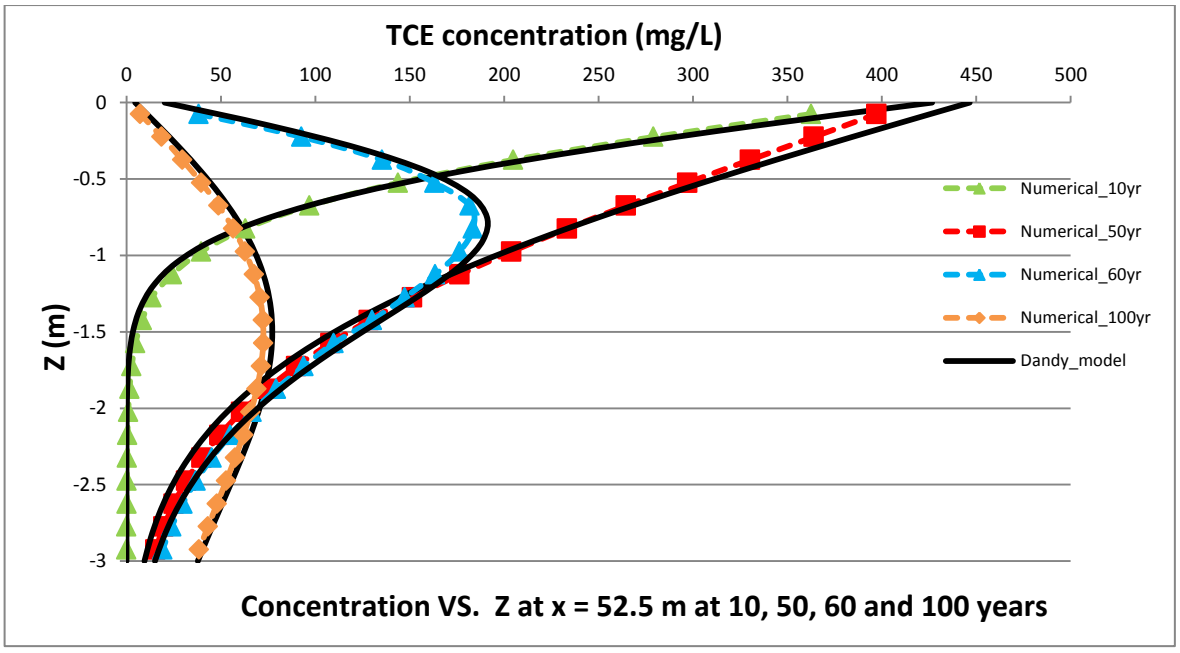

(d)

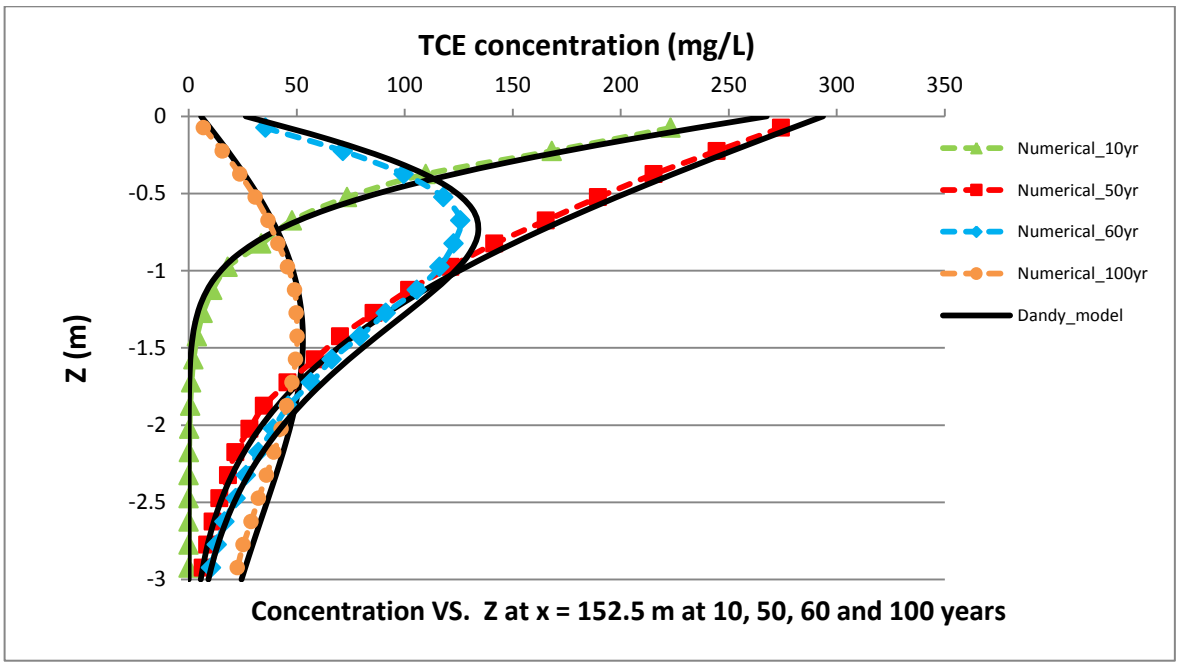

Figure 5.10 TCE concentration profiles in low-k layer for different times of 10, 50, 60 and 100 years at locations of: (a) x = 2.5 m (b) x = 12.5m, (c) x = 52.5m and (d) x = 152.5 m.

Table 5.3 Coefficient of determination between numerical and analytical solutions for concentration in the aquitard at different locations at various times.

Time / Location	10 years	50 years	60 years	100 years
X=2.5 m	0.994	0.995	0.986	0.993
X=12.5 m	0.992	0.993	0.978	0.991
X=52.5 m	0.988	0.989	0.965	0.986
X=152.5 m	0.985	0.986	0.946	0.982

CHAPTER 6

SEMI-ANALYTICAL SIMULATION

6.1 Introduction

A conventional numerical approach for modeling matrix diffusion of CVOCs from an aquifer into aquitard requires fine discretization of the aquifer and aquitard into tens of layers of gridblocks, resulting in large computational effort. Considering the inefficiency of numerical approaches, a semi-analytical method was developed to only discretize the aquifer and mathematically approximate the diffusive response in the underlying aquitard.

The semi-analytical method was originally developed in petroleum reservoir engineering for calculating the conductive heat flux from a permeable reservoir and overlying impermeable cap rock by Vinsome and Westerveld [1980]. This method was shown to be accurate for simulating heat exchange between reservoir fluids and confining beds in petroleum geothermal injection and production operations [Pruess and Wu, 1993; Pope et al., 1999; Varavei and Sepehrnoori, 2009]. The TMVOC code provides an option to use the heat transfer method of Vinsome and Westerveld [1980]. Instead of discretizing the confining bed, the semi-analytical method characterizes the vertical temperature profile in the confining bed by using an analytical trial function in each gridblock that is adjacent to the confining bed [Vinsome and Westerveld, 1980]. This trial function is updated at each time-step:

$$T(t,z) = (\theta + pz + qz^2)e^{-z/d} \tag{6-1}$$

Where T (t, z) is the temperature profile in the cap rock, θ is the temperature at interface between the reservoir and aquitard, p and q are the fitting parameters and z is the height (the zero level has been defined at interphace). The parameter d is the thermal penetration depth, determined by:

$$d = \frac{\sqrt{\alpha_T t}}{2}$$

where α_T is thermal diffusivity defined as:

$$\alpha_T = \frac{\kappa}{\rho c_r}$$

where κ is thermal conductivity and ρc_r is volumetric heat capacity.

The semi-analytical method can be theoretically applied to characterize the contaminant concentration distribution beneath the aquifer due to the mathematical analogy between the partial differential equations for chemical diffusion, and for heat conduction in low permeable zones.

$$R\frac{\partial C}{\partial t} = \tau D_w \frac{\partial^2 C}{\partial z^2} \qquad \rho C_r \frac{\partial T}{\partial t} = \kappa \frac{\partial^2 T}{\partial z^2} \tag{6-2}$$

where the chemical retardation factor, R, is analogous to the volumetric heat capacity (ρC_r); the contaminant concentration, C, is analogous to the temperature, T; and the effective diffusion coefficient (τD_w) is analogous to the thermal conductivity κ.

6.2 Semi-analytical Solution

The semi-analytical method for modeling CVOC matrix diffusion is conducted by performing numerical simulation for only the aquifer and mathematically approximating matrix diffusion effects in the aquitard by using an analytical trial function consisting of

two adjustable parameters. Following Vinsome and Westerveld (1980), the analytical trial function for the matrix diffusion problem can be represented as:

$$C(t,z) = (\theta + pz + qz^2)e^{-z/d} \tag{6-3}$$

where C(t, z) is the concentration profile in the aquitard beneath the aquifer grid block, z is the depth into the aquitard, θ is the concentration at interface between the aquifer and aquitard, p and q are the fitting parameters. The parameter d is the diffusion penetration depth, determined by

$$d = \frac{\sqrt{\alpha t}}{2} \tag{6-4}$$

where α is the effective molecular diffusivity divided by the retardation factor (R):

$$\alpha = \frac{\tau D_W}{R} \tag{6-5}$$

Based on mass conservation law, two conditions must be satisfied at aquitard/aquifer interface:

$$\frac{\partial C}{\partial t} = \alpha \left.\frac{\partial^2 C}{\partial z^2}\right|_{z=0} \tag{6-6}$$

$$\frac{\partial}{\partial t}\int_0^\infty C dz = \alpha \left.\frac{\partial C}{\partial z}\right|_{z=0} \tag{6-7}$$

Equation (6-6) illustrates the partial differential equation for chemical diffusion is satisfied at aquitard/aquifer interface; equation (6-7) illustrates that the rate of change of total chemical mass in the aquitard must be equal to the diffusive mass flux across the interface.

Taking the derivatives with respect to z:

$$\frac{\partial C}{\partial z} = \frac{\partial[(\theta + pz + qz^2)e^{-\frac{z}{d}}]}{\partial z} = -\frac{\theta}{d}e^{-\frac{z}{d}} - \frac{pz}{d}e^{-\frac{z}{d}} + pe^{-\frac{z}{d}} - \frac{qz^2}{d}e^{-\frac{z}{d}} + 2qze^{-z/d}$$

$$\frac{\partial^2 C}{\partial z^2} = \frac{\theta}{d^2}e^{-z/d} + \frac{pz}{d^2}e^{-z/d} - \frac{2p}{d}e^{-\frac{z}{d}} + \frac{qz^2}{d^2}e^{-\frac{z}{d}} - \frac{4qz}{d}e^{-\frac{z}{d}} + 2qe^{-\frac{z}{d}}$$

At the interface z = 0,

$$\left.\frac{\partial C}{\partial z}\right|_{z=0} = \frac{\theta}{d} - p$$

$$\left.\frac{\partial^2 C}{\partial z^2}\right|_{z=0} = \frac{\theta}{d^2} - \frac{2p}{d} + 2q$$

Using finite difference approximation for the time derivative, equation (6-6) can be written as:

$$\frac{\theta^{t+\Delta t} - \theta^t}{\Delta t} = \alpha\left(\frac{\theta}{d^2} - \frac{2p}{d} + 2q\right) \qquad (6\text{-}8)$$

The integral of C (t, z) with respect to z is:

$$\int Cdz = \int(\theta + pz + qz^2)e^{-\frac{z}{d}}dz = -\theta de^{-z/d} - pd(z+d)e^{-\frac{z}{d}} - qdz^2e^{-\frac{z}{d}}$$

$$- 2qzd^2e^{-\frac{z}{d}} - 2qd^3e^{-z/d}$$

At z = ∞, $\int Cdz = 0$

At z = 0, $\int Cdz = -\theta d - pd^2 - 2qd^3$

So, $$\int_0^\infty Cdz = \theta d + \mathrm{p}d^2 + 2qd^3$$

Equation (6-7) becomes:

$$\alpha \int_0^\infty \frac{\partial C}{\partial z} = \alpha(\frac{\theta}{d} - p)$$

Using a finite difference approximation for the time derivative, equation (6-7) becomes:

$$\frac{(\theta d+\mathrm{p}d^2+2qd^3)^{t+\Delta t}-(\theta d+\mathrm{p}d^2+2qd^3)^t}{\Delta t} = \alpha\left(\frac{\theta}{d} - p\right) \quad (6\text{-}9)$$

The algebra expression of parameters p and q can be derived from equations (6-8) and (6-9):

$$\mathrm{p} = \frac{\frac{\alpha\Delta t\theta^{t+\Delta t}}{d} + I^t - \frac{\theta^{t+\Delta t} - \theta^t}{\alpha\Delta t}d^3}{3d^2 + \alpha\Delta t}$$

$$\mathrm{q} = \frac{\frac{\theta^{t+\Delta t} - \theta^t}{\alpha\Delta t}d^2 - \theta^{t+\Delta t} + 2pd}{2d^2}$$

where $I^t = (\theta d + \mathrm{p}d^2 + 2qd^3)^t$.

At each time-step, the value of I^t is stored for use in the next time-step and the previous and current values of concentration θ^t and $\theta^{t+\Delta t}$ are used to compute p and q.

Then the diffusive mass flux across the interface, F, can be quantified by combining Fick's law and Equation (6-3).

$$F = -\phi\tau D_w \left.\frac{\partial C}{\partial z}\right|_{z=0} = \phi\tau D_w \left(\frac{\theta}{d} - p\right)$$

In the semi-analytical simulation, the semi-analytical diffusion term is only applied to the grid blocks adjacent to the aquitard to mathematically evaluate the concentration and mass flux in the aquitard.

6.3 Testing

The semi-analytical method was tested with the exact error function analytical solution [Parker et al., 1984] and the Dandy-Sale solution [Sale et al., 2008].

6.3.1 Error Function Analytical Solution

The test model was set up by a single aquifer grid block with diffusion into a large thickness aquitard (Figure 6.1). The initial condition of TCE concentration was set to zero everywhere. At time zero, TCE concentration in the aquifer was raised to 100mg/L instantaneously and maintained this value for 50 years, and then it was dropped to zero immediately. The concentration profile of two solutions is generated in Figure 6.2.

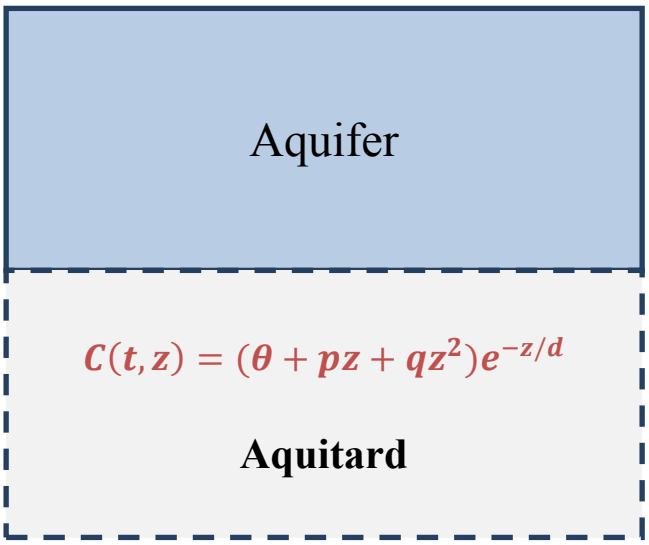

Figure 6.1 The domain of test model.

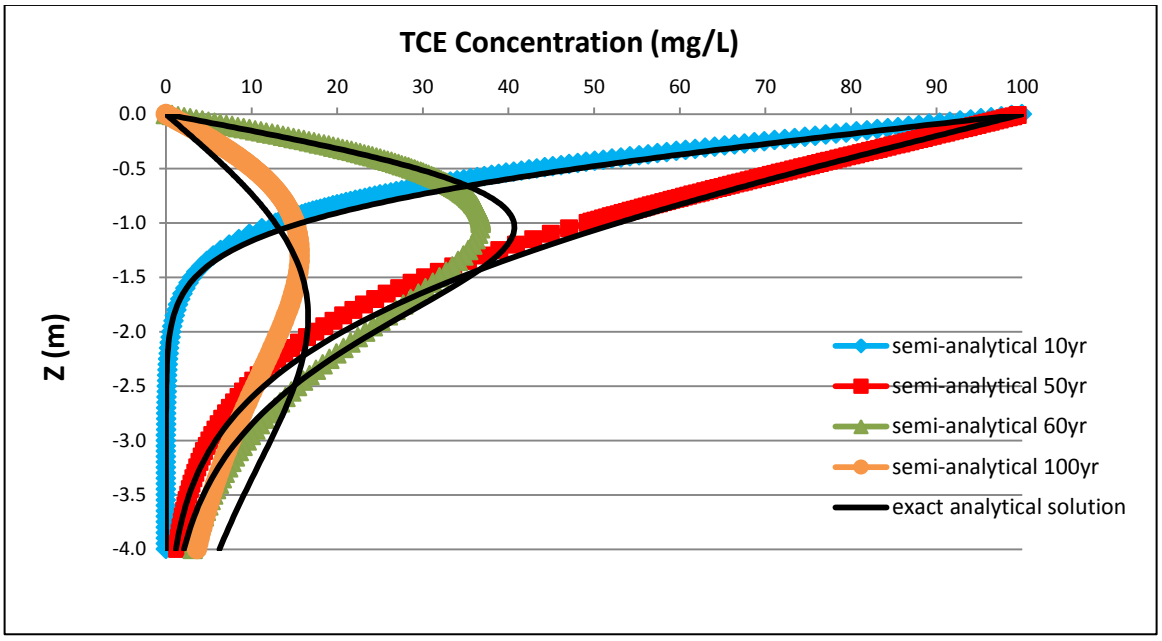

Figure 6.2 Comparison of semi-analytical method with the exact error function analytical solution for matrix diffusion at times of 10, 50, 60, and 100 years. The contaminant source is removed after 50 years.

Table 6.1 Coefficient of determination between numerical and analytical solutions for concentration at different times.

Time	R^2
10 years	0.994
50 years	0.991
60 years	0.976
100 years	0.981

In the first 50 years, the semi-analytical results were almost overlapped by the exact analytical solution. In Table 6.1, it is observed that the values of R^2 are more than 0.99 during the first 50 years, indicating that the semi-analytical method was highly accurate for estimating the concentration when the source is active. However, after removing TCE source at t= 50 years, it can be seen in that there was a deviation between semi-analytical and exact analytical solution, which may be due to the fact that the trial function cannot accurately resolve the approximation of concentrations after a sudden removal of source. The application of a different form of the trial function may provide better results for the concentration distribution during the unloading period.

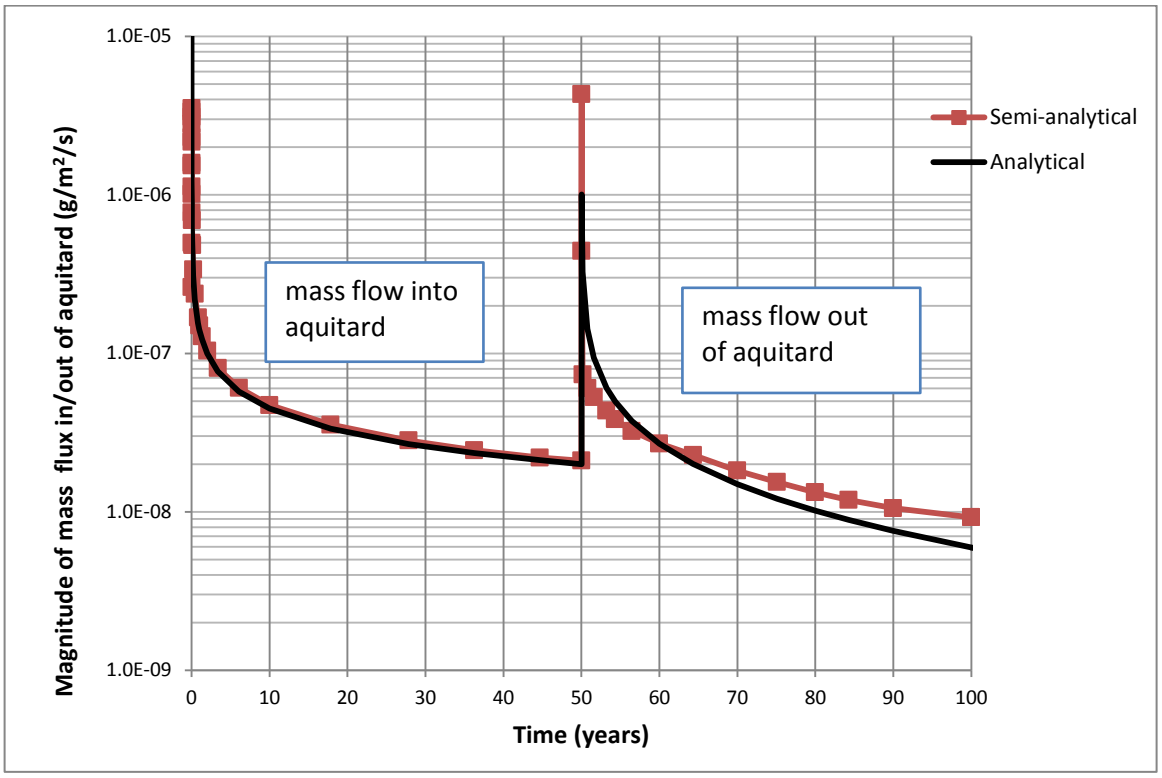

Figure 6.3 Magnitude of diffusive mass flux across the aquifer/aquitard interface.

The diffusive flux time-series can illustrate the mass flux between the aquifer and aquitard more clearly (Figure 6.3). During the first 50 years, the mass flow diffused gradually into the aquitard and the semi-analytical results are consistent with analytical solution. After the source was removed at t = 50 years, the mass diffused out of the aquitard due to the reversal of concentration gradient at the interface. Moreover, it is observed that there is a flux error after the sudden removal of the source. This flux error occurs because the trial function cannot accurately calculate the concentration gradient at z=0 m immediately after removing the source.

The total mass of TCE in the aquitard was derived by integrating the mass flux across the aquifer/aquitard interface with time [Seyedabbasi et al., 2012]. The contaminants gradually diffused from the aquifer into the aquitard over the first 50 years, resulting in a continuous increase of total mass in the aquitard until reaching its maximum value at t=50 years. After taking out the source, the chemicals diffused back into the aquifer, resulting in a sudden drop of the total mass in aquitard. The comparison of two solutions is presented in Figure 6.4. Although there is some difference between two solutions, the match of the total mass balance is still reasonably good.

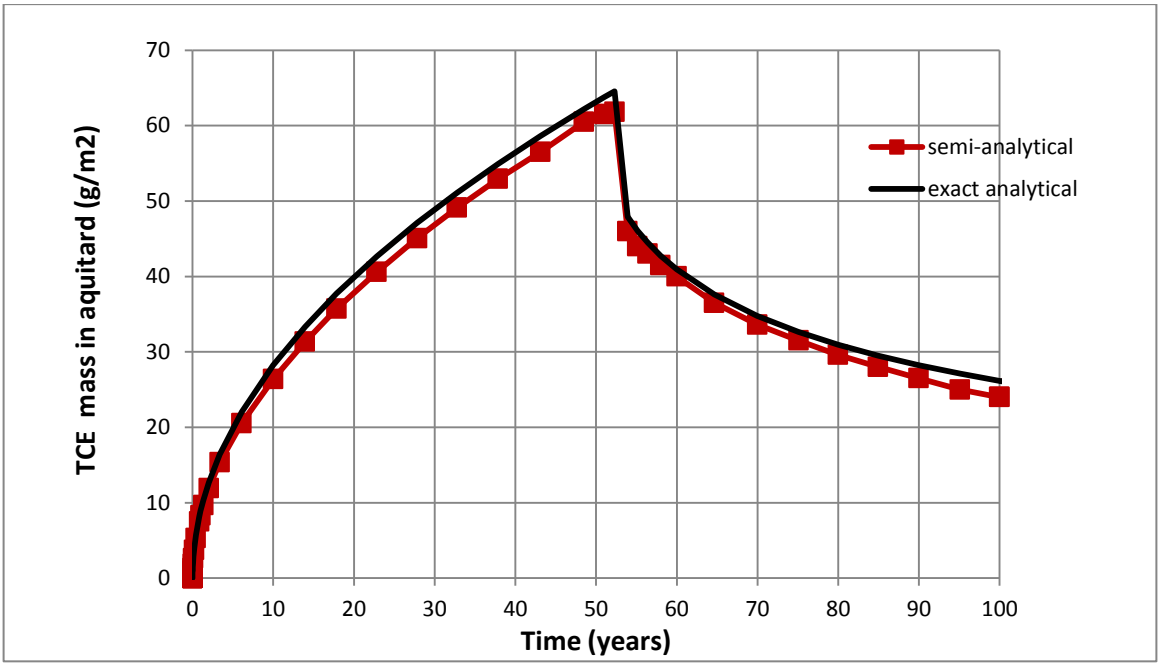

Figure 6.4 Comparison of the semi-analytical method with the exact solution for the TCE mass in the aquitard.

6.3.2 Dandy-Sale Analytical Solution

The semi-analytical method can be further validated by comparing it with the complex Dandy-Sale analytical solution when applied to a two-layer system model (Chapter 5). In this test, the semi-analytical simulation was conducted by repeating the numerical simulation for only the aquifer and mathematically estimating diffusive response in the aquitard using the trial function.

6.3.2.1 TCE Concentration in the Aquitard

The comparisons of semi-analytical and analytical solutions are shown in Figure 6.5 and the coefficient of determination between two solutions is presented in Table 6.2. As the values of σ at x=2.5m are less than 15 for all the time, we can conclude that the semi-analytical solution compare well with the Dandy-Sale solution at x= 2.5 m. However, as the location gets far away from the source, there is a deviation between the two solutions especially after removing the source (Figures 6.5-b, c, d), which can be attributed to the same reason that the trial function is not highly accurate to estimate concentrations in the aquitard especially after switching the source. However, the semi-analytical solution still provided a reasonably good representation of the concentration profiles in the aquitard.

(a)

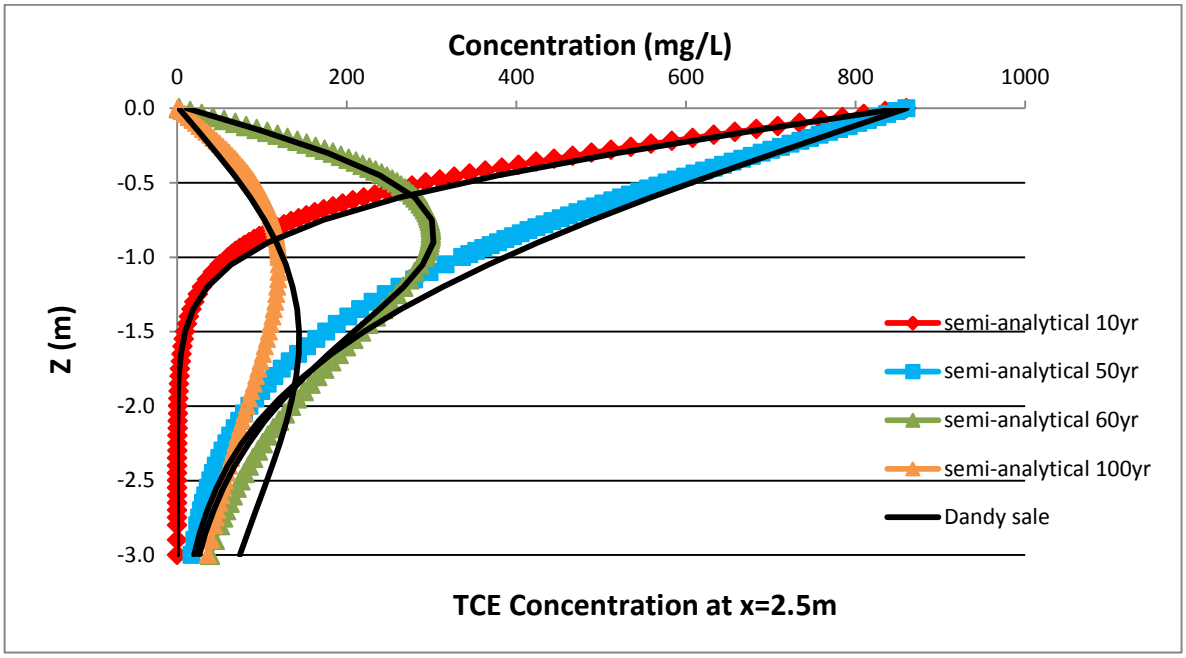
Concentration (mg/L)
0
200
400
600
800
1000
0.0
-0.5
-1.0
-1.5
-2.0
-2.5
-3.0
Z (m)
semi-analytical 10yr
semi-analytical 50yr
semi-analytical 60yr
semi-analytical 100yr
Dandy sale
TCE Concentration at x=2.5m

(b)

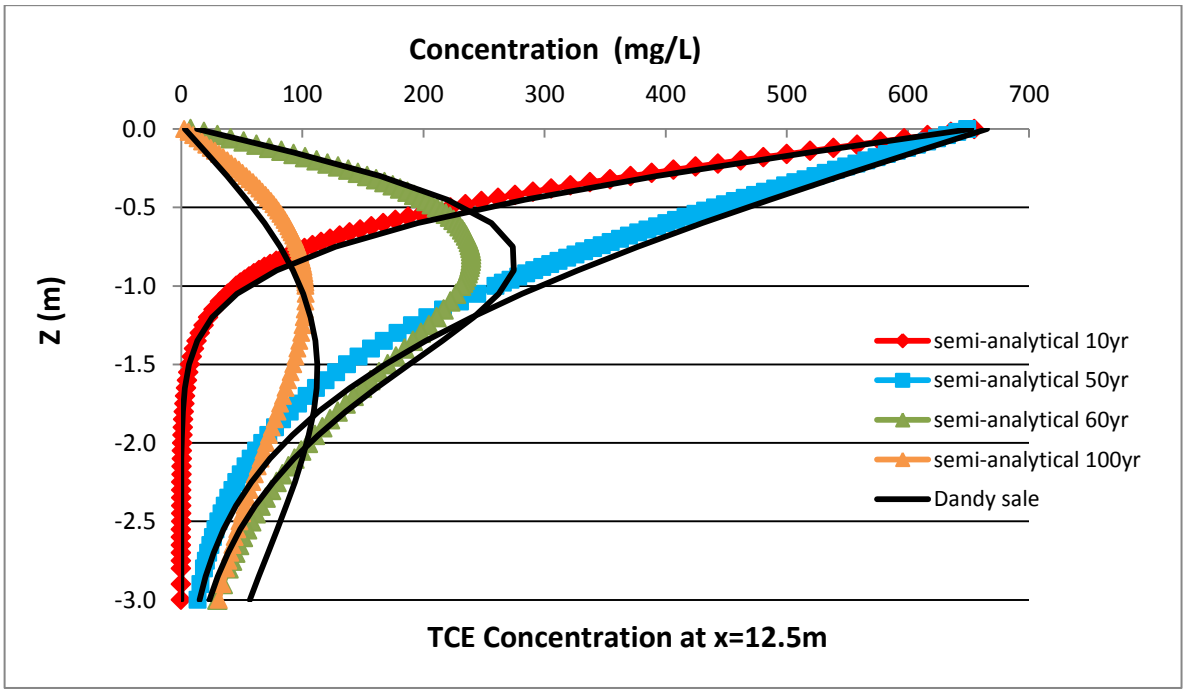
Concentration (mg/L)
0
100
200
300
400
500
600
700
0.0
-0.5
-1.0
-1.5
-2.0
-2.5
-3.0
Z (m)
semi-analytical 10yr
semi-analytical 50yr
semi-analytical 60yr
semi-analytical 100yr
Dandy sale
TCE Concentration at x=12.5m

(c)

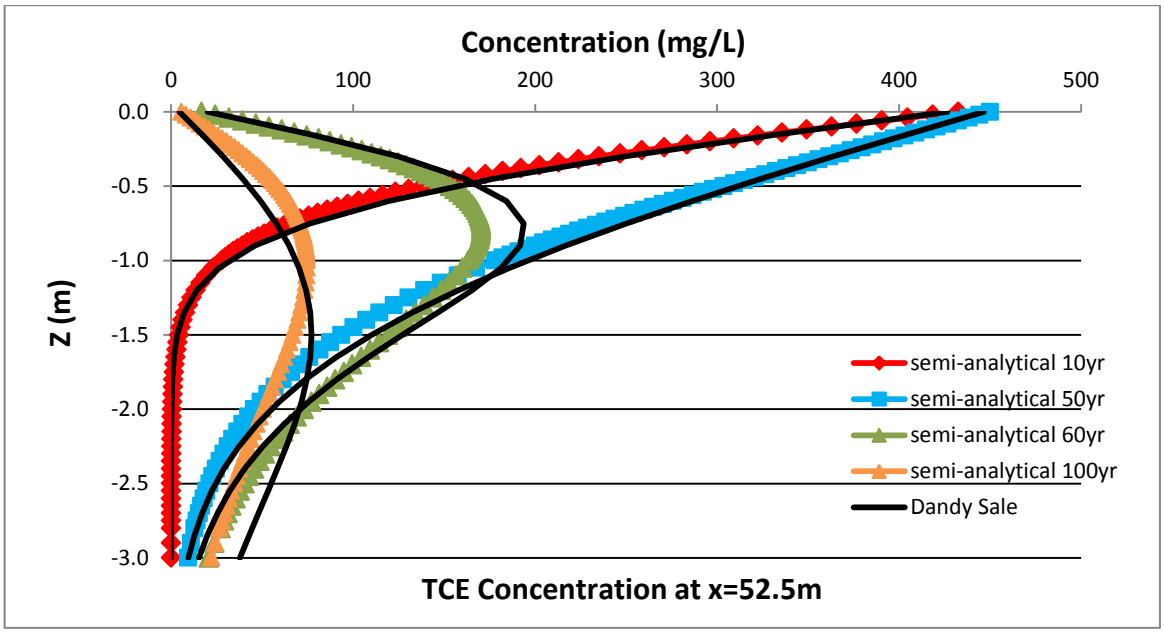

(d)

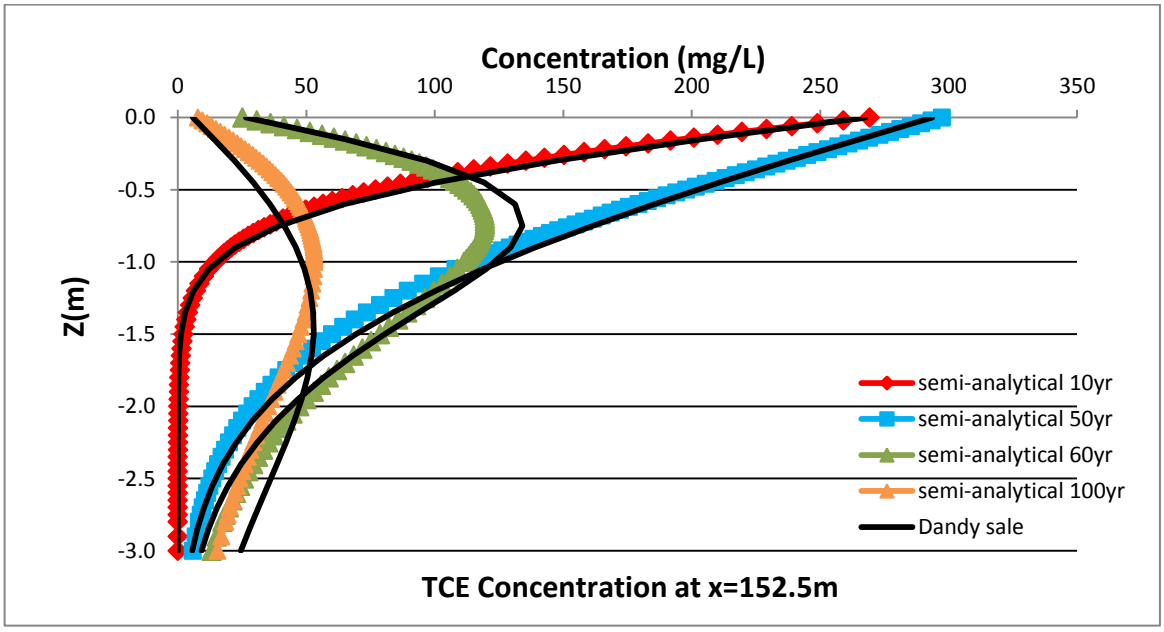

Figure 6.5 Comparison of semi-analytical method with the Dandy-Sale solution for TCE concentration profiles in low-k layer for at times of 10, 50, 60 and 100 years at locations of: (a) x = 2.5 m (b) x = 12.5m, (c) x = 52.5m and (d) x = 152.5 m.

Table 6.2 Coefficient of determination between semi-analytical and analytical solutions for concentration in the aquitard at different locations at various times.

Time / Location	10 years	50 years	60 years	100 years
X=2.5 m	0.994	0.995	0.992	0.991
X=12.5 m	0.988	0.990	0.989	0.987
X=52.5 m	0.985	0.986	0.943	0.946
X=152.5 m	0.983	0.984	0.972	0.978

6.3.2.2 TCE Concentration in the Aquifer

TCE concentrations as a function of lateral distance from the source in the aquifer are illustrated in Figure 6.6. As discussed before (Chapter 5), the concentration was calculated by assuming a 10-foot (3 m) screened interval. Based on the results of coefficient of determination (Table 6.3), the overall semi-analytical results show a good agreement with the Dandy-Sale solution, although there is a small deviation between two solutions at later times (Figures 6.6-d), which may be mainly attributed the reason that the trial function cannot accurately approximate the concentration profile during the unloading period. Another possible reason is that the Dandy-Sale analytical solution that we use to validate the semi-analytical results has neglected the process of longitudinal dispersion in the aquifer.

(a)

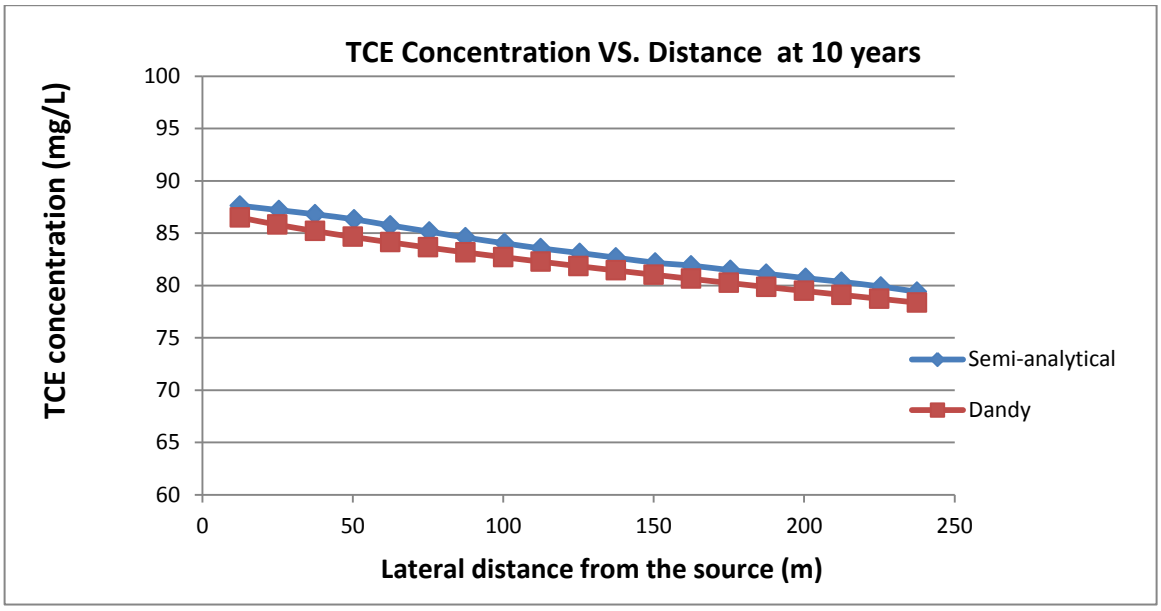
TCE Concentration VS. Distance at 10 years
TCE concentration (mg/L)
100
95
90
85
80
75
70
65
60
0
50
100
150
200
250
Lateral distance from the source (m)
Semi-analytical
Dandy

(b)

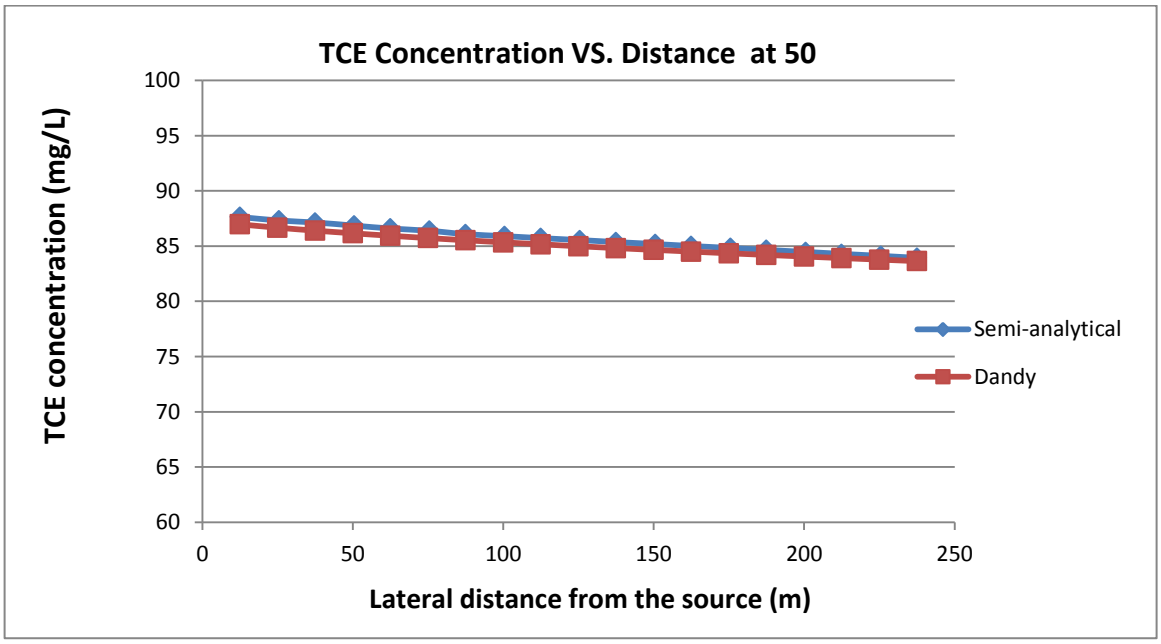
TCE Concentration VS. Distance at 50
TCE concentration (mg/L)
100
95
90
85
80
75
70
65
60
0
50
100
150
200
250
Lateral distance from the source (m)
Semi-analytical
Dandy

(c)

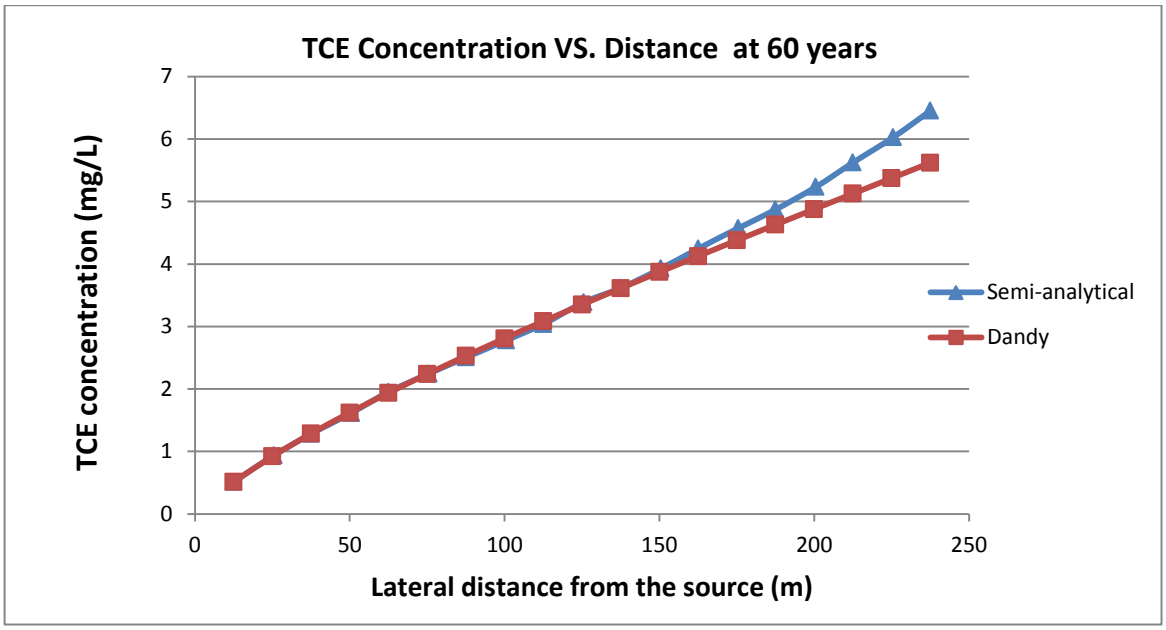

(d)

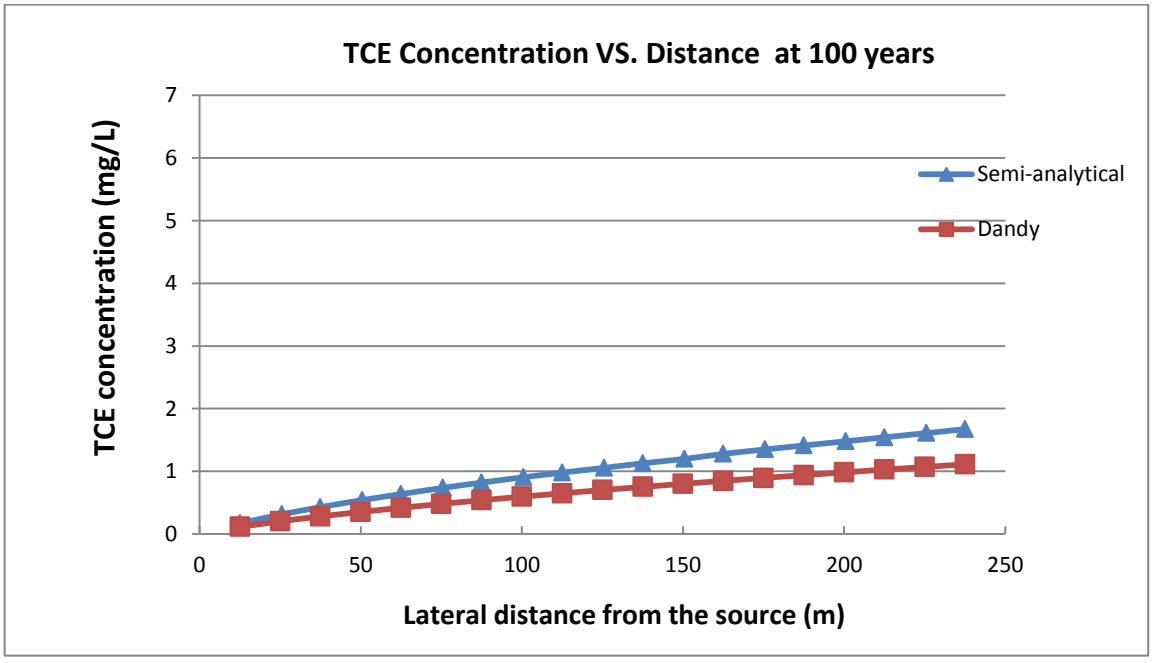

Figure 6.6 Comparison of semi-analytical method with the Dandy-Sale solution for TCE concentration profiles in aquifer layer at the times of: (a) 10 years, (b) 50 years, (c) 60 years and (d) 100 years.

Table 6.3 Coefficient of determination between semi-analytical and analytical solutions for concentration in the aquifer at various times.

Time	R^2
10 years	0.990
50 years	0.992
60 years	0.956
100 years	0.923

6.3.2.3 Mass Discharge in the Aquifer

Figure 6.7 presents the mass discharge in the aquifer as a function of lateral distance from the source at the times of 60 and 100 years. It is observed that the mass discharge increases with lateral distance during the unloading period. At t = 60 year, the comparison of the semi-analytical and Dandy-Sale solutions is excellent. At t = 100 years, there exists some difference between the two solutions (Figures 6.7-b), which can be attributed to the inaccurate approximation for aquifer concentrations as shown in Figure 6.6-d.

(a)

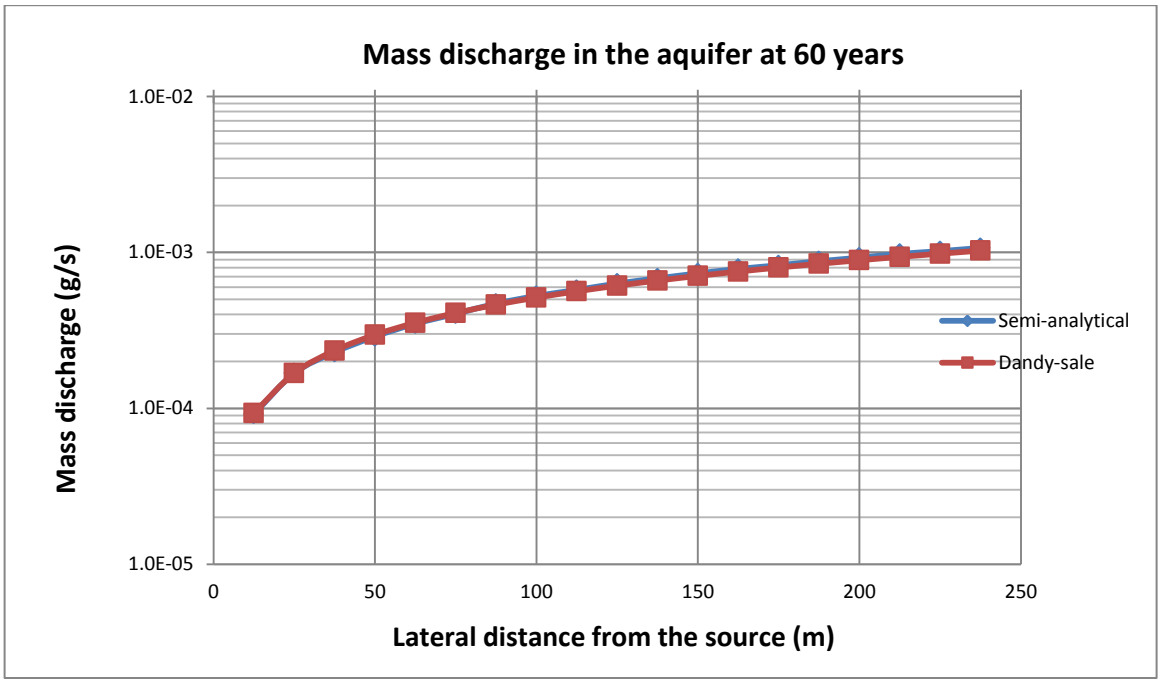

(b)

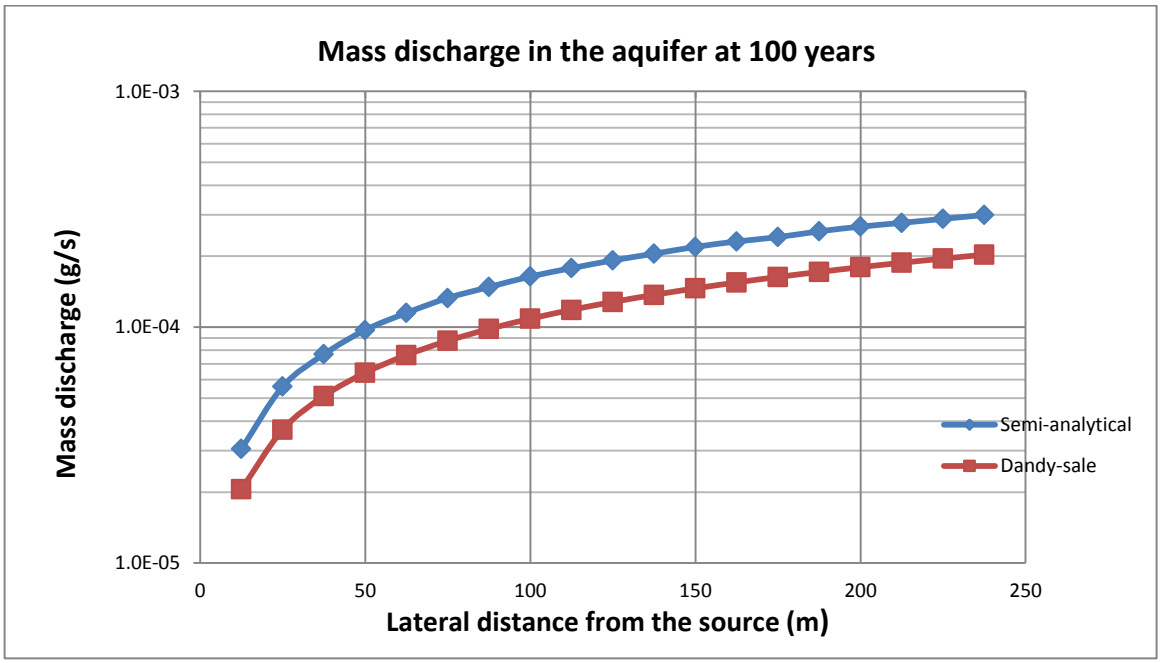

Figure 6.7 Comparison of semi-analytical method with the Dandy-Sale solution for TCE mass discharge in aquifer layer at the times of: (a) 60 years, (b) 100 years.

CHAPTER 7

CONCLUSIONS AND RECOMMENDATIONS

In this study, the accuracy of numerical and semi-analytical solutions for simulating the CVOC matrix diffusion between an aquifer and an aquitard was examined by comparing with published analytical solutions.

In the first part of this work, two simple numerical models were constructed to simulate the DNAPL pool dissolution in aquifers and matrix diffusion in aquitards, respectively. The numerical simulations with different levels of grid refinement were tested against two simple analytical solutions. The results indicated that in practical application, the numerical models are not necessary to be finely discretized into tens of layers of grid blocks. In these two cases, the grid spacing of $\Delta z = 0.2$ m and $\Delta x = 1$m is fine enough to provide accurate results for investigating the evolution of matrix diffusion in aquitards and DNAPL pool dissolution in aquifers.

In the second part of this work, to further validate the numerical method, an additional test was performed by comparing a two-layer numerical model with a more complex Dandy-Sale model (Sale et al., 2008). The numerical solutions were in good quantitative agreement with analytical solutions in Dandy-Sale model.

Finally, a new semi-analytical method was employed for the problem of CVOC matrix diffusion. The accuracy of the semi-analytical method was also verified by comparing with the complex analytical solutions in Dandy-Sale model. The comparison of two solutions indicated that the semi-analytical solution was an accurate

approximation of CVOC matrix diffusion effects between an aquifer and an aquitard especially during the loading period.

Recommendations

Some recommendations for application and future research from this study are listed below:

- Future studies need to consider more realistic situation, where the contaminant source in aquifer changes more smoothly with time instead of the simple "on-off" source scenario.
- Try different forms of the trial function to improve the inaccurate approximation for concentration profiles during the unloading period after a sudden removal of source.
- Consider the effect of decay in semi-analytical method. This semi-analytical method assumes no decay in the groundwater. To be more realistic, we can add a first order decay to the partial differential equation of chemical transport and develop new functions for the parameters p and q.

REFERENCES

Banerjee, S, Solubility of organic mixtures in water. *Environmental Science Technology*, **1984**, 18, 587-591.

Baston, D.P. Analytical and numerical modeling of thermal conductive heating in fractured rock. *M.S. Thesis*, Queen's University, Kingston, Ontario, Canada, **2008**.

Chapman, S. W. and B. L. Parker, Plume persistence due to aquitard back diffusion following dense nonaqueous phase liquid source removal or isolation, *Water Resource Research* **2005**, 41, (12), W12411.

Chen, G., G. E. Hoag, P. Chedda, F. Nadim, B. A. Woody, and G. M. Dobbs.The Mechanism and Applicability of In Situ Oxidation of Trichloroethylenewith Fenton's Reagent. J. Haz. Mat., **2001**, 87, 171-186.

Christ, J.A., Ramsburg, C.A., Pennell, K.D., Abriola, L.M., Estimating mass discharge from dense nonaqueous phase liquid source zones using upscaled mass transfer coefficients: an evaluation using multiphase numerical simulations. *Water Resource Research* **2006**, 42, (11), W11420.

Chrysikopoulos, C.V., 1995. Three-dimensional analytical models of contaminant transport from nonaqueous phase liquid pool dissolution in saturated subsurface formations. *Water Resource Research* **1995**, 31, 1137–1145.

Chrysikopoulos, C.V., Lee, K.Y., Harmon, T.C.: Dissolution of a well-defined trichloroethylene pool in saturated porous media: experimental design and aquifer characterization. *Water Resource Research* **2000**, 36, (7), 1687–1696.

Chrysikopoulos, C.V., Voudrias, E.A., Fyrillas, M.M.. Modeling of contaminant transport resulting from dissolution of non-aqueous phase liquid pools in saturated porous media. *Transport Porous Media* **1994**, 16, 125–145.

Falta, R. W., Pruess, K., Finsterle, S., and Battistelli, A. T2VOC user's guide. **1995**, LBL-36400, Lawrence Berkeley Laboratory.

Falta, R. W., C. M. Lee, S. E. Brame, E. Roeder, J. T. Coates, C. Wright, A. L. Wood, and C. G. Enfield. Field Test of High Molecular Weight Alcohol Flushing for Subsurface Nonaqueous Phase Liquid Remediation. *Water Resource Research* **1999**, 35, 2095-2108.

Falta, R.W. Dissolved chemical discharge from fractured clay aquitards contaminated by DNAPLs. In Dyanmics of Fluids in Fractured Rocks, Faybishenko, B.; Witherspoon, P.A., Gale, J., Eds; *American Geolophysical Union: San Francisco* **2005**, 165-174.

Falta, R.W., 2003. Modeling sub-grid-block-scale dense nonaqueous phaseliquid (DNAPL) pool dissolution using a dual-domain approach. *Water Resource Research* **2003**, 39, (12), 1360.

Fountain, J.C.: Field Test of Surfactant Flooding: Mobility Control of Dense Nonaqueous Phase Liquids, Chapter 15 in Transport and Remediation of Subsurface Contaminants, D.A. Sabatini and R.C. Knox (eds.), *American Chemical Society Symposium Series* **1992**.

Fure, A.D., Jawitz, J.W., Annable, M.D., DNAPL source depletion: linking architecture andflux response. Journal of *Contaminant Hydrology* **2006**, 85, (3–4), 118–140.

Heron, G., Parker, K., Galligan, J., & Holmes, T.C. Thermal Treatment of Eight CVOC Source Zones to Near Nondetect Concentrations. *Ground Water Monitoring & Remediation* **2009**, 29, 56-65.

Hunt, J.R.; Sitar, N.; Udell, K.S. Nonaqueous phase liquid transport and cleanup 1. Analysis of mechanisms. *Water Resource Research* **1998a**, 24, (8), 1247-1258.

Jawitz, J. W., R. K. Sillan, M. D. Annable,P. S. C. Rao, and K. Warner. 2000. In Situ Alcohol Flushing of a DNAPL Source Zone at a Dry Cleaner Site. *Enivironmental Science Technology* **2000**, 34, 3722-3729.

Johnson, P., Dahlen, P., Triplett, J., Foote, E., and Williams, S. State-of-the-Practice Overview: Critical Evaluation of State-of-the-Art in-Situ Thermal Treatment Technologies for DNAPL Source Zone Treatment **2009**.

Johnson, R.L., Pankow, J.F., 1992. Dissolution of dense chlorinated solventsinto groundwater. 2. Source functions for pools of solvent. *Enivironmental Science Technology* **1992,** 26, (5), 896–901.

Kueper, B.H., McWhorter, D.B., The behavior of dense no aqueous phase liquids in fractured clay and rock. *Journal of Ground Water* **1991** 29, 716–728.

Lee, K.Y., Chrysikopoulos, C.V., 1995. Numerical modeling of three-dimensional contaminant migration from dissolution of multicomponent NAPL pools in saturated porous media. *Environmental Geology* **1995**, 26, 157–165.

Lee, K.Y., Chrysikopoulos, C.V., Dissolution of a multicomponent DNAPL pool in an experimental aquifer. *Journal of Hazardous Material* **2006**, 128, 218–226.

Lee, K.Y., Chrysikopoulos, C.V., Dissolution of a well-defined trichloroethylene pool in saturated porousmedia: experimental results and model simulations. *Water Resource Research* **2002**, 36, 3911–3918.

Leinonen, P. J. and Mackay, D., The multicomponent solubility of hydrocarbons in water. Can. *Journal of Chemical Engineering* **1973**, 51, 230-233.

Lipson, D. S., Kueper, B. H., and Gefell, M. J. 2005, Matrix Diffusion-Derived Plume Attenuation in Fractured Bedrock, Ground Water, 43 (1), 30-39.

Liu, G., Ball, W.P., Back diffusion of chlorinated solvent contamination from a natural aquitard to a remediated aquifer under well-controlled field conditions: predictions and measurements, *Journal of Ground Water* **2002**, 40, 175-184.

Lunn, S. R. D. and B. H. Kueper. 1997. Removal of Pooled Dense, Nonaqueous Phase Liquid from Saturated Porous Media Using Upward Gradient Alcohol Floods. *Water Resource Research* **1997**, 33, 2207-2219.

Mackay, D. M. and J. A. Cherry (1989), Groundwater contamination - Pump-and-Treat remediation. *Environmental Science & Technology* **1989**, 23, 630-636.

Mayer, A.S., Miller, C.T., The influence of mass transfer characteristicsand porous media heterogeneity on nonaqueous phase dissolution. *Water Resource Research* **1996**, 32, (6), 1551–1567.

Miller, C.T., Christakos, G., Imhoff, P.T., McBride, J.F., Pedit, J.A., Trangenstein, J.A. Multiphase flow and transport modeling in heterogeneous porous media: Challenges and approaches. *Advance Water Resource* **1998**, 21, (2), 77-120.

Nambi, I.M., Powers, S.E., 2000. NAPL dissolution in heterogeneous systems: anexperimental investigation in a simple heterogeneous system. , *Journal of Contaminant Hydrology*, **2000,** 44, (2), 161–184.

Nambi, I.M., Powers, S.E., Mass transfer correlations for nonaqueousphase liquid dissolution from regions with high initial saturations. *Water Resource Research* **2003**, 39, (2), 1030.

National Research Council (NRC), Contaminants in the Subsurface: Source Zone Assessment and Remediation. *National Academies Press, Washington, D.C*, **2005**.

Pankow, J. F. and J. A. Cherry, Dense Chlorinated Solvents and Other DNAPLs in Groundwater, Waterloo, Portland, **1996**.

Parker, B. L., R. W. Gillham, and J. A. Cherry, Diffusive Disappearance of Immiscible-Phase Organic Liquids in Fractured Geologic Media, *Ground Water* **1994**, 32, 805-820.

Parker, B.L., Chapman, S.W., Guilbeault, M.A., Plume resistance caused by back diffusion from thin clay layers in a sand aquifer following TCE source-zone hydraulic isolation, *Journal of Contaminant Hydrology* **2008** 102, 72-85.

Parker, B.L.; McWhorter, D.B.; Cherry, J.A. Diffusive loss of non-aqueous phase organic solvents from idealized fracture networks in geologic media. *Ground Water* **1997**, 36, (6), 1077-1088.

Parker, J.C., Park, E., Modeling field-scale dense nonaqueous phaseliquid dissolution kinetics in heterogeneous aquifers. *Water Resource Research* **2004**, 40, (5), W05109.

Pearce, A.E., Voudrias, E.A., Whelan, M.P., Dissolution of TCE and TCA pools in saturated subsurface systems. *Journal of Environmental Engineering* **1994**, 120, 1191 – 1206.

Pearce, A.E., Voudrias, E.A., Whelan, M.P., Dissolution of TCE and TCA pools in saturated subsurface systems. *Journal of Environmental Engineering* **1994**, 120, 1191–1206.

Pierce, Robert R.; Perlman, Howard A., Estimated use of water in the United States in 1990. *USGS Numbered Series* **1990**, 1081.

Pope, G.A., K. Sepehrnoori, M.M. Sharma, D.C. McKinney, G.E. Speitel, and R.E. Jackson, Three-dimensional NAPL fat and transport model. *Technical Report*, **1999**, 600, 99-110.

Powers, S. E., I. M. Nambi, and G. W. Curry Jr, Non-aqueous phase liquid dissolution in heterogeneous systems: Mechanisms and a local equilibrium modeling approach, *Water Resource Research* **1998**, 34, (12), 3293-3302.

Pruess, K., and Y.S. Wu, A new semi-analytical method for numerical simulation of fluid and heat flow in fractured reservoirs, *SPE Advanced Technology Series* **1993,** 1, (2), 63-72.

Ramsburg, C.A., and K.D. Pennell: Experimental and economic assessment of two surfactant formulations for source zone remediation at a former dry cleaning facility, *Ground Water Monitoring and Remediation* **2001**, 21, (4), 68-82.

Rao, P. S. C., M. D. Annable, R. K. Sillan, D. Dai, K. Hatfield, W. D. Graham, A. L. Wood, and C. G. Enfield. Field-Scale Evaluation of In Situ Cosolvent Flushing for Enhanced Aquifer Remediation. *Water Resource Research* **1997,** 33, 2673-2686.

Saba, T., Illangasekare, T.H., Effect of groundwaterflow dimensionality on mass transfer from entrapped nonaqueous phase liquid contaminants. *Water Resource Research* **2000**, 36, (4), 971–979.

Sale, T. C., Zimbron, J., Dandy, D., Effects of reduced contaminant loading on downgradient water quality in an idealized two-layer granular porous media, *Journal of Contaminant Hydrology* **2008**, 102, 72-85.

Sale, T.C., McWhorter, D.B., 2001. Steady state mass transfer from singlecomponent dense nonaqueous phase liquids in uniform flowfields. *Water Resource Research* **2001**, 37, (2), 393–404.

Sale, T.C., McWhorter, D.B., Steady state mass transfer from singlecomponent dense nonaqueous phase liquids in uniform flowfields. *Water Resource Research* **2001**, 37, (2), 393–404.

Schipper, L.A., Robertson, W.D., Gold, A.J., Jaynes, D.B., Cameron, S.C., Denitrifying bioreactors – an approach for reducing nitrate loads to receiving waters. *Ecology Engineering* **2010**, 36 (11), 1532–1543.

Schwille, F, Dense Chlorinated Solvents in Porous and Fractured Media: Model Experiments, *Lewis Publishers* **1988**, 146.

Seagren, E.A., Rittmann, B.E., Valocchi, A.J., An experimental investigation of NAPL pool dissolution enhancement by flushing. , *Journal of Contaminant Hydrology* **1999,** 37, 111 – 137.

Shackelford, CJD., Laboratory diffusion testing for waste disposal - A review, *Journal of Contaminant Hydrology* **1991,** 7, 177-217.

Stegemeier, G.L.; Vinegar, H.J. Thermal conduction heating for in-situ thermal desorption of soils. In Hazardous & Radioactive *Waste Treatment Technologies Handbook* **2001,** 1-22.

Tase, N., Groundwater contamination in Japan. *Environonmetal Geology Water Science* **1992**, 20, (1), 15–20.

Triplett Kingston, J.L., Dahlen, P.R., & Johnson, P.C. 2010. State-of-Practice Review of In Situ Thermal Technologies. *Ground Water Monitoring & Remediation* **2010,** 30, 64-74.

Varavei, A., and K. Sepehrnoori, An EOS-based compositional thermal reservoir simulator, *SPE Reservoir Simulation Symposium* **2009**.

Vinsome, P.K.W., and J. Westerveld, A simple method for predicting cap and base rock heat losses in thermal reservoir simulators, *The Journal of Canadian Petroleum Technology* **1980**, July-September, 87-90.

Voudrias, E.A., Yeh, M.F., Dissolution of a toluene pool under constant and variable hydraulic gradients with implications for aquifer remediation. *Groundwater* **1994**, 32, 305–311.

West, C.C. and J.H. Harwell: Surfactants and Subsurface Remediation, *Environmental Science Technology* **1992**, 26, (12), 2324-2330.

Whelan, M.P., Voudrias, E.A., Pearce, A., DNAPL pool dissolution in saturated porous media: Procedure development and preliminary results *Journal of Contaminant Hydrology* **1994,** 15, 223–237.

Zoh, K.-D, M. K. Stenstrom. Fenton Oxidation of Hexahydro-1,3,5-Triazine (RDX) and Octahydro-1,3,5,7-Tetrazocine (HMX). *Water Resource Research* **2002**, 36, 1331-1341.